Uso de métodos avanzados para la monitorización y el análisis de los cambios de la humedad del suelo en Europa

Tesis doctoral

Física Aplicada y Tecnología

Universidad de Salamanca

Laura Almendra Martín

Directores

José Martínez Fernández

María Piles Guillem

Instituto de Investigación en Agrobiotecnología - CIALE Salamanca 2022

Dr. Luis Plaja Rustein, Coordinador del Programa de Doctorado en Física Aplicada y Tecnología de la Universidad de Salamanca.

CERTIFICO:

Que la presente Memoria titulada **"Uso de métodos avanzados para la monitorización y el análisis de los cambios de la humedad del suelo en Europa"**, ha sido realizada en el Programa de Doctorado en Física Aplicada y Tecnología de la Universidad de Salamanca por **Laura Almendra Martín**, bajo la dirección del Prof. **Dr. José Martínez Fernández** y la Prof. **Dra. María Piles Guillem,** y cumple las condiciones exigidas para optar al grado de Doctor por la Universidad de Salamanca.

Para que así conste, firmo el presente certificado en Salamanca a 21 de octubre de 2022

Fdo: Dr. L. Plaja Rustein

Haciendo uso de la posibilidad que ofrece la Universidad de Salamanca, esta tesis doctoral se presenta como un compendio de artículos científicos, siendo la estudiante de doctorado Laura Almendra Martín la autora principal de todos ellos:

- Almendra-Martín, L., Martínez-Fernández, J., Piles, M., González-Zamora, Á., 2021. Comparison of gap-filling techniques applied to the CCI soil moisture database in Southern Europe. Remote Sens Environ 258. https://doi.org/10.1016/j.rse.2021.112377

  Status: publicado

- Almendra-Martín, L., Martínez-Fernández, J., Piles, M., González-Zamora, Á., Benito-Verdugo, P., Gaona, J., 2022. Analysis of soil moisture trends in Europe using rank-based and empirical decomposition approaches. Glob Planet Change 215. https://doi.org/10.1016/j.gloplacha.2022.103868

  Status: publicado

- Almendra-Martín, L., Martínez-Fernández, J., Piles, M., González-Zamora, Á., Benito-Verdugo, P., Gaona, J., 2022. Influence of atmospheric patterns on soil moisture dynamics in Europe. Science of The Total Environment 846, 157537. https://doi.org/10.1016/j.scitotenv.2022.157537

  Status: publicado

Autores

Almendra-Martín, Laura[1]

Benito-Verdugo, Pilar[1]

Gaona, Jaime[1]

González-Zamora, Ángel.[1]

Martínez-Fernández, José[1]

Piles, María[2]

[1]Instituto de Investigación en Agrobiotecnología, CIALE, Universidad de Salamanca, Villamayor, 37185 Salamanca, Spain.

[2]Image Processing Laboratory, Universitat de València, 46980, València, Spain

Dr. José Martínez Fernández, Catedrático de Geografía Física del Departamento de Geografía de la Universidad de Salamanca y Dra. María Piles Guillem, Investigadora Ramón y Cajal en el *Image Processing Laboratory* de la Universitat de València.

CERTIFICAMOS:

Que la presente Memoria titulada "**Uso de métodos avanzados para la monitorización y el análisis de los cambios de la humedad del suelo en Europa**", ha sido realizada en el Instituto de Investigación en Agrobiotecnología de la Universidad de Salamanca, bajo nuestra dirección, por Laura Almendra Martín, se presenta como un compendio de artículos científicos, y cumple las condiciones exigidas para optar el grado de Doctor por la Universidad de Salamanca.

Para que así conste, firmamos el presente certificado en Salamanca a 21 de octubre de 2022.

Firmado:

MARTINEZ FERNANDEZ JOSE - 74432086S

Firmado digitalmente por MARTINEZ FERNANDEZ JOSE - 74432086S
Fecha: 2022.10.21 18:20:28 +02'00'

Dr. José Martínez Fernández

MARIA| PILES| GUILLEM

Firmado digitalmente por MARIA|PILES| GUILLEM
Fecha: 2022.10.21 17:59:14 +02'00'

Dra. María Piles Guillem

Fdo: Laura Almendra Martín

AGRADECIMIENTOS

Quiero agradecer a todas las personas que, de alguna manera, me han ayudado a realizar este trabajo de tesis doctoral. Como los despistes existen, voy a obviar los nombres en grupos de gente numerosos porque no quiero de dejar a nadie en el olvido.

En primer lugar, quiero agradecer a mis directores de tesis José Martínez Fernández y María Piles por su esfuerzo y dedicación durante estos años. A Pepe por todo el interés que ha volcado en mi formación y aprendizaje, por orientarme y apoyar mi investigación y mi carrera investigadora desde el primer día. A María, porque a pesar de la distancia, todos los correos, mensajes o videoconferencias han sido de inmensa ayuda.

En segundo lugar, quiero agradecer a Rafael Muñoz Carpena, por acogerme en su grupo de investigación durante mi estancia en el *Department of Agricultural and Biological Engineering, University of Florida*. También quiero agradecer a todos los miembros de su grupo, por hacer de mi estancia allí una experiencia única.

En tercer lugar, quiero agradecer a todos mis compañeros del CIALE, y allegados, por haber hecho de mi lugar de trabajo un sitio divertido todos estos años. Quiero hacer mención especial a mis compañeros de laboratorio por ofrecerme el mejor ambiente de trabajo siempre: a Carlos, Jaime, Pilar y, cómo no, a Ángel, que me ha ayudado y apoyado desde mi primer día en el laboratorio.

En cuarto lugar, quiero agradecer a las personas ajenas a mi lugar de trabajo, que directa o indirectamente me han apoyado durante estos años. A Oscar y Alberto del M3 por tan deliciosos y divertidos desayunos, cafés, comidas o meriendas. A Laura del "Bar la Gaso" por sus reponedores cafés y bocadillos en las salidas de campo. A Marta y a todas mis compañeras y amigas de Espacio Endanza por hacerme amar la danza, mi gran aliada durante estos años. A todos mis amigos y familia, que siempre me han apoyado y animado cuando más lo necesitaba. Pero, en especial, quiero agradecer a mi hermana Sara, a mis padres Mariángeles y Evelio, y a mi pareja Juan por su apoyo incondicional y por animarme e inspirarme a crecer profesional y personalmente.

Por último, quiero agradecer a las instituciones que han financiado mi investigación: a la consejería de Educación de la Junta de Castilla y León y al Fondo Social Europeo por la ayuda para financiar la contratación predoctoral de personal investigador, a la Universidad de Salamanca por la ayuda de movilidad para estancias en centros extranjeros para estudiantes de doctorado, al MCIN/AEI/10.13039/501100011033/ por los proyectos ESP2017-89463-C3-3-R, RTI2018-096765-A-I00 y PID2020-114623RB-C33, y al gobierno de Castilla y León y el Fondo Europeo de Desarrollo Regional (FEDER) por los proyectos SA112P20 and CLU-2018-04.

RESUMEN

La humedad del suelo (SM, *soil moisture*) es una variable clave en el ciclo hidrológico, fundamental para una gran diversidad de aplicaciones desde la de gestión de recursos hídricos y la productividad agrícola, hasta la predicción de la variabilidad climática. Considerada una variable climática esencial (ECV, *essential climatic variable*) por el GCOS (*Global Climate Observing System*), en las últimas décadas se ha puesto de manifiesto el interés creciente por disponer de bases de datos de SM de larga duración, continuas en el tiempo y el espacio. Además, el todavía incierto impacto del cambio climático en el ciclo hidrológico del planeta realza la necesidad de comprender y definir los cambios en la dinámica de la SM. Estos cambios son de particular interés en Europa, donde se prevé que el calentamiento global afecte negativamente a los recursos hídricos. Con ánimo de explorar diferentes métodos y enfoques de análisis para el estudio de la tendencia de cambio de la SM, su interacción con los patrones atmosféricos y la obtención de bases de datos apropiadas para el continente europeo, en esta tesis doctoral se han planteado tres objetivos específicos.

En primer lugar, se destaca la necesidad de contar con bases de datos de SM continuas y de larga duración, tanto modelizadas como observacionales. Las misiones satelitales han facilitado esta labor enormemente, sin embargo, la continuidad de las series se ve comprometida debido a la existencia de lagunas en los datos, provocadas por diversos factores como la presencia de nieve o interferencias de radiofrecuencia que no hacen posible la medición. Motivado por esta necesidad, el primer objetivo de esta tesis doctoral busca comparar diferentes técnicas de *gap-filling* para estimar los valores ausentes en la base de datos de SM satelital más larga disponible en Europa, la proporcionada por la *Climate Change Initiative* (CCI). Para ello, se evaluaron diferentes técnicas, desde las más sencillas como interpolaciones lineales o cúbicas hasta técnicas más complejas como métodos autorregresivos (AR, *autoregressive*) o de aprendizaje automático (ML, *machine learning*) como las s*upport vector machine* (SVM) y los *random forest* (RF), donde se evaluó el uso de diferentes variables de entrada relacionadas con la dinámica de la SM. Todas estas técnicas fueron evaluadas tanto en el domino espacial como en el temporal.

En segundo lugar, el impacto del cambio climático en la dinámica de la SM en Europa y la magnitud de estos cambios es todavía incierto. Por ello, se definió como segundo objetivo de esta tesis doctoral el estudio de las tendencias de la SM de los últimos 30 años en Europa utilizando diferentes tests estadísticos, escalas temporales (anual y mensual) y bases de datos. Los métodos utilizados fueron el test de Mann-Kendall (MK), ampliamente utilizado y basado en el comportamiento monótono, y el *empirical mode decomposition* (EMD), basado en una descomposición empírica de las series temporales. Además, se analizó la tendencia de los principales atributos que caracterizan la sequía agrícola (inicio, duración e intensidad). La significación estadística de las tendencias y sus signos fueron evaluados

en los diferentes tipos de clima presentes en el continente europeo, según la clasificación de Köppen-Geiger.

En tercer y último lugar, es sabido que la variabilidad de la SM está íntimamente ligada a los procesos atmosféricos. Sin embargo, muchos aspectos sobre las interacciones entre los sistemas suelo-atmósfera aún son inciertos. Aunque en Europa están bien definidas las teleconexiones atmosféricas, la relación de los diferentes patrones de circulación atmosférica con la SM no ha recibido especial atención. Además, rara vez se han analizado sus relaciones causales. En este contexto, se planteó como tercer y último objetivo de esta tesis doctoral el análisis de la influencia y las relaciones causales entre la *North Atlantic Oscillation* (NAO), la *Arctic Oscillation* (AO) y *El Niño Southern Oscillation* (ENSO) y la variabilidad de la SM en Europa. Para ello, se consideraron dos bases de datos de SM y se evaluaron, a una escala de tiempo mensual, la correlación y las relaciones causales entre los patrones atmosféricos y la SM.

Los resultados obtenidos en esta tesis han permitido, por un lado, evaluar diferentes técnicas para el relleno de lagunas de datos de series satelitales de forma precisa. Los SVM aplicados al dominio espacial, utilizando la textura y las series de SM anteriores como *inputs*, han demostrado ser una buena herramienta para hacer frente a la limitación de las lagunas de datos presentes en las series satelitales. Por otro lado, haciendo uso de datos procedentes de la modelización se ha podido observar una tendencia general a condiciones más secas en el suelo en casi todo el continente europeo en los últimos 30 años, independientemente del tipo de clima, la escala temporal analizada o el método aplicado. También se ha encontrado un incremento de la intensidad y la duración de le periodos de sequía agrícola. Por último, los resultados de esta tesis han demostrado que existe una relación causal predominantemente negativa entre la NAO y AO, y la variabilidad de la SM en la mayor parte de Europa, sin apenas retraso temporal, mientras que con ENSO se observó una respuesta retardada de uno o dos meses en Europa central y noroeste. Los resultados obtenidos en esta tesis aportan nuevos conocimientos sobre los cambios que ha experimentado la SM en Europa y su interacción con los patrones atmosféricos, poniendo de manifiesto la importancia de la aplicación de metodologías avanzadas para llevar a cabo estos análisis, así como de obtener bases de datos apropiadas para los mismos.

ABSTRACT

Soil moisture (SM) is a key variable in the hydrological cycle, essential for a wide variety of applications from water resource management and agricultural productivity to the climate variability forecast. Considered an essential climatic variable (ECV) by the GCOS (Global Climate Observing System), in recent decades there has been an increasing interest in having long-term SM databases continuous over time and space. In addition, the still uncertain impact of climate change on the hydrological cycle highlights the need to understand and define the changes in the SM dynamics. These changes are of particular interest in Europe, where global warming is expected to negatively affect water resources. To explore different methods and analysis approaches for the study of the SM change trend, its interaction with atmospheric patterns, and obtaining appropriate databases for the European continent, three specific objectives have been proposed in this doctoral thesis.

First, the need of having continuous and long-term SM databases, both modeled and observational, is highlighted. Satellite missions have considerably facilitated this challenge; however, the continuity of the series is compromised due to the existence of gaps in the data, caused by several factors such as the presence of snow or radio frequency interference that prevents from having measurements. Motivated by this need, the first objective of this doctoral thesis sought to compare different gap-filling techniques to estimate the missing values in the longest satellite SM database available in Europe, the one provided by the Climate Change Initiative (CCI). For this, different techniques were evaluated, from the simplest such as linear or cubic interpolations to more complex techniques such as autoregressive (AR) or machine learning (ML) methods, such as the support vector machine (SVM) and random forest (RF), evaluating the use of different input variables related to SM dynamics. All these techniques were applied in both the spatial and temporal domains.

Second, the impact of climate change on the SM dynamics in Europe and the magnitude of its changes is still uncertain. Therefore, the second objective of this doctoral thesis was the study of SM trends over the last 30 years in Europe using different statistical tests, time scales (annual and monthly) and databases. The methods utilized were the Mann-Kendall (MK) test, widely used and based on monotonic behavior, and the empirical mode decomposition (EMD), based on an empirical decomposition of time series. In addition, the trend of the main attributes that characterize agricultural drought (onset, duration, and intensity) were analyzed. The statistical significance of the trends and their signs were evaluated in the different types of climates of Europe, according to the Köppen-Geiger classification.

Third and last, it is known that the variability of the SM is closely linked to atmospheric processes. However, many aspects of the interactions between soil-atmosphere systems are still uncertain. Although atmospheric teleconnections are well defined in Europe, the relationship of the different atmospheric circulation patterns with SM has not received

special attention. In addition, their causal relationships have rarely been analyzed. In this context, the third and final objective of this doctoral thesis was to analyze the influence and causal relationships between the North Atlantic Oscillation (NAO), the Arctic Oscillation (AO) and the El Niño Southern Oscillation (ENSO) with SM variability in Europe. For this, two SM databases were considered and the correlation and causal relationships between atmospheric patterns and SM were evaluated on a monthly time scale.

The results obtained in this thesis have allowed, on the one hand, to evaluate different approaches for filling data gaps in satellite series accurately. SVMs applied to the spatial domain, using soil texture and previous SM series as inputs, have proven to be a good tool to deal with the limitation of data gaps present in satellite series. On the other hand, using data from modeling, it has been possible to observe a general trend towards drier conditions in the soil in almost the entire European continent in the last 30 years, regardless of the type of climate, the time scale analyzed, or the method applied. An increase in the intensity and duration of agricultural drought has also been found. Finally, the results of this thesis have shown that there is a predominantly negative causal relationship between the NAO and AO, and the SM variability in most of Europe, with hardly any time delay, while wit ENSO a delayed response of one or two months was observed with in central and northwestern Europe. The results obtained in this thesis provide new insights into the changes that SM has experienced in Europe and its interaction with atmospheric patterns, highlighting the importance of applying advanced methodologies to carry out these types of analyses, as well as obtaining appropriate data for them.

ÍNDICE

LISTA DE FIGURAS

LISTA DE TABLAS

LISTA DE ACRÓNIMOS

AMSR	Advanced Microwave Scanning Radiometer
AMSR-E	Advanced Microwave Scanning Radiometer - Earth Observation System
ANN	Artificial neural network
AO	Arctic Oscillation
AR	Autoregressive
C3S	Copernicus Climate Change Service
CCI	Climate Change Initiative
CI	Cubic interpolation
CIMR	Copernicus Imaging Microwave Radiometer
CRU	Climatic research unit
DEM	Digital elevation model
EA	East Atlantic
ECV	Essential climate variable
EDO	European Drought Observatory
EFAS	European Flood Awareness System
EMD	Empirical mode decomposition
ENSO	El Niño Southern Oscillation
ENVISAT	Environmental Satellite
EOF	empirical orthogonal function
ERA	ECMWF Re-Analysis
ERA5L	ERA5-Land
ERS	European Remote Sensing
ESA	European Space Agency
EUMETSAT	European Organisation for the Exploitation of Meteorological Satellites
FAO	Food and Agriculture Organization
FDR	Frequency domain reflectometry
FY-3B/MWRI	Fengyun-3B Microwave Radiation Imager
GCOS	Global Climate Observing System
GIS	Geographical information system
GLDAS	Global Land Data Assimilation System
GLM	General linear model
GOLD	*Global Offline Land-surface Dataset*
GP	Gaussian Processes
GRNN	General regression neural network
HBV	*Hydrologiska Byråns Vattenbalansavdelning*
HTESSEL	Hydrology Tiled ECMWF Scheme for Surface Exchanges over Land
IP	Iberian Peninsula
IPCC	Intergovernmental Panel on Climate Change
ISMN	International Soil Moisture Network
ISRO	Indian Space Research Organization

JERS	Japanese Earth Resources Satellite
JRC	Joint Research Centre
LI	Linear interpolation
LST	Land surface temperature
MCI	Momentary conditional independence
MERRA-Land	*Modern-Era Retrospective* Analysis for Research and Applications - Land
MetOp	Meteorological Operational satellite
MK	Mann-Kendall
ML	Machine learning
MODIS	Moderate Resolution Imaging Spectroradiometer
NAO	North Atlantic Oscillation
NASA	National Aeronautics and Space Administration
NASDA	National Space Development Agency of Japan
NDVI	Normalized difference vegetation index
NIR	Near Infrared
PCA	Principal component analysis
RF	Random forest
RFI	Radio frequency interference
SAR	Synthetic Aperture Radar
SCAND	Scandinavian Pattern
SCM	Structural causal models
SHE	*Système Hydrologique Européen*
SM	Soil moisture
SMADI	Soil moisture agricultural drought index
SMAP	Soil Moisture Active and Passive
SMDI	Soil moisture deficit index
SMI	Soil moisture index
SMMR	Scanning Multichannel Microwave Radiometer
SMOS	Soil Moisture Ocean Salinity
SOI	Southern Oscillation index
SSM/I	Special Sensor Microwave Imager
SST	sea surface temperature
SVM	Support vector machine
SWB	Soil Water Balance
SWDI	Soil water deficit index
SWIR	Shortwave-infrared
SZI	Standardized soil moisture anomaly index
TDR	Time domain reflectometry
TIR	Thermal infrared
WMO	World Meteorological Organization

LISTA DE SÍMBOLOS

$cRMSE$	Centered root mean square error
R	Pearson correlation coefficient
R_{max}	Maximum Pearson correlation coefficient
ε	Epsilon-insensitive loss
E_n	Energy of the n^{th} signal
Ep	Potential evaporation
θ	Soil moisture
θ_g	Gravimetric soil moisture
θ_v	Volumetric soil moisture
C_i	i^{th} intrinsic mode function
N	Number of data
Z	Mann-Kendall Z parameter
q_{10}	10^{th} percentile
T_n	Period of the n^{th} signal
P	Precipitation
p	P-value
R_n	Residual of the n^{th} signal
τ	Lag
$RMSE$	Root mean square error
r_o	Remain series before subtracting C_i
S	Mann-Kendall S parameter
t	Time
var	Variance

CAPíTVLO 1

INTRODUCCIÓN, OBJETIVOS Y MÉTODOS

1.1. Motivación

El agua es uno de los recursos naturales más importantes para los organismos vivos. Ésta se encuentra en continuo movimiento describiendo un ciclo, denominado ciclo hidrológico, que expresa el intercambio continuo de agua entre sus diferentes fuentes de almacenamiento. Aunque el agua cubre tres cuartas partes de la superficie terrestre solo el 2.5% es dulce (Igor Shiklomanov, 1993), siendo ésta clave en la sostenibilidad de la biosfera y la vida humana. El agua dulce se encuentra principalmente almacenada bajo la superficie terrestre o en forma de hielo en los glaciares, mientras que únicamente el 1.3% está almacenada en la superficie, presente en los diferentes estados. Esta agua superficial se encuentra mayoritariamente en forma de hielo y nieve, mientras que, el agua en estado gaseoso es la menos abundante y está almacenada en la atmósfera. El resto permanece en estado líquido, presente en ríos, lagos, pantanos, almacenada en el suelo o en los seres vivos (Figura 1.1).

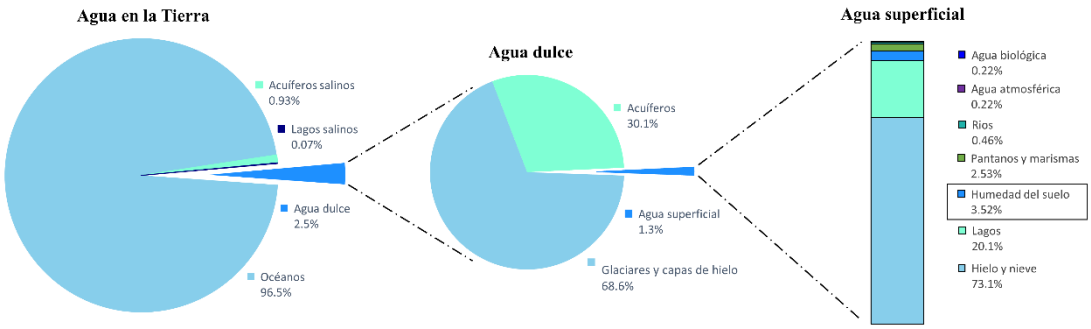

Figura 1.1 Distribución del agua en la Tierra. Información obtenida de Igor Shiklomanov (1993).

Aunque representa un pequeño porcentaje del agua del planeta, el agua almacenada en el suelo, conocida como humedad del suelo (SM, *soil moisture*), constituye uno de los componentes más relevantes dentro del ciclo hidrológico, ya que ejerce control sobre el intercambio de agua y energía entre el suelo y la atmósfera, gobierna la infiltración, la escorrentía y la evapotranspiración, y se comporta como un mecanismo de almacenamiento de la precipitación (McColl et al., 2017; Seneviratne et al., 2010). Como consecuencia, ejerce una gran influencia en el desarrollo de eventos extremos como sequías e inundaciones (Martínez-Fernández et al., 2015; Piles et al., 2022; Wanders et al., 2014). Además, expresa la cantidad de agua disponible para las plantas y está implicada en el desarrollo de múltiples procesos biológicos, siendo una variable clave en la gestión de los recursos hídricos, la productividad agrícola o el seguimiento de la salud de los ecosistemas (Entekhabi et al., 2014). Por todo ello, en el año 2010, el *Global Climate Observing System* (GCOS) incorporó la variable SM dentro de las variables climáticas esenciales (ECV, *essential climate variable*), reconociendo la importancia y la necesidad de obtener series de datos adecuadas de esta variable (GCOS, 2010).

El interés por monitorizar la SM es un asunto reciente con respecto al de otras variables hidro-climáticas, pues hasta cerca de comienzos del S.XXI no se disponía de la tecnología

para su medición, sobre todo de forma remota. Además, la dinámica de la SM es compleja y su variabilidad espacial y temporal depende de diversos factores geográficos, ambientales, meteorológicos y climáticos (Yoo and Kim, 2004). Por ello, diferentes técnicas de medición pueden proporcionar series de datos de características distintas en cuanto a la cobertura y resolución, tanto espacial como temporal, la capa del suelo que consideran para su estimación, o las incertidumbres asociadas. En las últimas décadas se han desarrollado diferentes técnicas capaces de proporcionar estimaciones de SM con sensores remotos. En concreto, avances tanto científicos como tecnológicos en el uso de las microondas para la estimación de esta variable permitió el desarrollo y lanzamiento de las dos primeras misiones espaciales dedicadas a medir la SM: la misión *Soil Moisture Ocean Salinity* (SMOS) de la Agencia Espacial Europea (ESA, *European Space Agency*) (Kerr et al., 2012, 2010, 2001) y la misión *Soil Moisture Active and Passive* (SMAP) de la NASA (*National Aeronautics and Space Administration*) (Bindlish et al., 2015; Entekhabi et al., 2010a). Existen también otras misiones satelitales con bandas de microondas que, aunque no fueron lanzadas con el objetivo de estimar la SM, son sensibles a esta variable. La *Climate Change Initiative* (CCI) de la ESA ha podido combinar todas las estimaciones provenientes de los diferentes sensores capaces de estimar esta variable hasta generar una serie climática de SM con cobertura global y duración de más de 30 años (Dorigo et al., 2017; Gruber et al., 2019). El desarrollo de los sensores remotos en plataformas satelitales ha permitido evolucionar de las series de datos de medidas *in situ*, obtenidas mediante sensores en estaciones puntuales, a poder monitorizar esta variable de forma continua en el tiempo y el espacio (Piles et al., 2019; Wigneron et al., 2003), demostrando ser una herramienta fundamental. No obstante, algunos aspectos de la monitorización de esta variable pueden aún ser mejorados (Kerr et al., 2016). Es el caso de las lagunas de datos, provocadas por diversos factores como son la contaminación por interferencia de radiofrecuencia (RFI, r*adio frequency interference*), o la dificultad de recuperación de los datos en alta topografía, en regiones con vegetación muy densa y bajo determinadas condiciones climáticas (Cui et al., 2019). Esta limitación condiciona el uso de las series de datos satelitales de SM en un gran número de aplicaciones. Por ello, el estudio de diferentes técnicas capaces de hacer frente a dicha restricción es un tema relevante y de creciente interés en la comunidad científica.

Por otra parte, además de los datos observacionales, los datos provenientes de modelos también poseen un enorme potencial para monitorizar y estudiar esta variable, sus variaciones y conexiones en los diferentes procesos de intercambio de agua y energía suelo-atmósfera. Series de datos de SM han sido desarrolladas por la comunidad científica a través de diferentes modelos de distintas características (Brocca et al., 2014). Esta aproximación posee la ventaja de poder proporcionar series continuas en el espacio y en el tiempo, para largos periodos y sin lagunas de datos. Además, los recientes avances tecnológicos han permitido disponer de una mayor capacidad de computación y almacenamiento, permitiendo obtener series de SM a resoluciones espaciales más finas, de hasta 5 km x 5 km, como en el caso del modelo LISFLOOD (de Roo et al., 2000; van der Knijff et al., 2010). Las estimaciones de los modelos están condicionadas por la precisión de cada uno, ya que diferentes enfoques en el modelado conducen a distintas

representaciones de esta variable (Brocca et al., 2017). Para hacer frente a esto, las series de datos de reanálisis permiten realizar una corrección continua de las predicciones del modelo utilizando observaciones complementarias (Medina-González et al., 2015). Este método aprovecha el potencial de utilizar en conjunto las series satelitales y las de modelización, para beneficiarse de las ventajas de ambos (Parajka et al., 2006), como es el caso de ERA5-Land (ERA5L) (Muñoz-Sabater et al., 2021). Sin embargo, también existen fuentes de incertidumbre relacionadas principalmente con la incorporación de las series satelitales a los modelos (Muñoz-Sabater et al., 2021). De este modo, aunque actualmente existen diversas bases de datos de SM con diferentes características válidas para una multitud de aplicaciones (Beck et al., 2020; Peng et al., 2021), aún existen aspectos que pueden ser mejorados. Por ello es fundamental, por un lado, estudiar y hacer frente a las limitaciones de los productos existentes y, por otro lado, hacer uso de los diferentes recursos de datos de manera complementaria para poder aprovechar las diferentes ventajas y evaluar las posibles limitaciones de cada uno.

Una de las aplicaciones fundamentales de estos datos es el estudio de los cambios que ha experimentado la SM. Como consecuencia del cambio climático, se prevé una gran alteración de muchos procesos ambientales y económicos (Grillakis, 2019). No obstante, su impacto en los recursos hídricos del planeta todavía es incierto en muchos casos, por lo que conocer y definir la tendencia de cambio de las diferentes variables hidro-climáticas es un asunto urgente. En particular, definir los cambios en la dinámica de la SM es una tarea fundamental debido al papel que juega esta variable en el ciclo hidrológico (Seneviratne et al., 2010). En comparación con otras variables, no son muchos los estudios que han analizado la tendencia de la SM a escala climática, principalmente debido a la escasa disponibilidad hasta hace poco y, en algunos casos, todavía, de bases de datos adecuadas. Estos estudios, en general, o bien tienen un alcance global (Dorigo et al., 2012), o bien se han centrado en áreas de especial interés como el Sahel, Australia, India o América del Norte (Sheffield and Wood, 2007), en donde, sin duda, los problemas son acuciantes. Es notable que, a pesar del aumento previsto del riesgo de sequía en el continente europeo (Spinoni et al., 2018), y el notable aumento en las olas de calor, recientemente identificada como un punto caliente (*heatwave hotspot*) (Rousi et al., 2022), esta región no ha recibido la misma atención. Además, el uso extendido de métodos que asumen un comportamiento lineal en las variables, el estudio de diferentes periodos y el uso de diferentes bases de datos puede llevar en muchos casos a una difícil reconciliación de los resultados. En particular, en Europa se han observado pocas tendencias en la SM cuando se ha asumido un comportamiento lineal (Albergel et al., 2013; Dorigo et al., 2012; Zawadzki and Kędzior, 2014). Sin embargo, debido al incremento de las temperaturas (Luterbacher et al., 2004) y los diferentes patrones de cambio observados en la precipitación del continente (Caloiero et al., 2018), cabe pensar que la dinámica de la SM también se está viendo afectada, y por lo tanto es un asunto de enorme interés definir y cuantificar la tendencia de estos cambios.

Si bien los diferentes factores que gobiernan los cambios en la dinámica de la SM se han estudiado desde diferentes perspectivas (Daly and Porporato, 2005), algunos aspectos sobre las interacciones suelo-atmósfera aún son inciertos (Boé, 2013). Es el caso de la relación entre los patrones de circulación atmosférica y la SM; aunque es bien sabido que éstos

influyen en gran medida en las condiciones climáticas en todo el mundo (Hurrell and van Loon, 1997), su relación con la SM no ha sido todavía estudiada en profundidad. En concreto, en Europa diversos estudios han definido la relación entre los patrones de circulación atmosférica y las condiciones generales de temperatura y precipitación, es decir, basados en teleconexiones atmosféricas (Brönnimann, 2007; Trigo et al., 2002). Además, en muchos casos se ha asumido que estas relaciones explican los cambios en las diferentes variables estudiadas, pero rara vez se han analizado sus relaciones causales (Runge et al., 2019a). Esto revela la necesidad de estudiar las posibles relaciones causa-efecto entre los cambios en la dinámica de la SM y los patrones de circulación atmosférica.

En resumen, habiendo puesto de manifiesto la importancia de la SM para muchas aplicaciones y conociendo los factores, todavía presentes, que limitan la comprensión de su dinámica y sus variaciones como consecuencia del cambio climático, la aportación de nuevos enfoques y conocimiento sobre ello es fundamental para una buena gestión de los recursos hídricos. Motivada por las diferentes lagunas en los temas expuestos, esta tesis presenta la aplicación de diferentes métodos para abordar las lagunas de las series de datos satelitales, la identificación de tendencias de la SM y la relación que esta variable tiene con los patrones de circulación atmosférica. De esta manera, se pretende contribuir al mejor conocimiento de una variable esencial en una región de especial interés como es el continente europeo.

1.2. Objetivos

Bajo el escenario de cambio climático, y su todavía incierto impacto en los recursos hídricos del continente europeo, se plantea como objetivo general de esta tesis aportar nuevas herramientas, enfoques de análisis y conocimiento sobre una de las variables claves del ciclo hidrológico: la SM. Para ello, se han planteado tres objetivos específicos basados tanto en el estudio de los cambios de esta variable y su interacción con los patrones atmosféricos como en la obtención de bases de datos adecuadas para poder abordar este tipo de estudios. Estos objetivos específicos son:

1. Evaluar diferentes técnicas de relleno de lagunas de datos en la base de datos de SM satelital más larga disponible, la base de datos de la ESA CCI, en Europa.
2. Estudiar la tendencia de la SM en Europa durante las últimas tres décadas (1991 a 2020) comparando diferentes métodos, resoluciones temporales y bases de datos.
3. Evaluar la respuesta de la SM a los principales patrones de circulación atmosférica en Europa para el período 1991-2020. Los patrones considerados son la *North Atlantic Oscillation* (NAO), la *Arctic Oscillation* (AO) y *El Niño Southern Oscillation* (ENSO).

1.3. Humedad del suelo

El suelo se define como la capa externa de la superficie terrestre formada por la desintegración, descomposición y recomposición del material mineral y diferentes residuos orgánicos (Hillel, 2003). Las partículas minerales poseen diferentes tamaños que definen la textura del suelo y lo convierten en un sistema poroso capaz de almacenar gases y agua (Wang, 2018). El agua contenida en el suelo se puede clasificar como agua ligada, aludiendo a las moléculas estrechamente unidas a las partículas del suelo, y el agua libre, en referencia a las moléculas que pueden moverse libremente dentro del suelo (Wang, 2018). Esta se distribuye a través de la sección vertical, o perfil, y define dos capas en función de su contenido, la zona saturada, aquella en la que los poros están completamente rellenos de agua, y la zona no saturada o zona vadosa, aquella entre la superficie y el límite superior de la zona saturada, denominado nivel freático (Figura 1.2). La SM, por tanto, se define como la cantidad de agua, libre o ligada, que está contenida en la zona no saturada del suelo (Seneviratne et al., 2010).

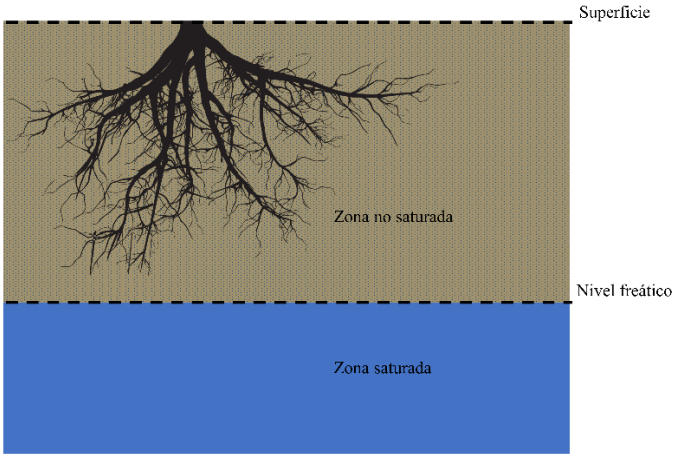

Figura 1.2 Capas del perfil del suelo definidas en función de la distribución del agua.

La SM, generalmente representada como θ, se puede cuantificar de forma gravimétrica (θ_g), es decir, como la masa de agua relativa a la masa del suelo (Ec. 1.1) expresada comúnmente en tanto por ciento (%), o de forma volumétrica (θ_v), como el volumen de agua relativo al volumen de suelo (Ec. 1.2) (Hillel, 2003). La forma volumétrica suele ser la más común y, generalmente, se expresa en $m^3 \cdot m^{-3}$.

$$\theta_g = \frac{m_{H_2O}}{m_{Suelo}} \tag{1.1}$$

$$\theta_v = \frac{V_{H_2O}}{V_{Suelo}} \tag{1.2}$$

La distribución espacial del agua en el suelo, tanto horizontal como vertical, es muy variable debido a la heterogénea distribución de los factores físicos que determinan la capacidad de un suelo para retener agua, como la textura, la topografía o la cobertura vegetal (Hillel, 1998). Esto implica que la SM estimada para diferentes volúmenes puede ser diferente (Hillel, 1998). Además, es muy variable en el tiempo debido a la falta de uniformidad de las precipitaciones, que constituyen la principal fuente natural de incorporación de agua al suelo, y la evapotranspiración, referida a la perdida de agua en el suelo por evaporación y por transpiración de las plantas (Engman, 1990).

Se diferencian, generalmente, dos capas dependiendo de la profundidad del suelo a la que se estime esta variable. La superficial, normalmente se refiere a los primeros 5 cm del suelo (Bao et al., 2018), especialmente en el caso de la SM satelital, aunque ésta puede llegar a representar hasta los primeros 15-25 cm (Feldman et al., 2022). Y la zona radicular, que se refiere a la capa del suelo donde se encuentran las raíces de las plantas. Aunque la profundidad de la zona radicular es variable ya que depende del tipo de vegetación y de la longitud de las raíces, es común asumir 100 cm para estimar la SM en dicha capa (Martínez-Fernández et al., 2019; Reichle et al., 2017). La SM, tanto superficial como radicular, se puede estimar mediante diferentes técnicas que se comentaran más adelante en este capítulo.

1.3.1. Humedad del suelo: una *essential climate variable* (ECV)

Aunque la SM representa una proporción muy pequeña del agua dentro del ciclo hidrológico, es una variable clave en diversos procesos biológicos, biogeoquímicos, hidrológicos y climáticos (Civeira, 2019). Es una variable fundamental para diversas aplicaciones tales como el pronóstico de la variabilidad meteorológica y climática, la monitorización de áreas de inundación o sequía, la gestión de diferentes recursos hídricos, la productividad agrícola o el seguimiento de la salud de los ecosistemas (Entekhabi et al., 2014).

Por un lado, juega un papel crucial en el acoplamiento de los sistemas suelo-atmósfera controlando el intercambio de agua y energía entre los dos sistemas. La SM ejerce un impacto significativo en la tasa de evapotranspiración, las condiciones térmicas del suelo y el albedo de la superficie (Cheng et al., 2017), y contribuye al reciclaje de la precipitación o la formación de nubes (Dominguez et al., 2006; Sehgal et al., 2021) así como a la persistencia del clima en la tierra (Entekhabi et al., 1996). Además, influye en el desarrollo y la duración de eventos extremos como sequías, inundaciones y olas de calor (Piles et al., 2022). Como consecuencia, el conocimiento del contenido de agua del suelo mejora la predicción de las variables climáticas en los modelos, pudiendo ayudar a cuantificar el impacto del cambio climático y el calentamiento global en la aparición de estos fenómenos (Hollmann et al., 2013).

Por otro lado, esta variable controla la distribución del agua procedente de la lluvia, funcionando como un componente de almacenamiento del agua en el suelo. Ejerce un gran impacto en la generación de escorrentía (Botter et al., 2007) y por tanto en la variabilidad

del caudal de los ríos, la circulación de agua a otras áreas y a la degradación de la capa superior del suelo por erosión (Kerr, 2007). Además, gobierna la infiltración y la recarga de los acuíferos (Wagner et al., 2007). Esto convierte a la SM en un factor clave para comprender muchos procesos hidrológicos y para numerosas aplicaciones de gestión de los recursos hídricos, como la mejora de predicciones de modelos hidrológicos y la estimación de escorrentía (Brocca et al., 2012; Fidal and Kjeldsen, 2020).

Además, la medición o estimación de la SM permite conocer el volumen de agua disponible para las plantas. Por este motivo, es una variable que juega un papel fundamental en aplicaciones vinculadas al desarrollo y crecimiento de la vegetación (González-Zamora et al., 2021; Martínez-Fernández et al., 2019). Como tal, esta variable ejerce una gran influencia en la producción agrícola (Gaona et al., 2022; González-Zamora et al., 2022) y es de gran utilidad en sistemas de gestión del riego (Brocca et al., 2018).

Como consecuencia, es una variable clave en la organización de los ecosistemas naturales y la biodiversidad (Medina-González et al., 2015). De forma directa o indirecta, juega un papel muy importante en la salud de los ecosistemas ya que influye en la respiración microbiana del suelo (Manzoni et al., 2012), siendo una variable muy ligada al ciclo del carbono (Scholze et al., 2016). Además, controla el flujo de productos químicos hacia los acuíferos (Martínez-Fernández and Ceballos, 2003) y advierte del peligro de incendios forestales (Bartsch et al., 2009).

Todas estas aplicaciones son de una enorme relevancia para el medio ambiente, la sociedad, la salud o la economía. Por este motivo, y desde muchos puntos de vista, disponer de datos de SM con la precisión y resolución espacial y temporal adecuadas es imperativo (Entekhabi et al., 2014). Como resultado, en el año 2010 el GCOS incluyó la SM entre las ECVs (GCOS, 2010), estableciendo una serie de requisitos para la monitorización de esta variable mediante sensores remotos, que se explicarán más adelante. Esto propició el lanzamiento de las dos primeras misiones espaciales dedicadas a la medición de esta variable.

1.3.2. Dinámica de la humedad del suelo

La variable SM posee una enorme variabilidad espacial y temporal dominada por diversos factores como la topografía, las características del suelo, la cobertura vegetal, la precipitación, la evapotranspiración o la escorrentía superficial y subterránea (Yoo and Kim, 2004). Por consiguiente, la dinámica del balance hídrico del suelo resulta extremadamente compleja (Daly and Porporato, 2005). Sin embargo, conocer esta dinámica y sus cambios a diferentes escalas espaciales y temporales es fundamental para una multitud de aplicaciones (de Jeu et al., 2008).

La SM es una variable de estado, es decir, expresa el contenido de humedad en un lugar del espacio en un momento determinado. El agua en el suelo se mueve de los puntos más húmedos a los más secos, generando diferentes flujos de agua cuyos gradientes están, en general, controlados por la energía potencial (Daly and Porporato, 2005). El balance total

de todos estos flujos, tanto de aporte como de pérdida de agua al suelo, constituye su balance hídrico, y permite conocer la dinámica de la SM.

Considerando un sistema con vegetación, el balance hídrico del suelo puede representarse de forma simple mediante el esquema de la Figura 1.3. La precipitación constituye la mayor aportación natural de agua al suelo (Martin et al., 2015). El agua que precipita será infiltrada, almacenada o desplazada por la superficie en forma de escorrentía. Esto vendrá determinado, por un lado, por diversos factores como la intensidad de la lluvia, el contenido de humedad previo en el suelo, las características geográficas y físicas del suelo, y la cantidad y tipo de vegetación. Por otro lado, las pérdidas, dominadas por la absorción de las raíces y la evapotranspiración (Daly and Porporato, 2005), también determinarán esta dinámica. Por tanto, mediante el cómputo del balance de todos estos flujos se puede determinar y estudiar la dinámica de la SM.

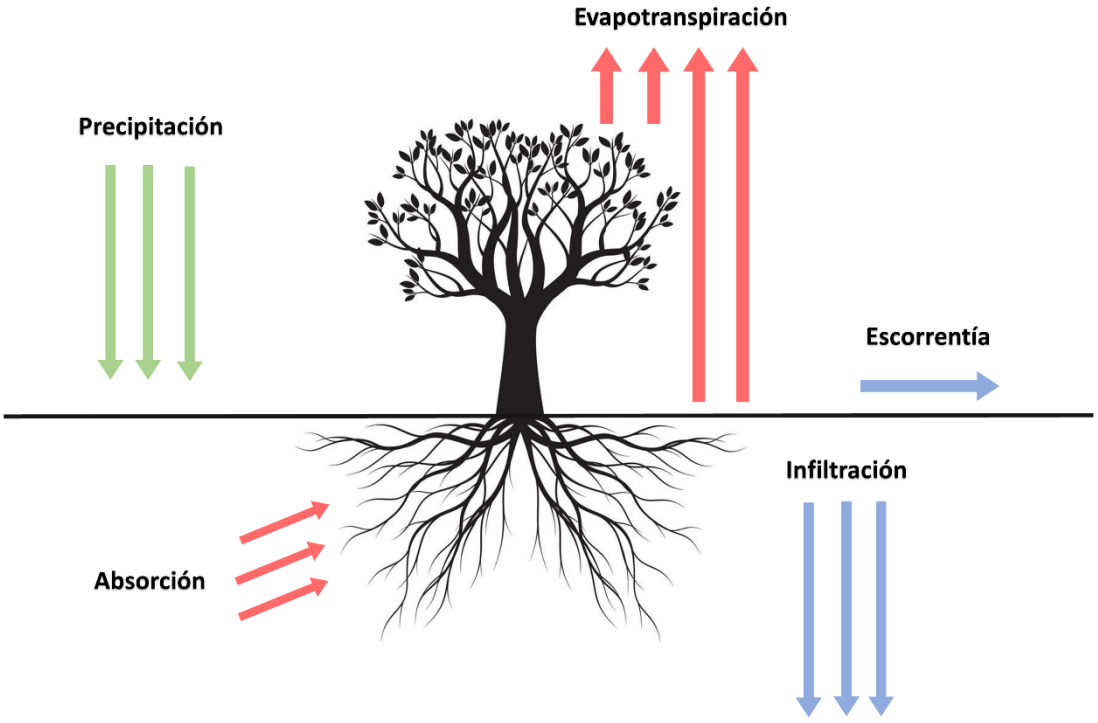

Figura 1.3 Esquema del balance hídrico del suelo en un sistema con vegetación.

Sin embargo, la dinámica real del agua es mucho más compleja, y los flujos de agua en el suelo son muy irregulares en el tiempo (Engman, 1990). Por consiguiente, obtener una representación coherente de todos los procesos involucrados en el balance hídrico y a todas las escalas espaciales y temporales es una tarea difícil de abordar (Daly and Porporato, 2005). Además, las interacciones con los diferentes factores que dominan la variabilidad de la SM pueden seguir un comportamiento no lineal (Entin et al., 2000). Por ello, obtener una representación lo más precisa posible es una tarea fundamental (McColl et al., 2017).

Uno de los atributos que describe la dinámica de la SM es la memoria, definida como el tiempo que tarda el suelo en disipar una anomalía, positiva o negativa, de su

almacenamiento de agua (McColl et al., 2017). La magnitud de este atributo es considerable, ya que, una anomalía en la SM puede tardar en disiparse desde días hasta meses. Esto influye en la generación de anomalías atmosféricas como tormentas, sequias o inundaciones (Orth and Seneviratne, 2012). Además, este atributo está estrechamente relacionado con las características del suelo, como la textura y el contenido de materia orgánica (Martínez-Fernández et al., 2021).

Debido a la alta variabilidad de la SM, el análisis de las diferentes escalas espaciales y temporales es fundamental para explicar la variación de esta variable. La variación espacial de la SM está controlada por factores de pequeña escala, generalmente de la superficie terrestre como el tipo de suelo, la topografía y la vegetación, y por componentes de gran escala, generalmente meteorológicos como la precipitación y la evapotranspiración (Entin et al., 2000). Sin embargo, la variabilidad temporal es, en muchos casos, mayor que la espacial (Brocca et al., 2010). Es sabido que las series temporales de las diferentes variables hidro-climáticas poseen diferentes componentes, generados por distintos mecanismos físicos y a diferentes escalas temporales; estos componentes son el ruido, la periodicidad y la tendencia (Yevjevieh, 1987). La identificación de cada componente y los mecanismos que influyen en sus cambios es fundamental para entender su dinámica. En especial, la identificación de tendencias en series hidrológicas es un problema de gran interés (Sang et al., 2013), debido a la incertidumbre del impacto del cambio climático sobre el ciclo hidrológico (Almendra-Martín et al., 2022). Motivado por esta cuestión, el Capítulo 3 de esta tesis presenta un estudio pionero en la identificación de tendencias de la SM en Europa en las últimas 3 décadas.

1.3.3. Cambio climático y humedad del suelo

El clima se define por el *Intergovernmental Panel on Climate Change* (IPCC) como el tiempo meteorológico promedio durante un período determinado, siendo 30 años el intervalo común establecido por la *World Meteorological Organization* (WMO). En este contexto, se define el cambio climático como un cambio en el estado del clima y que persiste durante un período prolongado (IPCC, 2007). Actualmente, se está experimentando un pronunciado cambio climático provocado por el calentamiento global de la Tierra (Thuiller, 2007). Los cambios observados en la composición y dinámica de la atmósfera son lo suficientemente abruptos como para superar los límites de la variabilidad natural, lo que indica que la acción del ser humano está constituyendo la fuente principal de cambio (Karl and Trenberth, 2003). Sin embargo, las tasas de cambio y el impacto del calentamiento global a largo plazo en los diferentes sistemas terrestres y, por tanto, en la sociedad y en la economía son todavía inciertos.

La circulación global de la atmósfera es responsable de la distribución de los diferentes climas en el mundo. Es por esto, que el estudio del cambio climático se basa, en gran medida, en el estudio de los cambios atmosféricos. Al mismo tiempo, el clima ejerce una influencia fundamental en la mayoría de los procesos naturales, por ello, es esencial conocer las conexiones entre la atmósfera y el resto de los sistemas terrestres. En particular,

el aumento constante de la temperatura global acelera los procesos hidrológicos, ya que aumenta la capacidad de retención de agua de la atmósfera, la evapotranspiración y la fusión de nieve y hielo, alterando, por tanto, los patrones de precipitación (Trenberth, 2011). Se estima que la temperatura media global puede llegar a aumentar hasta 4 °C para finales de siglo (Thuiller, 2007). Como consecuencia, se prevé una intensificación de los fenómenos climáticos extremos, como las sequías o inundaciones (IPCC, 2022).

Si bien se han realizado numerosos esfuerzos para estudiar los impactos del cambio climático en el ciclo del agua (Jiménez Cisneros et al., 2014), la SM no ha recibido especial atención, en gran medida por la escasa disponibilidad de bases de datos adecuadas. El patrón global de cambio en la SM estudiado hasta ahora es incierto y las predicciones sobre la magnitud de sus cambios abarcan un amplio rango de posibilidades (Wang, 2005). Se sabe que los cambios en la SM son inducidos por forzamientos regionales, como cambios en el uso de suelo, y globales, como cambios en la circulación atmosférica (Seneviratne et al., 2010). Sin embargo, en lo que se refiere a la influencia que ejercen los patrones de circulación atmosférica en la SM, se ha prestado poca atención (Trnka et al., 2009b). Motivado por esta cuestión, en el Capítulo 4 de esta tesis se presenta un estudio novedoso en esta materia a escala europea. Comprender estas relaciones es de especial interés en esta región ya que las predicciones futuras a largo plazo más representativas anuncian una fuerte disminución del contenido de humedad en el suelo en verano (Seneviratne et al., 2010) y una intensificación de extremos hidrológicos como las sequías (Grillakis, 2019).

1.3.4. Sequía agrícola

La sequía se define como un periodo prolongado de escasez de recursos hídricos capaz de provocar efectos adversos sobre el medio natural, la sociedad y los sistemas productivos (Berg and Sheffield, 2018), y constituye uno de los riesgos naturales con mayores consecuencias sobre los ecosistemas (Archaux and Wolters, 2006) y las actividades humanas (Wilhite, 2000). Se diferencian varios tipos de sequía dependiendo del proceso hidrológico que las origina y el ámbito natural al que afecta. En primer lugar, la sequía meteorológica, que se refiere a la sequía generada por la reducción de la precipitación durante un periodo prolongado (Hayes et al., 2011). Si esta reducción de la precipitación persiste, diferentes recursos hídricos, superficiales o subterráneos, llegan a verse afectados. En este supuesto, si, por un lado, el caudal de los arroyos y ríos, o el nivel de los lagos, pantanos y aguas subterráneas se reducen de forma anómala por un periodo de tiempo, estaríamos hablando de sequía hidrológica (Van Loon, 2015). Por otro lado, si es la SM la que se ve reducida llegando a afectar negativamente al rendimiento de los cultivos, estaríamos hablando de sequía agrícola (Martínez-Fernández et al., 2015; Sánchez et al., 2018).

La sequía agrícola suele tener un mayor impacto económico y social, ya que afecta directamente a la producción agrícola, pudiendo contribuir a la escasez regional de alimentos (Sheffield et al., 2014). Por este motivo, monitorizar el alcance de su impacto es clave para reducir sus posibles repercusiones. Sin embargo, este impacto no es inmediato

ni fácilmente cuantificable (Kumar and Panu, 1997). Los índices de sequía constituyen la forma más común para caracterizar estos eventos. En la actualidad existen una multitud de ellos basados en diferentes variables y que caracterizan los diferentes tipos de sequía (Liu et al., 2016).

En el caso de la sequía agrícola, atendiendo a su definición se advierte la conveniencia del uso de la SM para caracterizar este fenómeno (Martínez-Fernández et al., 2015; Salvia et al., 2021; Sánchez et al., 2016). Sin embargo, en el pasado, generalmente se han empleado índices basados en datos atmosféricos, como la lluvia o la temperatura (Quiring and Papakryiakou, 2003). Esto se ha debido, en gran medida, a la escasez de bases de datos de SM adecuadas. Actualmente, las bases de datos existentes han permitido el desarrollo de nuevos métodos que permiten monitorizar y evaluar la sequía agrícola a través de la SM (Tabla 1.1). La mayoría de ellos están basados en un reescalado de la SM en relación con propiedades específicas del suelo (Mladenova et al., 2020). Uno de los índices de uso más frecuente, es la anomalía de la SM, ya que es un índice simple de obtener y adecuado para monitorizar la sequía agrícola. Por este motivo, es el método estándar utilizado por el *European drought observatory* (EDO) (Toreti et al., 2022).

Tabla 1.1 Ejemplos de índices de sequía agrícola basados en la SM.

Índice de sequía	**Abreviación**	**Referencia**
Soil moisture index	SMI	(Hunt et al., 2009; Sridhar et al., 2008)
Soil water deficit index	SWDI	(Martínez-Fernández et al., 2015)
Standardized soil moisture anomaly index	SZI	(Zhang et al., 2015)
Soil moisture agricultural drought index	SMADI	(Sánchez et al., 2018)
Soil moisture deficit index	SMDI	(Narasimhan and Srinivasan, 2005)

1.4. Técnicas y métodos para la monitorización de la humedad del suelo

La importancia de monitorizar la SM es un asunto al que se le ha puesto especial atención durante las últimas décadas (Wigneron et al., 1998). Disponer de series de datos precisas de esta variable es fundamental para una multitud de aplicaciones como el estudio de su dinámica, su interacción con los ecosistemas, la atmósfera y las diferentes variables hidro-climáticas, la gestión del agua en agricultura o el estudio de sus cambios a largo plazo. Existen varios métodos o técnicas que permiten medir o estimar, directa o indirectamente, el contenido de agua del suelo (Dorigo et al., 2011; Robinson et al., 2008; Susha Lekshmi et al., 2014). Por la naturaleza de estos métodos, las series obtenidas abarcan una gran diversidad de coberturas temporales y espaciales, características intrínsecas y errores asociados (Beck et al., 2020; Brocca et al., 2017). A lo largo de esta sección se describen los métodos más relevantes utilizados para monitorizar esta variable y las posibles limitaciones y ventajas asociadas a cada uno.

1.4.1. Redes de estaciones *in situ*

Las observaciones *in situ* se refieren a aquellas tomadas de forma directa en el lugar o sitio en que se encuentra la magnitud a medir. En el caso de la SM, las que se realizan en el mismo suelo. Durante los últimos casi 90 años, se han desarrollado varias técnicas e instrumentos que permiten obtener series de datos *in situ* de esta variable (Walker et al., 2004b).

El único método directo para medir la SM es el denominado gravimétrico, que consiste en estimar la pérdida de peso de una muestra de suelo de masa conocida después de secarla (Reynolds, 1970). Se trata de un método muy preciso, sin embargo, es destructivo y requiere mucho tiempo, por lo que no permite obtener un muestreo repetitivo de un lugar (Muñoz-Carpena et al., 2004; Walker et al., 2004b). Como se trata del único enfoque directo, las medidas gravimétricas constituyen los valores de referencia para calibrar las estimaciones de SM obtenidas con otros métodos de medida.

Los métodos indirectos son métodos no invasivos que se basan en medidas de propiedades físicas del suelo más fáciles de obtener y que están relacionadas con el contenido de agua (González-Zamora, 2017). Una de las técnicas indirectas más utilizadas en el pasado para obtener datos *in situ* de SM han sido las sondas de neutrones, cuyas medidas se basan en la interacción de los neutrones de una fuente radiactiva con los átomos de hidrógeno del agua del suelo (Susha Lekshmi et al., 2014). Otro ejemplo son los sensores electromagnéticos, basados en medidas de la permitividad dieléctrica del suelo. Estos métodos destacan sobre el resto ya que permiten obtener medidas de la humedad de suelo continuas, en tiempo real y para una gran diversidad de sustratos a diferentes profundidades (Iturria et al., 2019). Se diferencian dos técnicas, una basada en la reflectometría de dominio de tiempo (TDR, t*ime domain reflectometry*) y otra basada en la capacitancia o la reflectometría de dominio de

frecuencia (FDR, *frequency domain reflectometry*) (Vaz et al., 2013). En general, los sensores TDR son más precisos que los sensores FDR, sin embargo, estos últimos son más asequibles en cuanto a su coste (Seneviratne et al., 2010). Este tipo de sensores se pueden instalar a lo largo del perfil del suelo, pudiendo obtener medidas de humedad a diferentes profundidades. El uso de estos sensores y de otros muchos (Muñoz-Carpena et al., 2004; Robinson et al., 2008), ha ido creciendo a lo largo de los años tanto en tareas y experimentos de campo específicos como para el monitoreo permanente o temporal de la SM en regiones específicas. Para este último caso, es relevante destacar el papel que juegan las redes de estaciones de SM.

Existen numerosas redes de estaciones *in situ* distribuidas por todo el mundo que monitorizan la SM. Las características de estas redes son muy diversas en función de la localización geográfica, los sensores utilizados o su extensión espacial (Robock et al., 2000). Además, la cobertura temporal de datos de cada red es muy variable ya que están gestionadas por un gran número de organizaciones diferentes (Dorigo et al., 2011). Estas redes son de gran utilidad para diferentes aplicaciones, por ese motivo, en el año 2000 se creó el *Global Soil Moisture Data Bank* (Robock et al., 2000), que reunía los datos de hasta 600 estaciones instaladas por todo el mundo. Actualmente la *International Soil Moisture Network* (ISMN), y desde hace ya una década, es quien realiza la tarea de preservar una base de datos de SM *in situ* mundial, agrupando la mayoría de las series obtenidas por las distintas redes existentes (Dorigo et al., 2021, 2011). Aunque existen redes de estaciones de SM repartidas por todo el mundo, la mayoría se encuentran ubicadas en regiones de latitudes medias. En concreto, en Europa se localizan 28 redes diferentes (Dorigo et al., 2021) (Figura 1.4).

Figura 1.4 Localización de las redes de estaciones in situ de SM de la ISMN. Imagen obtenida de https://www.geo.tuwien.ac.at/insitu/data_viewer/.

La cobertura espacial de las series de datos de SM *in situ*, al tratarse de medidas puntuales, es limitada. Sin embargo, juegan un papel fundamental en la validación de observaciones remotas o modelos de SM a diversas escalas (Loew et al., 2017; Muñoz-Sabater et al., 2021; Sánchez et al., 2020). Además, estos dispositivos permiten obtener datos tanto de SM de la superficie como de la zona radicular.

1.4.2. Teledetección: observaciones con satélite

La teledetección constituye una técnica de medición indirecta que permite obtener, de forma remota, información basada en la radiación electromagnética emitida o reflejada por el objeto que se quiere medir (Schmugge et al., 2002). Analizando la interacción de la cubierta terrestre con la radiación electromagnética a lo largo de todo el espectro electromagnético se pueden monitorizar una gran diversidad de parámetros y variables de forma global y espacialmente continua (Chuvieco, 1990). Esta información se obtiene a través de sensores a bordo de diferentes dispositivos aéreos o espaciales y se recoge en forma de imágenes. La SM se puede estimar mediante técnicas de teledetección estudiando la respuesta espectral del suelo en diferentes rangos del espectro electromagnético, desde el visible hasta el rango de las microondas (Engman, 1990). Estas técnicas han supuesto un enorme avance para la monitorización de la SM, y, por tanto, para una gran diversidad de aplicaciones como la modelización climática o de procesos hidrológicos, el pronóstico de inundaciones, o la monitorización de sequías (Peng et al., 2021). Actualmente, se pueden obtener estimaciones remotas de la SM de forma global cada 3 días (Panciera et al., 2014).

1.4.2.1. Observaciones con sensores de microondas

La región de las microondas en el espectro electromagnético comprende las longitudes de onda desde 1 m hasta 1 mm (frecuencias entre 300 MHz y 300 GHz). Las estimaciones de la SM en este rango del espectro se basan en la medida de la constante dieléctrica a partir de la emisividad o retrodispersión de la superficie (de Jeu et al., 2008). Las microondas no se ven atenuadas por la atmósfera y tienen más capacidad de penetración en la vegetación que ondas de longitud de onda más corta (frecuencias más altas). Además, la medición es independiente de la iluminación solar, esto permite obtener estimaciones diurnas o nocturnas en cualquier situación climática y en una gran variedad de ecosistemas (Schmugge et al., 2002). Sin embargo, la profundidad del suelo accesible a las microondas disminuye con el aumento de la frecuencia y el contenido de SM, por lo que las estimaciones de SM en este rango del espectro electromagnético se obtienen únicamente para la capa más superficial del suelo, comúnmente establecida como los primeros 5 cm (Wigneron et al., 2003), aunque recientemente se está observando que puede llegar a representar la humedad de hasta 15-25 cm de profundidad (Feldman et al., 2022).

Las bandas de microondas más importantes para la estimación de la SM son las que se encuentran entre 1 y 20 GHz: la banda L (1-2 GHz), la banda C (4-8 GHz), la banda X (8-12 GHz), la banda K_u (12-18 GHz) y la banda K (18-27 GHz) (Jackson, 2005; Wagner et

al., 2007). Numerosos estudios han demostrado que la banda L es más adecuada para la estimación de la SM (Kerr, 2007), pero puesto que las primeras misiones espaciales en banda L dedicadas a la estimación de la SM se lanzaron en 2009 (SMOS) y 2014 (SMAP) es necesario utilizar observaciones de diferentes bandas para construir la serie climática (Dorigo et al., 2015; Li et al., 2021; Piles et al., 2019).

Se diferencian dos técnicas de teledetección de microondas, pasiva si se examina la radiación electromagnética emitida naturalmente por la superficie del suelo y activa si se examina la radiación dispersada por el suelo después de haber sido sometido a una fuente de radiación conocida (Jackson, 2005). El estudio de la aplicación de estas técnicas para estimar la SM se remonta a los años 70 (Eagleman and Lin, 1976; Schmugge et al., 1974).

1.4.2.1.1. Sensores pasivos

El radiómetro de microondas es el sensor pasivo que recoge la radiación electromagnética emitida es ese rango del espectro. Para estimar la SM, esta radiación se expresa en términos de la temperatura de brillo, que es proporcional al producto entre la temperatura superficial y la emisividad de la superficie (Engman, 1990).

Conocida la emisividad del suelo se puede obtener su reflectividad y por tanto la constante dieléctrica, que está directamente relacionada con el contenido de agua en el suelo (Dobson et al., 1985). Sin embargo, la emisividad también depende de otros factores como la textura del suelo, la rugosidad de la superficie y la vegetación, lo que hace que la relación entre la SM y la emisividad sea compleja y no lineal (Dobson et al., 1985; Jackson and O'Neill, 1987). En la literatura se han propuesto diferentes algoritmos de recuperación de la SM a partir de la radiometría de microondas (Chan et al., 2016; Chaubell et al., 2022; Fernandez-Moran et al., 2017; Jackson, 1993; Jackson et al., 1995; Jackson and O'Neill, 1987; Njoku and Entekhabi, 1996; Owe et al., 2008; Wigneron et al., 1998). Estas técnicas pueden proporcionar series espacialmente continuas de SM de alta precisión (Ahmad et al., 2011). Sin embargo, estos sensores poseen una limitación con respecto a la resolución espacial, ya que es proporcional al diámetro de la antena e inversamente proporcional a la longitud de onda (Kerr et al., 2016). Esto conlleva limitaciones tecnológicas que explican el hecho de que, aunque se conoce desde los años 1980 que la banda L (la de mayor longitud de onda) es la óptima para estimar la SM, hasta la pasada década no haya sido posible lanzar las primeras misiones espaciales dedicadas a la estimación global de esta variable.

La primera misión satelital enviada con el propósito de estimar la SM se lanzó el 2 de noviembre de 2009 y sigue operativa actualmente. Se trata de la misión SMOS de la ESA, que lleva a bordo el primer radiómetro de microondas en banda L lanzado al espacio (Kerr et al., 2012, 2010, 2001). Las misiones SAC-D/Aquarius y SMAP de la NASA, fueron las siguientes enviadas al espacio que incluían radiómetros en banda L, pero equipadas también con sensores activos para aprovechar el potencial de ambas técnicas (Bindlish et al., 2015; Entekhabi et al., 2010a). Aunque su propósito no fuera la estimación de la SM, existen desde el año 1978 diferentes radiómetros a bordo de misiones espaciales operando en las frecuencias C, X y K de microondas que han permitido estimar esta variable, por ejemplo,

la banda C en el *Scanning Multichannel Microwave Radiometer* (SMMR) (Gloersen and Barath, 1977), la banda X en el *Advanced Microwave Scanning Radiometer - Earth Observing System* (AMSR-E) (Kawanishi et al., 2003) o la banda K en el *Special Sensor Microwave Imager* (SSM/I) (Jackson, 1997). La futura misión *Copernicus Imaging Microwave Radiometer* (CIMR), con fecha prevista de lanzamiento en 2027, proporcionará de manera operacional observaciones pasivas en las bandas L, C, X, K y K_u de microondas que permitirán la obtención de mapas globales de SM con una revisita diaria y una resolución espacial entre 60, 15 y 5 km, dependiendo de la banda utilizada (Piles et al., 2021).

1.4.2.1.2. Sensores activos

La técnica de teledetección activa se basa en la medida de la retrodispersión o *backscatter* de la superficie a medir. La retrodispersión representa la cantidad de radiación enviada por el sensor activo que refleja la superficie, conocida la longitud de onda, el ángulo de incidencia y la polarización de la señal enviada (Ahmad et al., 2011). Al igual que con los sensores pasivos, la estimación de la SM se basa en la relación que existe entre la reflectividad del suelo y su contenido de humedad. La retrodispersión total medida por el sensor se compone de la retrodispersión de la vegetación y la del suelo, sujeta a la atenuación de la cubierta vegetal (Engman, 1990), pero también es sensible a atributos de la geometría de la superficie como la rugosidad del suelo o la distribución de la vegetación. Se han desarrollado muchos modelos teóricos y empíricos que permiten estimar la SM a partir el coeficiente de retrodispersión (Dobson and Ulaby, 1986; Dubois et al., 1995; Quesney, 2000; Wang and Qu, 2009).

El radar de apertura sintética (SAR, *Synthetic Aperture Radar*) es el sensor activo más común para estimar la SM debido a su fina resolución espacial, del orden de las decenas de metros (Wigneron et al., 1998). Sin embargo, poseen una menor frecuencia de revisita y mayor sensibilidad a la geometría de la superficie que los sensores pasivos. La mayoría de los sensores activos han trabajado en la banda C de microondas, como los de las misiones *European Remote Sensing* (ERS-1 y ERS-2), *Environmental Satellite* (ENVISAT) de la ESA (Altese et al., 1996; Paloscia et al., 2008; Walker et al., 2004a) y *Meteorological Operational satellite* (MetOp) de la *European Organisation for the Exploitation of Meteorological Satellites* (EUMETSAT) (Bartalis et al., 2007). Algunas misiones han incluido sensores activos de microondas en banda L como el Japanese Earth Resources Satellite (JERS-1) de la NASDA (*National Space Development Agency of Japan*) (Narayanan and Hegde, 1995) y, SMAP y Aquarius de la NASA en combinación con radiómetros de microondas (Bindlish et al., 2015; Entekhabi et al., 2010a). Además, la futura misión de la NASA e ISRO (*Indian Space Research Organization*) NISAR (NASA-ISRO SAR) con fecha de lanzamiento 2023, junto con la futura misión ROSE-L del programa de observación de la Tierra de la Unión Europea Copernicus con fecha de lanzamiento 2027, permitirán consolidar las técnicas y productos de SM con sensores activos de microondas.

1.4.2.1.3. *Climate Change Initiative*

La observación de la Tierra a través de técnicas de teledetección ha supuesto una enorme fuente de información de los sistemas terrestres y ha permitido mejorar nuestra comprensión sobre su dinámica y sus interacciones. Además, la capacidad de estas técnicas de monitorizar globalmente una gran diversidad de variables ha facilitado la comprensión, modelización y predicción de muchos procesos hidro-climáticos. Con el fin de permitir la monitorización del clima a largo plazo, el GCOS estableció una serie de requisitos para los productos satelitales de las ECVs (GCOS, 2016). En este contexto, la ESA inició en el año 2010 la CCI, cuyo objetivo es aprovechar todo el potencial de los datos procedentes de teledetección de observación de la Tierra que han proporcionado las diferentes misiones tanto de la ESA como de terceros (Hollmann et al., 2013). De las 50 ECVs establecidas por el GCOS, actualmente CCI proporciona series de datos de teledetección para 22 de ellas, entre las que se incluye la SM (https://climate.esa.int/).

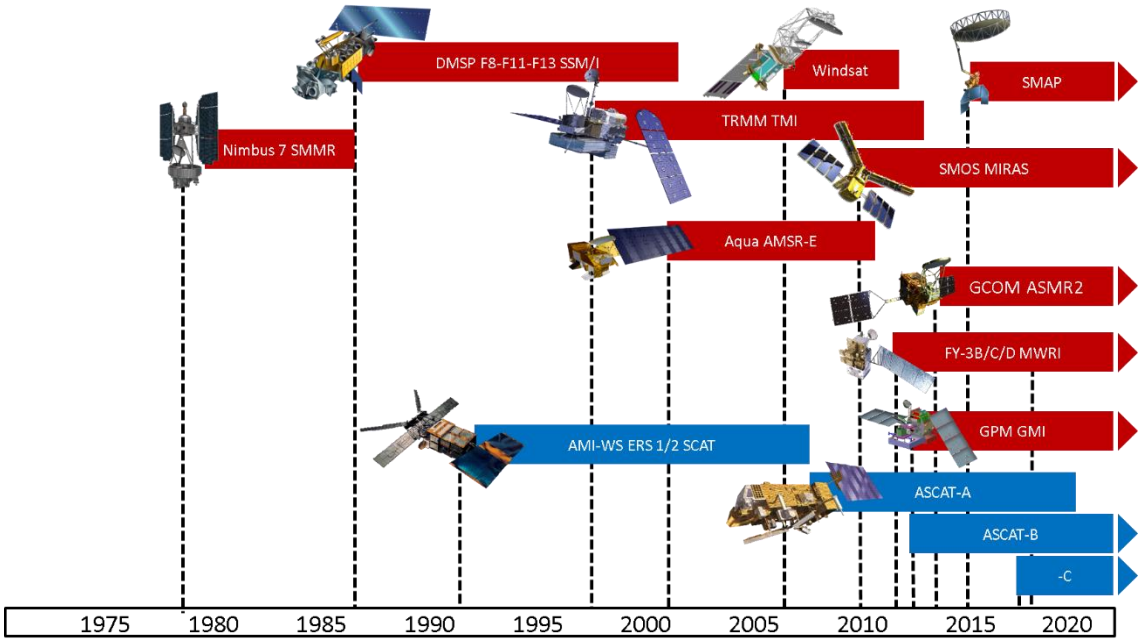

Figura 1.5 Cronología de los sensores de teledetección de microondas pasivos (rojo) y activos (azul) utilizados para generar el producto de SM de CCI v07.1. Imagen obtenida de https://esa-soilmoisture-cci.org/node/93.

Las series de datos de SM de CCI se basan en un algoritmo de fusión que armoniza las estimaciones de esta variable obtenidas con sensores de microondas activos y pasivos desde el año 1978. El resultado son 3 productos, uno derivado únicamente de los sensores pasivos (PASSIVE), otro de los sensores activos (ACTIVE) y un último producto combinado (COMBINED). Todos ellos se producen con una resolución temporal diaria y en una malla regular de 0,25° (Dorigo et al., 2017; Gruber et al., 2019). Por el momento, se han publicado hasta 13 versiones diferentes con el objeto de actualizar las series de datos, incorporando nuevos sensores al algoritmo o mejorando las técnicas utilizadas para su armonización.

Actualmente, la versión más reciente es la v07.1, publicada en mayo del año 2022, que utiliza un total de 12 sensores pasivos y 5 activos (Figura 1.5 y Tablas 1.2 y 1.3). Hoy por hoy, es la base de SM satelital de más larga duración que existe.

Las especificaciones de los diversos sensores incluidos en el algoritmo son muy diferentes, por lo que, para obtener datos de calidad en el proceso de fusión es necesario caracterizar los errores de las estimaciones de SM procedentes de cada sensor, realizar correcciones del sesgo y reescalar las series de datos (Scanlon et al., 2022). Se ha observado que la fusión de varios productos generalmente ha superado a los de un solo sensor, y que su calidad ha ido mejorando con cada nueva versión (Dorigo et al., 2017).

Tabla 1.2 Descripción de los sensores pasivos incluidos en el algoritmo del producto de SM de CCI v07.1 (Scanlon et al., 2022).

Sensor	**Plataforma**	**Periodo**	**Frecuencia de microondas**	**Resolución espacial (km^2)**	**Cobertura espacial**
SMMR	Nimbus 7	11/1978 – 08/1987	6.6 GHz	150×150	Global
SSM/I	DMSP	09/1987 – 12/2007	19.3 GHz	69 × 43	Global
TMI	TRMM	01/1998 – 12/2013	10.7 GHz	59 × 36	N40 - S40
AMSR-E	Aqua	07/2002 – 10/2011	6.9/10.7 GHz	76 × 44	Global
AMSR2	GCOM-W1	05/2012 – 12/2019	6.925/10.65 GHz	35 x 62	Global
Windsat	Coriolis	10/2007 – 07/2012	6.8/10.7 GHz	25 x 35	Global
MIRAS	SMOS	01/2010 – 12/2021	1.4 GHz	40 x 40	Global
SMAP	SMAP	04/2015 – 12/2021	1.4GHz	38 x 49	Global
GMI	GPM	03/2014 – 12/2021	10.7 GHz	19 x 32	N70 - S70
MWRI	FY-3B	06/2011 – 08/2019	10.7 GHz	51 x 85	Global
MWRI	FY-3C	06/2011 – 08/2019	10.7 GHz	51 x 85	Global
MWRI	FY-3D	06/2011 – 08/2019	10.7 GHz	51 x 85	Global

Tabla 1.3 Descripción de los sensores activos incluidos en el algoritmo del producto de SM de CCI v07.1 (Scanlon et al., 2022).

Sensor	**Plataforma**	**Periodo**	**Frecuencia de microondas**	**Resolución espacial (km^2)**	**Cobertura espacial**
AMI-WS	ERS1/2	07/1991 – 12/2006	5.3 GHz	50 × 50	Global
AMS-WS	ERS2	05/1997 – 02/2007	5.3 GHz	25 x 25	Global
ASCAT	Metop-A	01/2007 – 12/2020	5.3 GHz	25 × 25	Global
ASCAT	Metop-B	11/2012 – 12/2021	5.3 GHz	25 × 25	Global
ASCAT	Metop-C	11/2018 – 12/2021	5.3 GHz	25 × 25	Global

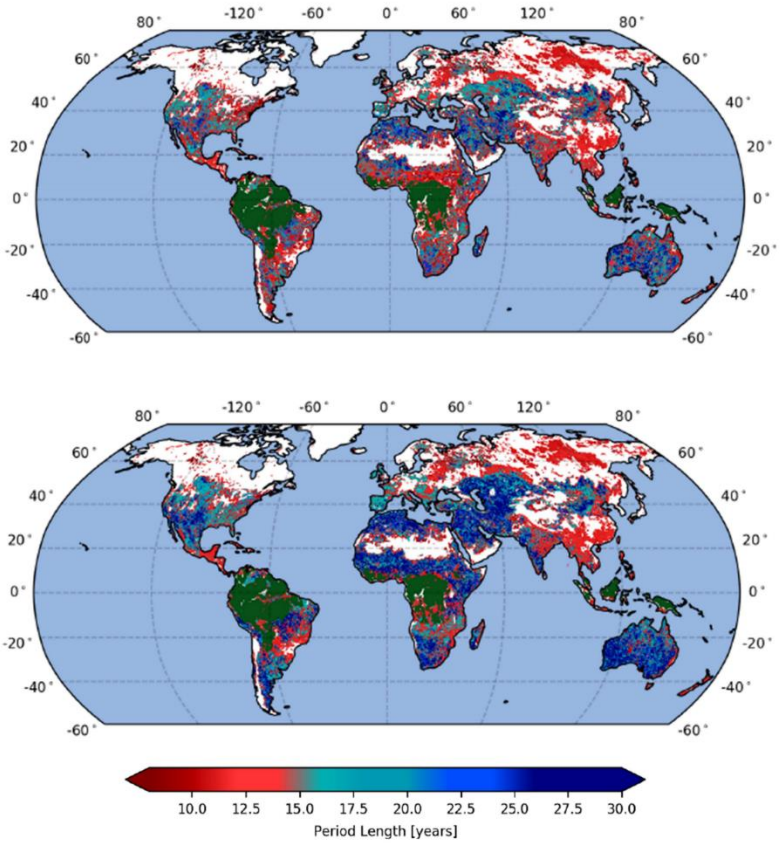

Figura 1.6 Período homogéneo más largo del producto de SM de CCI COMBINED v04.4 antes (arriba) y después (abajo) de la corrección de las roturas (Scanlon et al., 2022).

Los productos de SM de CCI han sido ampliamente validados (Al-Yaari et al., 2019; Dorigo et al., 2015; González-Zamora et al., 2019) y usados para diversas aplicaciones (Dorigo et al., 2012; Martínez-Fernández et al., 2019; Nicolai-Shaw et al., 2017). Sin embargo, existen algunas limitaciones intrínsecas al método de estimación de la SM como son las lagunas de datos, causadas por diversos factores como los tiempos de revisita de los satélites, presencia de hielo, nieve o vegetación muy densa y contaminación por RFI, entre otros (Almendra-Martín et al., 2021b). Motivado por el gran potencial para la investigación emprendida en esta tesis doctoral de esta base de datos, el Capítulo 2 expone un estudio pionero sobre la comparación de diferentes métodos para hacer frente esta limitación considerando tanto aproximaciones temporales como espaciales, como diferentes conjuntos de variables de entrada.

Recientemente, y durante el transcurso del desarrollo de esta tesis, se ha puesto de manifiesto una limitación debida al propio algoritmo de fusión. Preimesberger et al. (2021) observaron discontinuidades o *breaks* en las series de datos como resultado de la fusión de los diferentes sensores a lo largo del tiempo. En su sexta versión se incorpora un nuevo producto auxiliar obtenido a partir del COMBINED y que ha sido sometido a un método de detección y corrección de estas discontinuidades (*Break-adjusted* COMBINED) (Scanlon et al., 2022). Aunque las mejoras han sido significativas, existen todavía muchas regiones en el mundo donde aún se observan discontinuidades o artefactos debidas

principalmente a cambios en la cantidad de datos (sensores) disponibles para la estimación de SM en un determinado período. Como resultado, el periodo homogéneo total disponible es muy diverso espacialmente y en algunos casos limita considerablemente la duración temporal de la serie climática. Concretamente, en Europa no se han podido obtener períodos homogéneos con duración mayor de 20 años (Figura 1.6).

1.4.2.2. Observaciones en el rango visible e infrarrojo

Aunque no son los métodos más comunes, la SM se puede estimar de forma indirecta a partir de observaciones remotas con sensores que trabajan en los rangos visible, infrarrojo cercano (NIR, *near infrared*), infrarrojo de onda corta (SWIR, *shortwave-infrared*) e infrarrojo térmico (TIR, *thermal infrared*) del espectro electromagnético (Petropoulos et al., 2015; Wang and Qu, 2009; Zhang and Zhou, 2016).

Diversos estudios han observado una relación entre la reflectividad de diferentes suelos en las bandas del visible NIR y SWIR y su contenido de humedad (Dalal and Henry, 1986; Leone and Sommer, 2000; Weidong et al., 2002). Sin embargo, las características espectrales del suelo dependen de muchos otros factores además del contenido de agua, lo que lleva en muchos casos a una difícil calibración y por tanto estimaciones deficientes (Lobell and Asner, 2002). Por otro lado, las bandas del visible y NIR proporcionan información sobre el estado y el estrés hídrico de la vegetación (Bannari et al., 1995). Las condiciones de sequía pueden, por tanto, estimarse a través de índices de vegetación como el *normalized difference vegetation index* (NDVI). De esta forma se pueden estimar índices de sequía a partir del estado de la vegetación y estimar así el contenido de humedad en el suelo. Sin embargo, la precisión de este enfoque depende del tipo de vegetación o ecosistema en el que se aplique y en el retardo de la respuesta de la vegetación a la escasez de agua (Zhang and Zhou, 2016).

Sensores de teledetección con bandas en el TIR también permiten obtener estimaciones de la SM basadas en la influencia que esta variable ejerce en las variaciones de la temperatura de la superficie del suelo (LST, *land surface temperature*). Los métodos más comunes son los basados en la inercia térmica, propiedad física intrínseca al suelo definida como la resistencia a las variaciones de temperatura (Zhang and Zhou, 2016). Estos métodos se basan en principios físicos bien definidos que relacionan las propiedades térmicas del suelo con su contenido de agua. De esta forma se puede estimar la SM a partir de los cambios o la amplitud diurna de la LST (Price, 1980). Sin embargo, únicamente es aplicable en regiones con poca o muy escasa cobertura vegetal (Wang and Qu, 2009).

Como se ha expuesto, la SM guarda una estrecha relación con el estado de la vegetación y con las características térmicas del suelo. Por tanto, también es posible estimar el contenido de SM combinando ambos parámetros, la LST y el estado de la vegetación estimado a partir de índices de vegetación, en concreto el NDVI. La representación gráfica de valores de LST frente al NDVI consiste en una dispersión de puntos que definen un triángulo, conocido como el "Triángulo Universal" (Gillies and Carlson, 1995; Heim, 2002) y que aúna la relación entre estas dos variables y la SM.

Actualmente, muchos de los sensores de teledetección que trabajan en este rango del espectro electromagnético proporcionan imágenes de alta resolución espacial, sin embargo, estas ondas tienen una escasa capacidad de penetración en la superficie del suelo, y las ondas son absorbidas por las nubes o la vegetación densa (Zhang and Zhou, 2016), lo que imposibilita en muchos casos su aplicación. En especial, las nubes se consideran un tipo de contaminación de datos que en la mayoría de los casos supone la pérdida de estos (Shen et al., 2014). Además, este este rango del espectro, a excepción del TIR, depende de la iluminación del sol, por lo que no se pueden obtener medidas durante la noche (Wagner et al., 2007). Debido a estas limitaciones la continuidad espaciotemporal de los datos se ve comprometida con estos métodos. No obstante, la información obtenida con sensores de teledetección que trabajan en este rango del espectro electromagnético se ha utilizado, complementariamente con los sensores de microondas, para obtener estimaciones de SM con una resolución espacial más fina a través de técnicas de *downscaling* (Piles et al., 2011; Sánchez-Ruiz et al., 2014).

1.4.3. Humedad del suelo modelizada

Una de las técnicas más comunes para estimar series de datos en una infinidad de campos, es la modelización. Un modelo representa, de forma simplificada, el comportamiento de un sistema y permite estimar la respuesta de diferentes variables (*output*) a partir de diversos factores que condicionan su variabilidad (*inputs*). La SM se ha estimado a través de una multitud de modelos con diferentes características y diferente grado de complejidad, requerimiento de datos o cobertura espacial, entre otras.

En el caso de las variables hidrológicas, los modelos hidrológicos representan la parte del sistema terrestre que controla el movimiento y almacenamiento del agua. De este modo, un modelo hidrológico consiste en una representación simplificada, física o matemática, del ciclo hidrológico terrestre. Su objetivo general es simular los flujos de energía, humedad u otra materia a través de los límites del sistema considerado, siendo la cuenca el sistema más común en modelización hidrológica (Solomatine and Wagener, 2011). Sin embargo, en el pasado, estos modelos casi nunca consideraban la SM (Engman, 1990) y la usaban principalmente para estimar la escorrentía o el caudal. Se trata de los conocidos como modelos de lluvia-escorrentía (Birkel and Barahona, 2019).

Los modelos hidrológicos se pueden clasificar en base al enfoque usado para la simulación de los procesos en tres clases diferentes (Brocca et al., 2014). Por un lado, los modelos de base física, que abordan la solución de la ecuación de Richard, ecuación no lineal que describe la transferencia del flujo en medios porosos y no saturados (Ross, 1990). Un ejemplo, es el modelo *Système Hydrologique Européen* (SHE) conocido como uno de los modelos hidrológicos más complejos (Abbott et al., 1986). Por otro lado, los modelos estadísticos, que basan las simulaciones en el tratamiento estadístico de los datos, como, por ejemplo, modelos basados en técnicas de *machine learning* (ML) (Jiang and Cotton, 2004). Por último, los modelos conceptuales, construidos sobre la base de relaciones empíricas observadas o supuestas entre diferentes variables hidrológicas (Liu et al., 2017).

Estas relaciones suelen estar basadas en el balance hídrico o energético del suelo (Rodríguez-Iturbe et al., 1999; Sheikh et al., 2009). Ejemplos de modelos conceptuales son el modelo *Soil Water Balance* (SWB) desarrollado por Brocca et al. (2008), el HBV (*Hydrologiska Byråns Vattenbalansavdelning*) (Bergström, 1976) o, con una base más física, el TOPMODEL (Beven and Kirkby, 1979). Estos últimos han sido los más utilizados para simular la SM, ya que, debido a las simplificaciones en la representación del sistema, permiten estimar esta variable de forma precisa y sin necesidad de conjuntos de datos detallados para su calibración y parametrización (Brocca et al., 2014).

En las últimas décadas, en paralelo al desarrollo de los modelos hidrológicos, la necesidad de disponer de datos sobre los recursos hídricos motivó el desarrollo de otro tipo de modelos con un enfoque diferente (Overgaard et al., 2006). Entre los límites de la modelización atmosférica e hidrológica, nacen los modelos de superficie terrestre (LSM, *land surface model*). Los LSM tienen como objetivo simular la dinámica de la superficie terrestre y su papel dentro del sistema terrestre. Estos modelos consisten en modelos numéricos que resuelven los flujos acoplados de agua, energía y carbono entre la superficie terrestre y la atmósfera, dentro de un contexto de forzamientos (Fisher and Koven, 2020). Los LSM originalmente se desarrollaron para actividades de predicción y modelización atmosférica-climática, por lo que exigen condiciones de contorno físicas para representar la influencia de la superficie terrestre en los procesos meteorológicos. Como consecuencia, es necesario un forzamiento atmosférico para poder proporcionar las condiciones de contorno adecuadas y obtener los parámetros asociados al modelo (Ek, 2018). El desarrollo de este tipo de modelos ha permitido ir incorporando las representaciones de diferentes procesos, entre ellas la dinámica de la SM (Fisher and Koven, 2020). Además, los LSM actualmente incorporan la dinámica del agua en las capas más profundas, incluidos los acuíferos, y los flujos horizontales, lo que mejora la representación de la variabilidad de la SM (Maxwell et al., 2007). La integración de estos procesos ha permitido la aplicabilidad de los LSM a una amplia gama de aplicaciones hidrológicas (Yassin et al., 2019). Este tipo de modelos se han convertido en una herramienta fundamental, proclamándose como una alternativa atractiva a los modelos hidrológicos conceptuales (Overgaard et al., 2006).

A pesar de su enorme desarrollo, existen todavía retos a los que tanto los modelos hidrológicos como los LSM deben hacer frente. Un ejemplo es la resolución espacial (Bierkens et al., 2015), que en el pasado ha estado marcada por la resolución espacial de los modelos meteorológicos (20 km) y climáticos (100 km) (Wood et al., 2011). Los avances experimentados en las últimas décadas, tanto en capacidad de computación como en capacidad de almacenamiento, han permitido modelizar la SM en grandes superficies a una resolución espacial más fina. Un ejemplo es el modelo LISFLOOD, un modelo hidrológico espacialmente distribuido, pero con base física, ya que el uso de sistemas de información geográfica (*geographical information system*, GIS) permite desarrollar modelos de transporte (de Roo et al., 2000). Desarrollado por el *Joint Research Centre* (JRC) para la simulación de procesos hidrológicos en grandes cuencas fluviales europeas, proporciona series de SM a una resolución espacial de 5 km x 5 km (van der Knijff et al., 2010).

En resumen, la modelización posee la ventaja de ser capaz de proporcionar series continuas en el espacio y en el tiempo, para largos periodos, sin lagunas de datos, y posibilita estimar la SM a diferentes profundidades. Sin embargo, la resolución y cobertura espaciotemporal dependen de la estructura y las características del modelo. Además, las estimaciones están condicionadas por la precisión y disponibilidad de los datos de entrada, y por la adecuación del modelo (Holgate et al., 2016). Este último factor está íntimamente ligado a la parametrización de diferentes sistemas dentro del modelo, que en algunos casos puede ser extremadamente compleja (Brocca et al., 2017). Por este motivo, aunque los datos de SM modelizados se presentan como una destacada herramienta para numerosas aplicaciones, deben ser tratados con precaución considerando los posibles errores asociados a las series de datos. Diferentes enfoques de modelado conducen a diferentes representaciones de la SM (Brocca et al., 2017). Esto hace imprescindible una correcta validación de las bases de datos y por tanto la continuidad y disponibilidad de las redes de estaciones *in situ*.

1.4.3.1. Asimilación de datos: reanálisis

Como se ha expuesto, las series de SM modelizada pueden no ser adecuadas para determinadas aplicaciones, ya que las diversas incertidumbres asociadas a los modelos pueden suponen una limitación a la hora de proveer estimaciones lo suficientemente precisas. Por este motivo, cada vez es más frecuente el uso de métodos que permiten una corrección continua de las predicciones del modelo utilizando observaciones complementarias (Medina-González et al., 2015). Este procedimiento se denomina asimilación de datos y permite integrar las estimaciones, tanto de satélite como *in situ*, en los modelos (Boni et al., 2001; Georgakakos and Baumer, 1996). De esta forma se obtienen las llamadas series de datos de reanálisis.

Inicialmente la asimilación de datos se desarrolló para la predicción meteorológica, pero posteriormente comenzó a aplicarse en la modelización de los sistemas de la superficie terrestre (Parajka et al., 2006). Gracias a las extensas series de datos proporcionadas por los sensores de teledetección, actualmente podemos disponer de observaciones temporal y espacialmente continuas de numerosas variables. Haciendo uso de estas series, es posible integrar los datos satelitales de manera consistente con estimaciones de modelos. De esta manera, la asimilación de datos aprovecha el potencial de los dos métodos de estimación de la SM, teledetección y modelización, para beneficiarse de las ventajas de ambos (Parajka et al., 2006). Ejemplos de bases de datos de reanálisis de superficie terrestre que estiman la SM son el *Global Offline Land-surface Dataset* (GOLD) (Dirmeyer and Tan, 2001), el *Modern-Era Retrospective* Analysis for Research and Applications - Land (MERRA-Land) (Reichle et al., 2011) o los ECMWF Re-Analysis (ERA), como ERA-Interim/Land (Balsamo et al., 2015) y su versión mejorada ERA5L (Muñoz-Sabater et al., 2021).

Esta técnica puede mitigar errores intrínsecos a los modelos y mejorar la representación de los sistemas hídricos y de la superficie terrestre allí donde existen observaciones (Albergel et al., 2012). Sin embargo, las bases de datos de estas observaciones también poseen sus propias fuentes de error que pueden dar lugar a incoherencias temporales y espaciales

cuando se incorporan a los modelos (Muñoz-Sabater et al., 2021). Además, esta técnica está sujeta a la disponibilidad de estas observaciones. Por lo que, se hace imprescindible la disponibilidad de redes de estaciones *in situ* y de datos satelitales para una correcta validación de las series de datos.

1.5. Métodos estadísticos para el análisis de la evolución de la humedad del suelo

1.5.1. Técnicas de regresión para la reconstrucción de series

Las series de datos satelitales de SM han demostrado un gran potencial para una multitud de aplicaciones, ya que ofrecen estimaciones precisas espacial y temporalmente continuas. Sin embargo, una de las limitaciones más significativas es la existencia de lagunas de datos, algo que condiciona sobremanera su uso para el análisis de las variaciones de la SM. Esta limitación está presente en todas las series de datos provenientes de estimaciones a partir de sensores, ya sean *in situ* o remotos. La ausencia de datos en las series puede ser debida a una multitud de factores. Por ejemplo, en las redes *in situ*, el fallo de un sensor, observaciones interrumpidas o inexactas, o problemas con la trasferencia de datos pueden provocar perdidas de datos (Dumedah and Coulibaly, 2011). En el caso de los sensores de teledetección que estiman la SM, la contaminación por RFI, los diferentes tiempos de revisita del satélite, la presencia de hielo, nieve y vegetación muy densa, o la complejidad y alta incertidumbre de recuperación en zonas costeras y áreas montañosas, provocan perdidas de datos (Almendra-Martín et al., 2021b).

Varios trabajos han estudiado como afrontar esta limitación evaluando la precisión de diferentes técnicas capaces de rellenar estas lagunas a diversas escalas espaciales y temporales. En el caso de las series *in situ*, se han aplicado desde técnicas simples como el reemplazo con promedios diarios o mensuales, hasta técnicas más complejas como el *kriging* o las redes neuronales (Dumedah et al., 2014; Dumedah and Coulibaly, 2011; Ford and Quiring, 2014; Kornelsen and Coulibaly, 2014). Algunas de estas técnicas también se han aplicado a la reconstrucción de las lagunas de datos en imágenes de teledetección, sin embargo, la heterogeneidad espacial y temporal de los datos ausentes incorpora una dificultad con respecto a las series *in situ*. Por este motivo, las técnicas basadas en geoestadística (Llamas et al., 2020) o inteligencia artificial (Cui et al., 2019, 2016; Salcedo-Sanz et al., 2020) han destacado sobre otras. Como algunos de estos métodos requieren variables de referencia (*inputs*), una herramienta recurrente en la literatura ha sido el uso de otras bases de datos de SM, ya sean *in situ* (Xing et al., 2017; Zhang and Chen, 2016), de modelos (Xiao et al., 2016) o de satélite (Liu et al., 2020). Sin embargo, métodos más simples como las interpolaciones (Militino et al., 2019) o el suavizado de series (G. Wang et al., 2012), también han sido comúnmente empleados.

En esta tesis se ha evaluado la capacidad de diferentes métodos de relleno de lagunas de datos en los dominios temporal y espacial, desde los más simples, como la regresión lineal, hasta los más sofisticados como los basados en ML. Estos métodos incluyen la interpolación lineal y cúbica, un modelo autorregresivo (*autoregressive*, AR), las *support vector machine* (SVM) y los *random forest* (RF). Las interpolaciones en el dominio espacial se basaron en la triangulación de Delaunay (de Berg et al., 2008) y en el dominio temporal se realizaron por *splines* (Fritsch and Carlson, 1980). Además, en el dominio

temporal se aplicó un modelo AR, que estima los valores faltantes mediante una extrapolación iterativa (Rigling, 2012). Las SVM se emplearon utilizando su enfoque a problemas de regresión. El fundamento de este método consiste en encontrar una función de regresión óptima, lo más plana posible y que minimice el riesgo empírico o error fijando previamente un máximo de desviación ε del valor real (Smola and Schölkopf, 2004). Por último, los RF, también aplicados a problemas de regresión, consisten en un conjunto de árboles de decisión independientes, entrenados con una muestra aleatoria distinta, pero con la misma distribución en todos los árboles (Breiman, 2001). Estos dos últimos métodos requieren series de datos de diferentes variables (*inputs*) que permitan entrenar los modelos. Además, la selección de estas variables juega un papel fundamental en la precisión de las estimaciones. La selección de variables empleadas se presenta en el Capítulo 2 junto con una explicación detallada de los métodos mencionados.

1.5.2. Técnicas para la detección de tendencias

Según la teoría de la hidrología estocástica, las variaciones de las variables hidrológicas están causadas por diferentes mecanismos físicos que actúan a diferentes escalas temporales, por lo que se pueden diferenciar distintos componentes en una serie temporal: la estocasticidad o ruido, la periodicidad y la tendencia (Yevjevieh, 1987). Para identificar con precisión los diferentes componentes de las series hidrológicas, se han empleado en la literatura diferentes métodos. Sin embargo, la identificación de tendencias en series temporales de variables hidrológicas no es una tarea simple debido a su naturaleza no lineal y no estacionaria (Sang et al., 2018).

(Sang et al., 2013) clasifica los métodos más comunes para la identificación de tendencias en cuatro categorías. En primer lugar, los métodos basados en el ajuste de datos, como el ajuste por mínimos cuadrados o por máxima verosimilitud. Estos métodos son simples, pero requieren una función predefinida y sus parámetros pueden llevar asociadas incertidumbres, lo que hace que sean subjetivos y poco fiables en algunos casos. La segunda categoría se refiere a los métodos basados en el dominio temporal, como la prueba de Mann-Kendall (MK), el coeficiente de correlación de Spearman o la regresión lineal. El uso de estos métodos está muy extendido. En concreto, el test de MK es el método más común para el análisis de tendencias de variables hidro-climáticas (Gocic and Trajkovic, 2013; Yue et al., 2002), entre ellas la SM (Albergel et al., 2013; An et al., 2016; Dorigo et al., 2012). Es un método simple y no paramétrico capaz de tratar series de datos con lagunas, sin embargo, no es robusto frente a la autocorrelación de las series (Hamed and Rao, 1998), observada en la mayoría de las variables hidro-climáticas. La tercera categoría se refiere a los métodos basados en el dominio de frecuencias, como el test de medias móviles o la trasformada de Fourier. Estos métodos requieren establecer, *a priori*, una escala de tiempo predeterminada, ya que se basan en suposiciones de estacionariedad y linealidad. Sin embargo, los cambios observados en las variables hidrológicas suelen mostrar un comportamiento no lineal y no estacionario (Coulibaly and Baldwin, 2005). Por último, los métodos basados en ambos dominios, temporal y de frecuencias, como el test

basado en *wavelets* o el *empirical mode decomposition* (EMD). El uso de estos métodos está cada vez más extendido, siendo su principal atractivo que permiten analizar datos no estacionarios e identificar procesos no lineales a través de la descomposición de las series (Sang et al., 2018, 2014).

Diferentes métodos pueden llevar a diferentes resultados. Además, las tendencias dependen en gran medida del período de estudio y la escala temporal analizada (Gudmundsson and Seneviratne, 2015; Hänsel et al., 2019), especialmente cuando se aplican enfoques lineales. Esto hace que los resultados obtenidos por diferentes estudios no sean directamente comparables y por tanto deban interpretarse con precaución. En esta tesis se hace uso de dos métodos diferentes para analizar las tendencias de las 3 últimas décadas de la SM y de la sequía agrícola en Europa a diferentes escalas temporales. Este análisis se presenta en el Capítulo 3, que, además, incluye una descripción detallada de ambos métodos. Estos son, por un lado, el más utilizado en la literatura y basado en el comportamiento monótono de las series temporales, el MK, y, por otro lado, un método no lineal, que ha demostrado un gran potencial en la detección de tendencias de series hidro-climáticas, el EMD (Sang et al., 2014).

Cabe destacar que el estudio de tendencias requiere disponer de series de datos con una cobertura temporal suficientemente larga. Además, es necesario tener en cuenta que son pocos los métodos capaces de tratar con series de datos incompletas, como, por ejemplo, las series satelitales. Por este motivo, las bases de datos apropiadas para el estudio de tendencias de la SM son limitadas. Aunque la serie de SM de CCI presenta un gran potencial para este tipo de estudios, y aun completando en gran medida las lagunas de datos (Almendra-Martín et al., 2021b), las discontinuidades provocadas por la fusión de los diferentes sensores (Preimesberger et al., 2021) limitan la duración de las series y por tanto su aplicabilidad en algunas zonas, como es el caso del continente europeo (ver Figura 1.6). Por este motivo, actualmente las series de modelos o reanálisis generalmente resultan más apropiadas para el estudio de las tendencias SM que las series observacionales.

1.5.3. Métodos de causalidad

Las preguntas que motivan la mayoría de los estudios de diversos campos de investigación no son de naturaleza asociativa sino causal (Pearl, 2009). En el contexto de esta tesis, las relaciones causales pueden ayudar a comprender mejor las variaciones del contenido de agua del suelo a partir de los mecanismos físicos implicados en las interacciones entre la SM y la atmósfera. Los métodos de identificación de relaciones causales han demostrado un gran potencial para estudiar sistemas dinámicos complejos, ya que permiten obtener más información que los análisis de correlación (Runge et al., 2019a). Sin embargo, no es fácil formalizar un concepto general de causalidad.

La definición de Granger (Granger, 1969) es probablemente la más utilizada, ya que permite estudiar las relaciones causa-efecto de forma empírica sin necesidad de un modelo y cuantifica la asociación entre variables. La prueba de causalidad de Granger se basa en la capacidad de una serie temporal en predecir otra omitiendo parte de su pasado. Sin

embargo, esta formulación en ocasiones ha generado desconfianza ya que puede conducir a causalidades erróneas cuando no se incluyen determinadas variables que poseen vínculos indirectos (Eichler, 2012). Además, si se aumenta el número de variables, la alta dimensionalidad del conjunto de datos conduce a un poder de detección muy bajo (Runge et al., 2019b). Aunque existen otros métodos capaces de hacer frente al problema de la alta dimensionalidad, como la regresión de Lasso (Tibshirani, 1996) que combina un modelo de regresión con un procedimiento de selección de parámetros y permite realizar una selección de variables, este método se define principalmente en el contexto de la predicción y no del descubrimiento causal.

Más recientemente, la combinación de la estadística con los algoritmos de ML ha definido los *structural causal models* (SCM) (Pearl, 1995). En ellos se emplean modelos gráficos que identifican los efectos causales asumiendo la condición causal de Markov (Hausman and Woodward, 1999). Esta establece, a grandes rasgos, que en un modelo gráfico una variable Y es independiente de cualquier otra condicionada a las causas directas de Y (Runge et al., 2019a). Estos métodos son capaces de estimar los vínculos causales entre variables y su retraso o *lag* temporal (Runge et al., 2019b). Un ejemplo es el algoritmo PC (llamado así por sus inventores Peter y Clark) (Spirtes and Glymour, 1991), que parte de un gráfico completamente conectado y prueba la eliminación de vínculos de forma iterativa. La independencia condicional se puede probar de manera flexible con diferentes tipos de pruebas lineales y no lineales (Zhang et al., 2011). En esta tesis se ha empleado el método PCMCI, desarrollado por Runge et al. (2019b), para estudiar las relaciones causales entre la SM y los principales patrones de circulación atmosférica en Europa. En el Capítulo 3 se presenta este estudio, junto con una explicación más detallada del PCMCI, que recibe el nombre por la combinación del PC y el test *momentary conditional independence* (MCI). Este método ha demostrado ser preciso a la hora de identificar los vínculos causales, y más robusto frente a la no estacionariedad que otros métodos como Lasso y PC. Además, a diferencia de la prueba de causalidad de Granger, este método presenta la ventaja de poder identificar vínculos causales si la causalidad ocurre en el intervalo temporal de muestreo observable (Runge, 2020).

Las lagunas en las series de datos pueden limitar la identificación de relaciones causales con algunos métodos, o incluso imposibilitar su aplicación. Esto refleja la idoneidad del uso de bases de datos de SM provenientes de la modelización y/o el reanálisis. Además, una corta longitud de las series puede presentar limitaciones al estudiar la influencia de fenómenos como ENSO. Esto restringe el uso de series satelitales, ya que, aun completando en gran medida las lagunas de datos de la serie satelital más larga disponible, la CCI SM, las discontinuidades provocadas por la fusión de los diferentes sensores (Preimesberger et al., 2021) limitan su duración.

CAPÍTVLO 2

COMPARISON OF GAP-FILLING TECHNIQUES APPLIED TO THE CCI SOIL MOISTURE DATABASE IN SOUTHERN EUROPE

Almendra-Martín, L., Martínez-Fernández, J., Piles, M., González-Zamora, Á., 2021. Comparison of gap-filling techniques applied to the CCI soil moisture database in Southern Europe. Remote Sens Environ 258. https://doi.org/10.1016/j.rse.2021.112377

Resumen

La humedad del suelo (*soil moisutre*, SM) es una variable clave que juega un papel importante en las interacciones tierra-atmósfera. La monitorización de SM es crucial para muchas aplicaciones y puede ayudar a determinar el impacto del cambio climático. Por lo tanto, es fundamental contar con bases de datos de esta variable continuas y largas en el tiempo. Las misiones satelitales han contribuido a esta tarea; sin embargo, la continuidad de las series se ve comprometida debido a las lagunas de datos provocadas por diferentes factores, como el tiempo de revisita, la presencia de hielo estacional o la contaminación por interferencia de radiofrecuencia (RFI, *radio frequency interference*). En este trabajo, se evalúa la aplicabilidad de diferentes técnicas de *gap-filling* al producto combinado SM de la *Climate Change Initiative* (CCI) de la *European Space Agency* (ESA), la información satelital de SM más larga disponible. Los métodos utilizados fueron la interpolación lineal, cúbica y autorregresiva y las *support vector machines* (SVM). Este estudio se centró en el sur de Europa entre los años 2003-2015. Los diferentes métodos se aplicaron en los dominios temporal y espacial y se evaluaron mediante la técnica *holdout cross-validation*. Para poder estimar SM se introdujeron un conjunto de variables al modelo SVM, a saber, la temperatura de la superficie terrestre, la precipitación, el *normalized difference vegetation index* (NDVI), la evaporación potencial, la textura del suelo y las coordenadas geográficas. Para las SVM, se consideraron varias combinaciones de estas variables, incluido un análisis de componentes principales (PCA, *principal component analysis*) con todas ellas. Aunque los diferentes métodos muestran un buen resultado, en general, el método SVM supera al resto. Utilizar la SM del día anterior (SM_{t-1}) es clave para obtener buenas estimaciones. La mediana del coeficiente de correlación (R) obtenida con SVM y las series de SM_{t-1} en el análisis temporal fue de 0,83 y el RMSE de 0,025 m^3m^{-3}. Se obtuvieron resultados similares en el análisis espacial, siendo el mejor resultado (R = 0.88; RMSE = 0.024 m^3m^{-3}) el obtenido con el modelo SVM y utilizando las series de SM_{t-1} y las variables estáticas. El uso de PCA con las variables de entrada no fue satisfactorio y los métodos de interpolación fallaron cuando se trataba de grandes lagunas de datos espaciales o temporales. También se realizó una validación de la serie CCI SM con datos SM *in situ* de cuatro redes localizadas en España, Francia, Alemania e Italia, y no se observaron diferencias sustanciales entre los resultados obtenidos con la serie original y con la reconstruida. Además, los mejores *inputs* obtenidos con las SVM se utilizaron para evaluar el método de *random forest* (RF) en el dominio temporal y espacial. Este método mostró una buena capacidad para estimar los valores de SM en el dominio temporal, pero en menor medida que SVM, mientras que para el dominio espacial no pareció ser tan preciso. Los resultados obtenidos confirman que se puede abordar de manera eficiente el relleno de las lagunas espacio-temporales en las bases de datos observacionales de SM utilizando el método SVM, y las series temporales anteriores de SM y la textura del suelo como información de respaldo.

Palabras clave: *Gap-filling*, Humedad del suelo, CCI, *Support vector machines*

Abstract

Soil moisture (SM) is a key variable that plays an important role in land-atmosphere interactions. Monitoring SM is crucial for many applications and can help to determine the impact of climate change. Therefore, it is essential to have continuous and long-term databases for this variable. Satellite missions have contributed to this; however, the continuity of the series is compromised due to the data gaps derived by different factors, including revisit time, presence of seasonal ice or Radio Frequency Interference (RFI) contamination. In this work, the applicability of different gap-filling techniques is evaluated on the European Space Agency (ESA) Climate Change Initiative (CCI) SM combined product, which is the longest available satellite-based SM data record. The methods used were linear, cubic and autoregressive interpolation and support vector machines (SVMs). This study focused on Southern Europe and spanned the years 2003–2015. The different methods were applied in the temporal and spatial domains and evaluated using the holdout cross-validation technique. A set of variables was introduced in the SVM model to estimate SM, namely, land surface temperature, precipitation, normalized difference vegetation index (NDVI), potential evaporation, soil texture and geographical coordinates. For the SVMs, several combinations of these variables were considered, including a principal component analysis (PCA) containing all of them. Although the different methods show a generally good performance, the SVM method outperforms the rest. Using the SM of the precedent day (SM_{t-1}) is key to obtain good estimates. The median value of the correlation coefficient (R) obtained with the SVM and the SMt-1 series in the temporal analysis was 0.83, and the RMSE was 0.025 m^3m^{-3}. Similar results were obtained in the spatial analysis, with the best performance (R = 0.88; RMSE = 0.024 m^3m^{-3}) obtained by the SVM using the SM_{t-1} series and the static variables. The application of PCA to input variables was not beneficial, and the interpolation methods failed when dealing with large spatial or temporal gaps. A validation of the CCI SM series with *in situ* SM data from four networks located in Spain, France, Germany and Italy was also performed and no substantial differences were observed between results obtained with the original and with the reconstructed series. In addition, best inputs obtained with SVM were used to evaluate the random forest (RF) method in the temporal and spatial domain. This method showed a good ability to estimate soil moisture values in the temporal domain but to a lesser extent than SVM while for the spatial domain it did not seem to be as accurate. Our results confirm that we can efficiently deal with spatio-temporal gaps on observational SM databases using the SVM method and the past time series and soil texture as supporting information.

Keywords: Gap-filling, Soil moisture, CCI, Support vector machines

2.1. Introduction

Soil moisture (SM) is a relevant variable in land-atmosphere interactions as it controls the water, energy and carbon cycles, behaves as storage for precipitation, governs runoff and limits plant transpiration (Seneviratne et al., 2010). It is also a crucial variable in agricultural applications (Champagne et al., 2019) and many environmental studies, such as flood forecasting (Brocca et al., 2011), drought monitoring (Liu et al., 2019; Martínez-Fernández et al., 2016) and evaporation modelling (Miralles et al., 2011). Given its importance within the Earth system, SM was listed as one of the 50 essential climate variables (ECVs) by the Global Climate Observing System (GCOS, 2010) in 2010, and many efforts have been dedicated to the global mapping of SM in recent decades. Several SM products have been developed and validated with different objectives, characteristics and data sources (Beck et al., 2020). Examples include the International Soil Moisture Network (ISMN) (Dorigo et al., 2011), which consists of soil moisture series from *in situ* networks from all over the world. This soil moisture database is extremely useful, but has obvious limitations in terms of spatial coverage. Other approaches are the microwave active or passive satellite missions (e.g., Soil Moisture Ocean Salinity, SMOS, and Soil Moisture Active and Passive, SMAP) that provide a continuous spatio-temporal monitoring of this variable. The estimations are based on the high sensitivity of the brightness temperature measured by passive sensors, or the radar backscattering coefficient measured by active sensors, to the dielectric constant of soil, which is directly related to the soil moisture content. However, the retrieval of the variable can be complex due to various factors such as dense vegetation (Jackson, 1993). Furthermore, by merging different soil moisture estimations from different remote sensing missions, multi-satellite databases can be obtained (e.g., Soil Moisture Operational Products System, SMOPS, and Climate Change Initiative, CCI). These kind of products present the advantage of having a better spatio-temporal coverage than those obtained with just one sensor. Lastly, land surface models and reanalysis products (e.g., ERA5-Land and Global Land Data Assimilation System, GLDAS) provide a complete spatio-temporal coverage, since soil moisture is estimated by mathematical models incorporating also other variables.

The CCI programme from the European Space Agency (ESA) aims to provide long-term observational datasets of biogeophysical variables by taking advantage of the satellite measurements acquired during the observational era, i.e., from 1970's to the present (https://www.esa-soilmoisture-cci.org). These variables are all integrated in the Copernicus Climate Change Service (C3S), a Copernicus Earth Observation Programme service focused on climate research that provides climate information and data (https://climate.copernicus.eu). SM is one of these variables (hereafter CCI SM). The CCI SM product integrates SM products from four active and seven passive microwave satellite sensors, making the largest available existing observational SM data record (Dorigo et al., 2017; Gruber et al., 2019, 2017). This database has been extensively validated in different regions of the world including Southern Europe (Al-Yaari et al., 2019; An et al., 2016; Dorigo et al., 2015; González-Zamora et al., 2019; Ikonen et al., 2018; McNally et al., 2016). All these studies found great accordance between the CCI product and the different

in situ or reanalysis soil moisture series, although with some uncertainties, especially for the first years of the period when the data series have more gaps. Furthermore, CCI is extensively used for different applications, such as the study of global trends in SM (Feng, 2016; Qiu et al., 2016; Wang et al., 2016), precipitation estimations (Ciabatta et al., 2018), crop models (Sakai et al., 2016), the relationship between drought and climatic variables (Nicolai-Shaw et al., 2017), the assessment of the impact of El Niño drought conditions (Dorigo et al., 2016) or even tree growth tracking (Martínez-Fernández et al., 2019).

The ESA CCI SM product quality has steadily increased with each successive release, and the merged products generally outperform the single-sensor input products (Dorigo et al., 2017). Nevertheless, this database poses some limitations for several applications. For example, higher spatial resolutions are required to serve regional applications. This problem has been addressed in some studies that applied downscaling techniques to microwave-based SM products (Mascaro et al., 2011; Peng et al., 2017; Piles et al., 2016, 2014; Srivastava et al., 2013). Additionally, many studies have problems dealing with the spatio-temporal gaps in the data, which are caused by a variety of factors (e.g., RFI contamination, different satellite revisit times, presence of ice or snow, high uncertainty of retrievals in coastal and mountain areas). Several methods have been proposed in the literature to overcome this non-uniform effective sampling of SM observational data at different spatial and temporal scales. For *in situ* SM databases, some studies have compared a suite of different gap-filling methods (Dumedah et al., 2014; Dumedah and Coulibaly, 2011; Ford and Quiring, 2014; Kornelsen and Coulibaly, 2014). Regarding satellite images, Zhang and Chen (2016) proposed the satellite and *in situ* sensor collaborated reconstruction (SICR) method for filling Gaofeng-1 SM gaps. They classified the missing pixels based on their characteristics and their similarity or proximity to the *in situ* data and established four rules for the reconstruction based on linear regression or ordinary kriging. Xing et al. (2017) improved the SICR method by applying machine-learning techniques. While the two methodologies offer good results, they can be applied only to regions where *in situ* SM data exist. Xiao et al. (2016) proposed a way to efficiently reconstruct the satellite series by using the GLDAS Noah model but only in one-year period. In that study, satellite data were used to estimate the model control variables, and meteorological data were incorporated to force the model to simulate the temporal dynamics. Wang et al. (2012) applied a penalized least square method based on three-dimensional discrete cosine transformation to the Advanced Microwave Scanning Radiometer - Earth Observing System (AMSR-E) SM product, which was originally proposed by Garcia (2010) for smoothing multidimensional data with missing values. This methodology enables the simultaneous consideration of spatial and temporal database information but leads to poor predictions when the spatial differences are large. Furthermore, Cui et al. (2016) proposed a reconstruction of the Fengyun-3B Microwave Radiation Imager (FY-3B/MWRI) SM product using Moderate Resolution Imaging Spectroradiometer (MODIS) products by applying artificial neural networks (ANNs). This method was able to capture the SM dynamics, but they found uncertainties regarding the algorithm, which should be improved in the freezing-thaw period.

Despite the previous research aimed at completing SM databases, only a few have been applied to the challenging case of the long-term multi-satellite CCI SM product. In Llamas et al. (2020), three spatial methodologies were evaluated over a region in the U.S. Midwest: ordinary kriging, regression kriging and general linear models (GLMs). These methods are based on the spatial distribution of SM or its relationship with other variables (temperature and precipitation) and show good performance, especially the two kriging approaches. Cui et al. (2019) applied a modified algorithm from Cui et al. (2016) to the CCI SM product in the Tibetan Plateau. This method was based on a general regression neural network (GRNN) and used the SM, land surface temperature (LST), normalized difference vegetation index (NDVI), albedo and digital elevation model (DEM) as inputs. Liu et al. (2020) proposed the use of SMAP data to complete the CCI gaps. While the resampled SMAP SM series proved to be able to reasonably fill CCI SM gaps, the complete series reconstruction depends upon the availability of SMAP data.

Studies comparing the performance of different gap-filling methodologies to SM databases are limited, and they only partially address the specific case of long-term multi-satellite observational SM series. In this study we aim to bridge this gap by analysing the performance of gap-filling methodologies with different levels of complexity to the ESA CCI SM product: from simple ones, such as linear interpolation, to more sophisticated ones, such as those based on machine learning (ML). We selected ML techniques since they can integrate multivariate information and have been shown to excel in a variety of SM applications, from nonparametric and nonlinear classification to regression techniques (Lary et al., 2016). Specifically, the support vector machines (SVMs) for regression problems allow good generalization even with small training datasets (Ali et al., 2015; Mountrakis et al., 2011) and, in some cases, work better than ANNs (Ahmad et al., 2010). The effectiveness of SVMs to fill temporal gaps in ground-based observation databases has been proven elsewhere (Gill et al., 2006), but they have not been previously used to complete satellite databases.

Knowledge of the SM spatial distribution and its dynamics, anomalies and trends across time is fundamental to assess and quantify the impact of climate change on the water cycle. This highlights the need to fill the data gaps and improve the temporal sampling and observation density of the current observational soil moisture databases spanning the last 40 years. This work evaluates a suite of gap-filling methods of varying complexities for the case of long-term satellite-based SM databases (the CCI SM). This research is focused on the Southern part of Europe and covers spatial and temporal domains. Among the wide range of possible features that could explain the SM variability, the LST, NDVI, precipitation, potential evaporation and soil texture were chosen and used as inputs for the SVM models. The remainder of this article is organized as follows. Section 2.2.1 provides a description of the databases used in this study; Section 2.2.2 introduces the methods, the developed models and the overall validation strategy. Section 2.3 shows the results obtained by the different methods in the temporal and spatial domains and discusses the best results obtained in each analysis and their applicability. Conclusions and perspectives from this article are provided in Section 2.4.

2.2. Material and methods

2.2.1. Datasets

The CCI SM product is based on a merging algorithm that harmonizes the SM retrievals from available active and passive microwave sensors. The single-sensor SM products are merged into three different products depending on the type of sensors used: the active, the passive and the combination of the two. All products are provided in global daily maps in a regular grid of 0.25° (Dorigo et al., 2017). This merging algorithm has been updated and improved in the different versions of the product, which incorporate an increasing number of microwave sensors (Gruber et al., 2019, 2017). In this study, the combined product of the latest version (v4.5) was used, and only the data with best quality were considered. This was achieved by screening out data with reported inconsistencies by using the quality flag variable. The CCI SM product also provides SM uncertainty values that are used to interpret the results. The combined product covers a 40-year period (November 1978 to December 2018) and includes eleven microwave sensors, seven of which are passive and four of which are active (Figure 2.1), with different technical characteristics and coverage periods (Gruber et al., 2019). The availability of a number of sensors for specific time periods leads to important differences in spatiotemporal coverage, resulting in periods when a single operating sensor was used to retrieve global SM but also in periods when up to five simultaneous estimations were merged. Due to this fact, the spatiotemporal distribution of data gaps is highly heterogeneous.

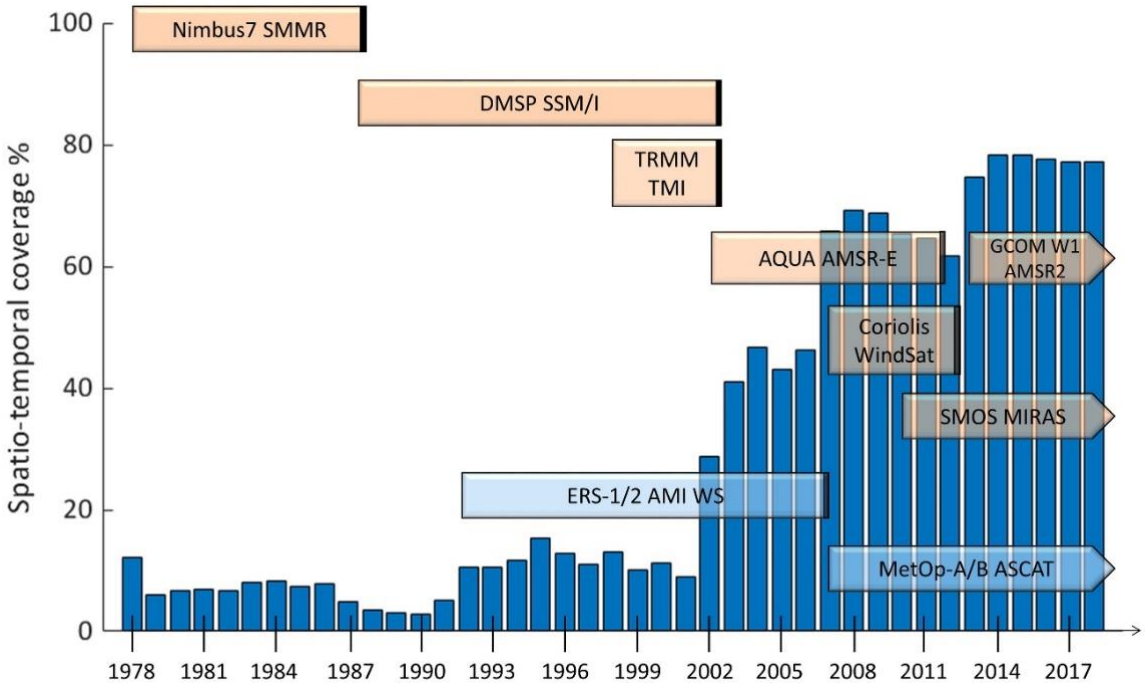

Figure 2.1 Timeline of the passive (orange) and active (blue) microwave sensors that generate the CCI SM product for version v4.5 and its annual percentage of available data in Southern Europe.

For the study area, the south of Europe, the percentage of data availability did not exceeded 20% in the first 20 years of the series (Figure 2.1). The amount of available data significantly increased notably to 40–50% in 2002–2003, when AMSR-E was added. Therefore, two periods can be clearly distinguished in the series in terms of data availability, with the tipping point being 2003. For this reason and due to the limited availability of complementary databases in the first period, this study focuses on the second period, i.e., 2003–2015. In this period, there was an increasing trend in data coverage over time until 2012, when AMSR-E operations ceased. The percentage of available data increased again in 2013 with AMSR-2 data, reaching a plateau of approximately 80% lasting until the end of the series. The mean percentage of SM data over Southern Europe for the study period is 62%, but its spatial distribution is non-homogeneous; some coastal pixels and mountain regions are the ones with the lowest percentage of data (see Figure 2.2a). But the majority of the area of study has between 70 and 80% of available data (Figure 2.2b). The temporal distribution and the gap length are also irregular. While the most common gaps last one or two days, there are also gaps of more than one year (Figure 2.2c).

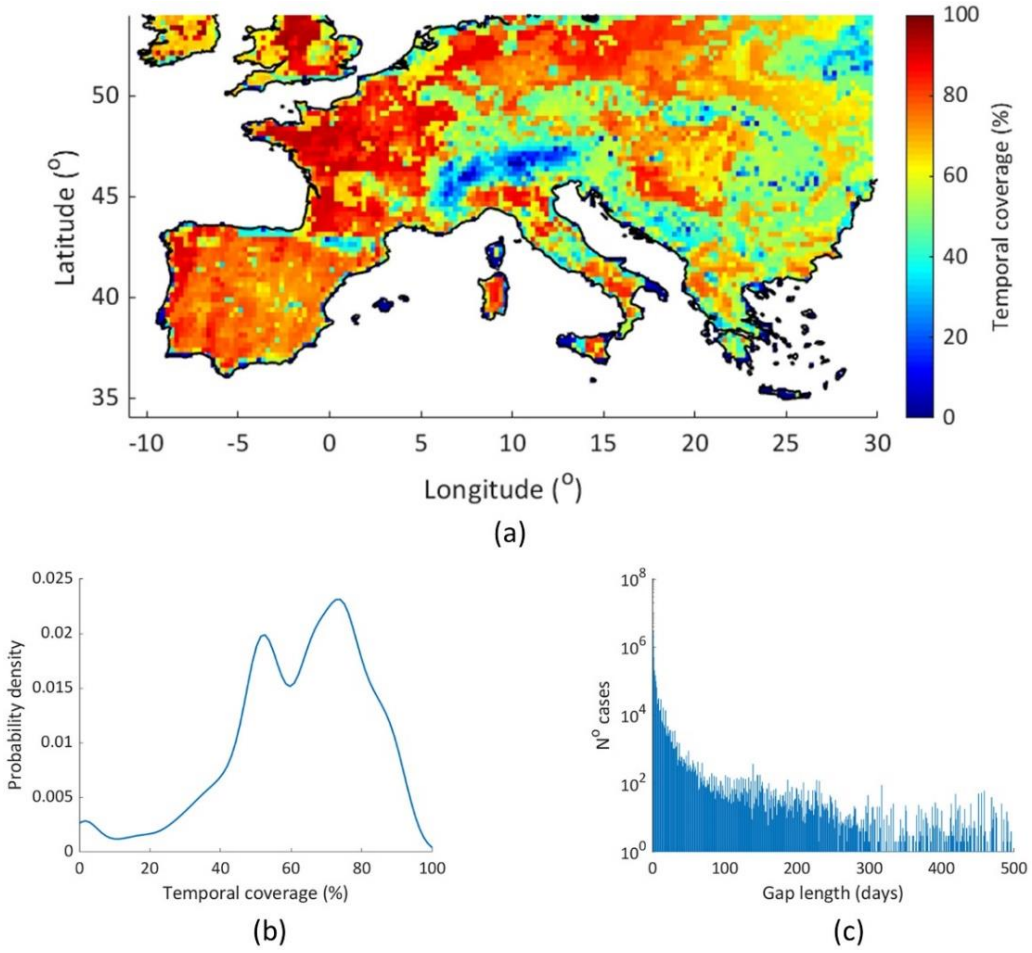

Figure 2.2 Temporal coverage of data available for the study period (2003–2015) (a). Its probability density function (b). Histogram of the data gap lengths for the period (2003–2015) in Southern Europe (c).

Several atmospheric, geophysical and hydrological variables are related to SM and can help capture its variability across space and time (Korres et al., 2013; Sandholt et al., 2002; Wang et al., 2007, 2017). In this study, the LST, NDVI, precipitation (P), potential evaporation (Ep) and soil texture were used to estimate the missing values of the CCI SM database (Table 2.1). The databases of these variables were chosen with the criteria of providing the longest temporal coverage and the fewest data gaps. Furthermore, remote sensing estimations rather than models were chosen when possible to avoid including additional uncertainties in the SM estimations. In addition, values were filtered using the provided quality flags to keep only the pixels with the highest quality. Due to the spatial resolution differences among the products used, all databases were projected to the WGS84 coordinate system and resampled into a common 0.25° grid by averaging the pixel values. This is a common and well-accepted practice when dealing with coarse resolution remote sensing data (Liu et al., 2020; Qu et al., 2019; Sandholt et al., 2002). In addition, the 16-day NDVI product was interpolated and the hourly LST product was averaged to obtain daily series. *In situ* SM data were also used to validate the CCI SM reconstructed series following the methodology of González-Zamora et al. (2019). For this, four SM networks of the ISMN over the south of Europe were used: REMEDHUS network (González-Zamora et al., 2016) located in Spain, the TERENO network (Zacharias et al., 2011) in Germany, the UMBRIA network (Brocca et al., 2008) in Italy, and the ORACLE network (Tallec et al., 2015) in France.

Table 2.1 Characteristics of the datasets used in the study.

Variable	Units	Product	Spatial resolution	Temporal coverage	Temporal resolution	Reference
SM	m^3m^{-3}	CCI SM combined v4.5	0.25°	1978/11/01 - 2018/12/31	1 d	(Dorigo et al., 2017; Gruber et al., 2019, 2017)
LST	K	LSA-001 CM SAF	0.05°	1991/01/01 - 2015/12/31	1 h	(Duguay–Tetzlaff et al., 2017)
P	mm	GPM IMERG Final Precipitation L3 v06	0.1°	2000/06/01 - Present	1 d	(Huffman et al., 2020)
NDVI	----	MOD13A2 v6	1 km	2000/02/18 - Present	16 d	(Didan et al., 2015)
Ep	mm/d	GLEAM ET v3.3 b	0.25°	2003/01/01 - 2018/09/30	1 d	(Martens et al., 2017; Miralles et al., 2011)
Soil texture	%	European Soil Data Centre (ESDAC) LUCAS topsoil	500 m	-----	-----	(Ballabio et al., 2016)

2.2.2. Gap-filling techniques

The gap-filling techniques chosen for this study were (i) linear interpolation, (ii) cubic interpolation, (iii) SVMs and (iv) SVMs combined with PCA. Furthermore, in the SVMs, an analysis of different combinations of input variables was carried out. The combination of inputs with the best accuracy was used to evaluate the random forest (RF) method. With the aim of evaluating the performance of the different methods, a holdout cross-validation was performed with nine replicates (Browne, 2000; Pérez-Planells et al., 2015). SM values were separated into the training and the test subsets (70% and 30% of the existing values, respectively). The partition of the datasets randomly reproduced the spatiotemporal distribution of the CCI SM gaps of the study area and is the same for all the methods to ensure robustness and consistency in the inter-comparisons. Once the reconstructed SM series were obtained from the training set, the new values were validated with the test set. The statistics calculated for the validation assessment with the test set were the Pearson correlation coefficient (R), the average error bias, the root mean square error (RMSE) and the centered RMSE (cRMSE). The last three are expressed in volumetric units (m^3m^{-3}). These metrics are commonly used in satellite SM validation exercises (Entekhabi et al., 2010b).

2.2.2.1. Interpolation methods

For the spatial domain, the objective was to complete each daily map of the CCI SM series. Delaunay triangulation-based 2-D linear interpolation (LI) and cubic interpolation (CI) were carried out to achieve this goal. Additionally, the missing values in the temporal domain (i.e., from each pixel time series) were estimated by using an LI and a CI by splines. This last algorithm preserves the monotony of the data in an interval by using a cubic function (Fritsch and Carlson, 1980).

For the temporal domain, an autoregressive (AR) model was used. This model performs interactive gap-filling to the temporal missing values by extrapolating data iteratively and has proven to obtain statistically consistent results (Rigling, 2012).

2.2.2.2. Support vector machine method

SVMs are based on statistical learning theory (Vapnik, 1995) and are commonly used for different applications, such as classification, regression estimation or pattern recognition (Camps-Valls et al., 2004; Gómez-Chova et al., 2010; Pal, 2006; Xie et al., 2008) . This technique was first developed for classification problems with the idea of obtaining the optimum separating hyperplane that maximizes the margin between patterns. Only the points that lie in the margin define the hyperplane, i.e., the data points most difficult to classify (Dibike et al., 2001). Later, it was developed for regression problems, where the goal consists of finding a function $f(x)$ that describes the dependency between the inputs (x_i) and the target output y with at most an ε deviation and at the same time being as flat as possible (Smola and Schölkopf, 2004). Last, to consider nonlinear relationships, the

kernel functions were added to the SVM algorithm. In this study, a Gaussian kernel function was used for that purpose and all the input variables were standardized before their incorporation to the models.

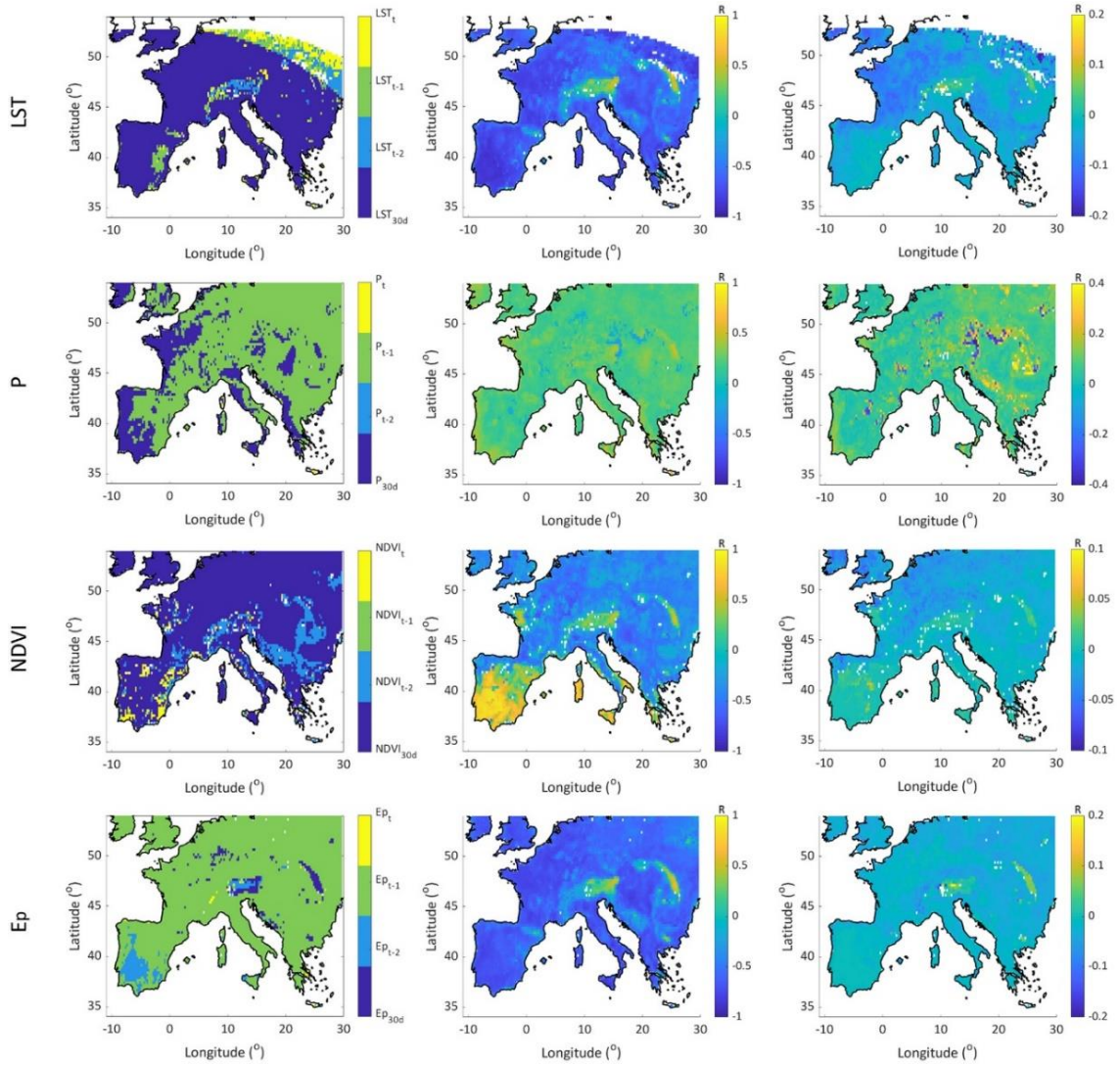

Figure 2.3 Relationship between the ESA CCI SM and complementary variables LST, P, NDVI and Ep (from top to bottom). Maps on the left column show the type of series with the strongest correlation with SM for each pixel. Maps in the middle column show the value of the Pearson correlation coefficient (R) of the majoritarian type of series in the left maps. The maps on the right column show the difference between the maximum R and the second highest R.

The SVM method has been extensively used in the remote sensing field due to its ability to generalize (Mountrakis et al., 2011), even with small training datasets. It has also proven to be a useful tool in SM estimation (Ahmad et al., 2010; Gill et al., 2006). Here, we implement the SVM model to estimate the missing values of the CCI SM series using all the variables of Table 2.1 as inputs. Khellouk et al. (2019) used these same variables to model SM with multiple linear regression methods. Nevertheless, not all the relationships between these variables and SM are linear, and sometimes disagreements exist between the changes in these variables and the SM response (Daly and Porporato, 2005). For this reason, a previous evaluation of these relationships was made. The level of correlation between the

SM series and the complementary variables (X) series was studied in four different scenarios (the coincident series X_t, the series one day before X_{t-1}, the series two days before X_{t-2} and the series smoothed by averaging with a centered 30-day window X_{30d}). For each pixel, the correlation of SM with the different series of each variable was determined. The series with the highest correlation was identified, and the difference between the maximum correlation and the second highest correlation was calculated for each variable (Figure 2.3). In view of the results, the series of LST_{30d}, P_{t-1}, $NDVI_{30d}$ and Ep_{t-1} were chosen since they provided the highest correlation for most of the pixels in the south of Europe. For NDVI, we decided to use the coincident series since it was already a smoothed series due to the daily interpolation of 16-day average values, and the differences obtained between the two maximum correlations were not remarkable.

In order to evaluate the ability of the SVM algorithm to estimate missing SM values, input variables were grouped. This approach allowed us to detect the crucial input variables for the SM estimation or those that could be expendable in the model. The groups were chosen based on the type of variables used; dynamic *d* (LST, P, NDVI and Ep), static *s* (soil texture and coordinates) or all of them *a* and on whether they used the SM_{t-1} series *h*. Thus, six groups were created for the spatial study *S* (*Sdh*, *Sd*, *Ssh*, *Ss*, *Sah* and *Sa*) and two were created for the temporal study *T*, where dynamic variables were used (*Td* and *Tdh*) (see Table 2.2).

A combination of SVM with PCA was also carried out. All input variables were considered for the analysis, i.e., group *Sah* for spatial and group *Tdh* for temporal. The components explaining up to 95% of the variance were used as inputs to the SVM model.

Table 2.2 Groups of input variables used to estimate missing SM values with the SVM model in the spatial and temporal domains.

	SVM	**Inputs**
Spatial	*Sah*	SM_{t-1} +LST_{30d} + P_{t-1} + $NDVI_{30d}$ + Ep_{t-1} + Soil texture + Latitude + Longitude
	Sa	LST_{30d} + P_{t-1} + $NDVI_{30d}$ + Ep_{t-1} + Soil texture + Latitude + Longitude
	Ssh	SM_{t-1} + Soil texture + Latitude + Longitude
	Ss	Soil texture + Latitude + Longitude
	Sdh	SM_{t-1} +LST_{30d} + P_{t-1} + $NDVI_{30d}$ + Ep_{t-1}
	Sd	LST_{30d} + P_{t-1} + $NDVI_t$ + Ep_{t-1}
Temporal	*Tdh*	SM_{t-1} +LST_{30d} + P_{t-1} + $NDVI_{30d}$ + Ep_{t-1}
	Td	LST_{30d} + P_{t-1} + $NDVI_{30d}$ + Ep_{t-1}

2.2.2.3. Random forest method

The RF consists on a combination of independent tree predictors that depend on random vectors with the same distribution for all trees but that are sampled independently (Breiman, 2001). As the SVM, this method can be applied to both classification (Pal, 2005) and

regression problems (Mutanga et al., 2012). In this study, the RF regression with 500 tree predictors was used to fill CCI SM gaps. The accuracy of the method was measured in the same way as for the other methods, thus the internal errors and correlation of the RF model were not considered. This ensured the results obtained with the different approaches are comparable. The combinations of input variables chosen for the spatial and temporal domain were the ones leading to the best estimates of SM using the SVMs.

2.3. Results and discussion

2.3.1. Temporal analysis

Six different approaches were evaluated (LI, CI, AR, SVM-*Tdh*, SVM-*Td* and SVM-PCA) to complete the CCI SM missing data in the temporal domain, i.e., to complete the time series of each pixel individually. The obtained parameters in the cross-validation analysis (Figure 2.4) show a good relationship between the estimated SM and the original SM CCI series for most of the pixels. The medians of R obtained in each approach range between 0.64 and 0.82 for CI and SVM-*Tdh*, respectively. The medians of the biases are practically zero in all cases. Some pixels provided negative (underestimation) and positive (overestimation) biases, but they very rarely exceeded 0.01 m^3m^{-3} in absolute values. There were hardly any differences between the RMSE and cRMSE due to the low bias; its medians range from 0.036 to 0.026 m^3m^{-3} for SVM with PCA and SVM-*Tdh*, respectively. These results are in line with those reported by Dumedah et al. (2014). The simplest methods resulted in the lowest accuracy, and the best results were obtained using a nonlinear autoregressive neural network, comparable to SVM-*Tdh*. When validation with the *in situ* SM series was performed (see Table 2.3), good accordance was obtained with SM CCI combined v4.5 product despite of the data gaps. Moreover, when reconstructed series were validated, the results obtained were also very similar to all the approaches. However, the correlation increases in most cases with the reconstructed CCI series by the SVM-*Tdh*, while the bias slightly increases or decreases, depending on the network. These results confirm that the SVM-*Tdh* method allows us to recreate the temporal dynamics of the original series without introducing significant errors.

Table 2.3 Validation of the CCI SM series, original and reconstructed in the temporal domain, with in situ networks (ORA, ORACLE; TER, TERENO; REM, REMEDHUS; UMB, UMBRIA).

CCI SM	**R**				**BIAS (m^3m^{-3})**			
	ORA	**TER**	**REM**	**UMB**	**ORA**	**TER**	**REM**	**UMB**
Original	0.51	0.63	0.83	0.63	-0.014	0.019	-0.099	-0.004
LI	0.50	0.60	0.84	0.66	-0.015	0.019	-0.100	0.001
CI	0.50	0.59	0.84	0.66	-0.015	0.019	-0.100	0.001
AR	0.50	0.62	0.84	0.68	-0.015	0.018	-0.101	0.001
SVM *Tdh*	0.49	0.65	0.84	0.71	-0.016	0.018	-0.100	-0.001
SVM *Td*	0.48	0.64	0.83	0.70	-0.016	0.018	-0.101	-0.001
SVM PCA	0.50	0.65	0.82	0.67	-0.014	0.018	-0.101	-0.001

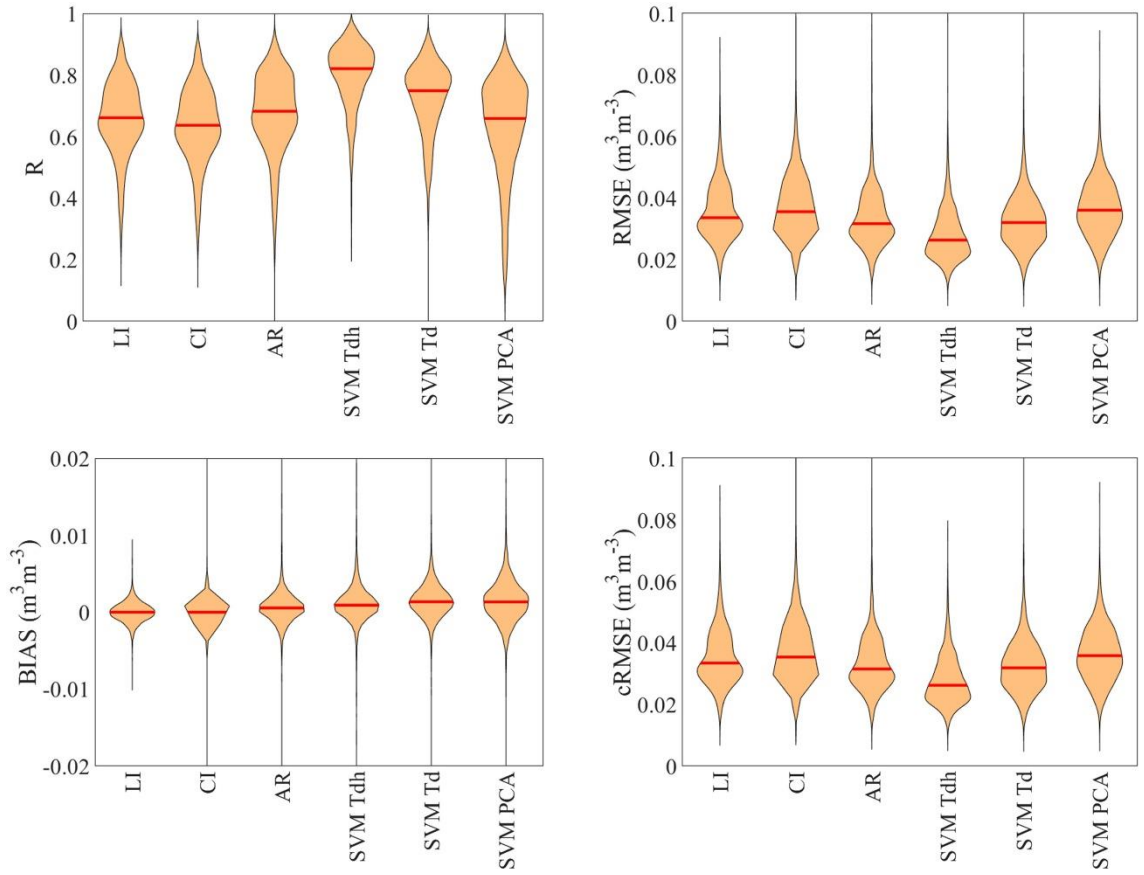

Figure 2.4 Statistical parameters of the cross-validation obtained for the six approaches of the CCI SM gap-filling procedure in the temporal domain.

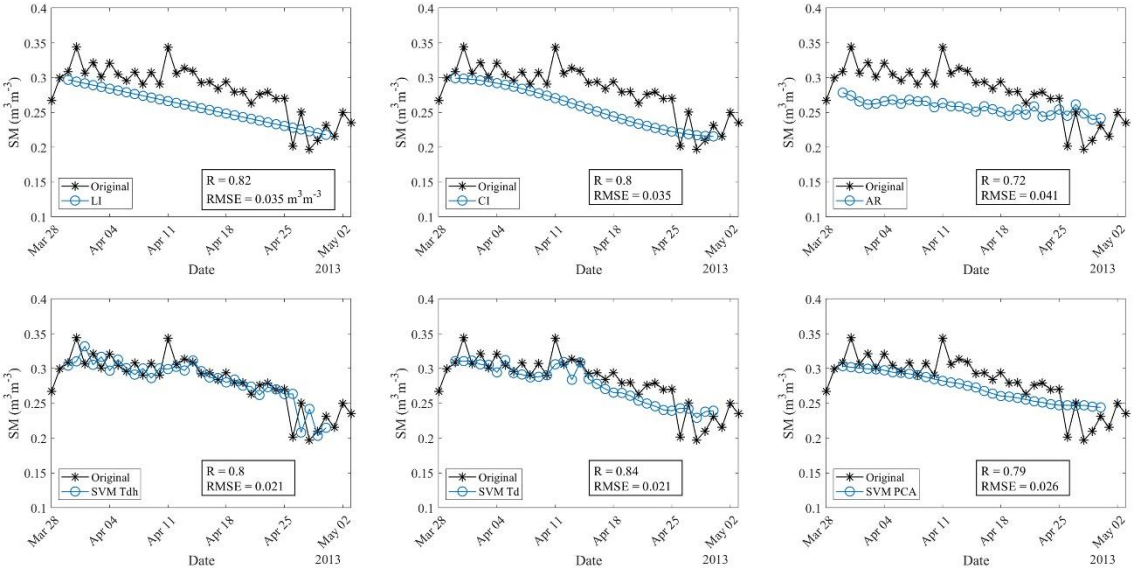

Figure 2.5 Pixel SM series reconstruction for each temporal approach. The original CCI SM series (black) and the reconstructed series according to a test set (blue) are shown for a period of three months.

While the obtained statistical scores seem to prove the effectiveness of all methods, a further examination of the results reveals that some of them might not be adequate. The LI, CI and AR methods have the advantage of being simple algorithms that require little processing time and do not need any auxiliary variables. However, we observed that their accuracy was compromised when dealing with large gaps (Figure 2.5). Among ML-based algorithms, the SVM with the original variables (no PCA applied) could capture the temporal dynamics, while the SVM with PCA failed. These results suggest that PCA is not well suited for this problem, perhaps because all variables are interdependent or because the number of variables used in the PCA is not high enough and the resulting principal components introduce noise to the SVM models. The SVM without PCA worked best, the chosen variables had already shown their ability to capture the SM dynamics (Khellouk et al., 2019), and the SVM could reproduce it. A clear improvement is seen when the SM_{t-1} series is incorporated into the SVM, in agreement with previous studies (Gill et al., 2006). Thus, the SVM-*Tdh* has proven to be the most efficient and accurate approach. The R obtained is higher than 0.7 in 85% of the study area, similar to that obtained by Cui et al. (2019) and Wang et al. (2012). An analysis of the spatial distributions of R showed that the poorest values were located in mountainous regions and highest values of RMSE were obtained in coastal areas and in the Balkan Peninsula (Figure 2.6). We observed that values of R lower than 0.6 corresponded to pixels with noisy SM series, i.e., with non-seasonal behaviour or with a high uncertainty of the original CCI SM values. This result suggests that the gap-filling performance depends on the quality of the original SM values to some extent. In fact, the mean CCI SM uncertainty and the RMSE obtained for each pixel showed a correlation coefficient of 0.78. A negative relationship between the correlation coefficient of the gap-filling method and the percentage of available data also exists but is lower (R = -0.64). This result could be attributed directly to the introduction of the SM series in the algorithm. However, this was also observed with all the methods. Ahmad et al. (2010) obtained lower accuracies at stations with a high vegetation density using SVMs. In this study no significant relationship was found between the accuracy and the mean values of NDVI, but a relationship was found between the RMSE obtained with all the methods and Ep mean values (R ranging between 0.51 and 0.64).

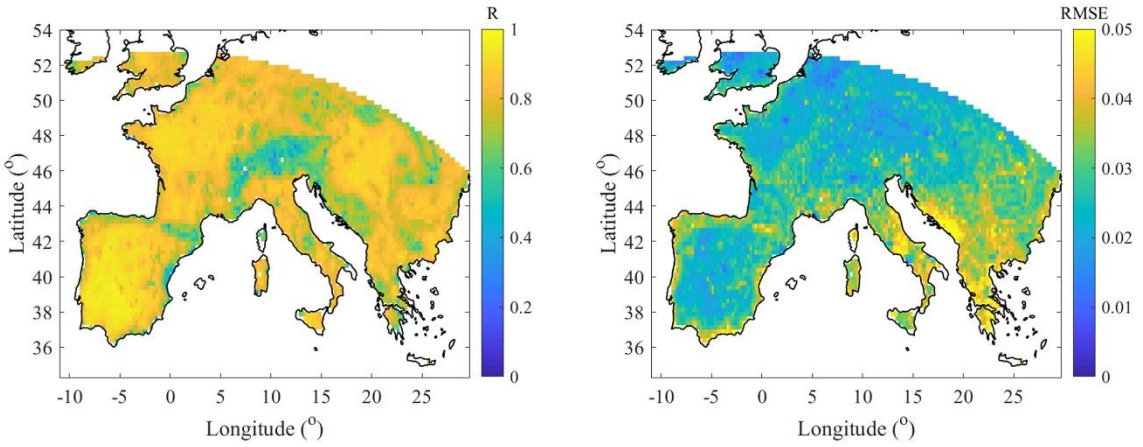

Figure 2.6 Spatial distribution of R (right) and RMSE (left) obtained with SVM Tdh in the temporal series study.

Table 2.4 Median values of the best combination for each group for the input variable combination analysis in the temporal domain.

Nº Variables	Combination	R	bias (m^3m^{-3})	RMSE (m^3m^{-3})	cRMSE (m^3m^{-3})
5	SM_{t-1}, LST_{30d}, P, $NDVI_{30d}$, E_p	0.834	0.000	0.025	0.025
4	SM_{t-1}, LST_{30d}, P, $NDVI_{30d}$	0.831	0.000	0.026	0.025
3	SM_{t-1}, LST_{30d}, P	0.826	0.000	0.026	0.026
2	SM_{t-1}, LST_{30d}	0.798	0.000	0.026	0.026
1	SM	0.755	-0.001	0.028	0.028

The SVM-*Tdh* has been proven to be accurate enough to complete the CCI SM series gaps for the study period. However, the availability of complementary databases with a coincident period is probably a limitation to complete the 40-year series. The SVMs do not determine the influence of each input variable on the output variable. However, with the aim of exploring whether some of the input variables would be expendable or crucial, all possible combinations were performed, starting with all of them and progressively eliminating one at a time until only the SM_{t-1} remained, similar to what (Yang et al., 2006) did. A total of 16 combinations were tested, and they were separated into groups based on the number of variables, which ranged from 5 to 1. The best results were obtained with the five variables (Table 2.4), i.e., with the original SMV-*Tdh* approach, but hardly any differences were observed with the remaining combinations. The accuracy was slightly reduced as the number of variables decreased.

Moreover, it was observed that the variables of the best datasets were consistent, showing more importance to LST, followed by P, NDVI and Ep (not shown). These results imply that it is possible to obtain good performance with the SVM model even if some of the input variables are not available. As expected, using only SM is not enough, and the results obtained in this case are equivalent to those obtained with simple interpolations.

2.3.2. Spatial analysis

For the spatial domain, missing values were estimated by applying a total of nine approaches to each CCI SM daily image. These methods were LI, CI, SVM-*Sah*, SVM-*Sa*, SVM-*Ssh*, SVM-*Ss*, SVM-*Sdh*, SVM-*Sd* and SVM with PCA (Table 2.2). The results of the cross-validation analysis show that most methods yield adequate SM estimations (Figure 2.7). The median values of R ranged between 0.48 and 0.88 for SVM with PCA and SVM-*Ssh*, respectively. The bias values, as for the temporal domain, are practically zero in all cases, implying few differences between the RMSE and cRMSE values. The RMSE and cRMSE medians range between 0.043 and 0.024 m^3m^{-3} for SVM with PCA and SVM-*Ssh*, respectively. These results are similar to those obtained by (Llamas et al., 2020), who reported higher RMSE values than those obtained with SVM-*Ssh* and similar

correlation coefficients with the ordinary kriging and regression kriging methods. In addition, their results with the generalized linear models showed lower R and higher RMSE than those obtained with LI and CU. Although our results cannot be directly comparable as they were focused on different study regions, they nonetheless provide an idea about the quality of each method to estimate the missing CCI SM values. The results obtained in the validation with *in situ* data (see Table 2.5) showed lower correlations between the reconstructed series and the ground measurements when using any of the interpolation methods. However, SVMs without using SM_{t-1} series offer similar results as the interpolations approaches (Figure 2.7). When the SM_{t-1} is used, the reconstructed series validation results barely differ from the ones obtained with the original series, confirming a good ability to estimate the CCI SM missing values in this input data configuration.

Again, it was observed that the SVM method performed better than the other methods but only when SM_{t-1} was used. SVM with PCA, as was found with the temporal domain, showed the poorest SM estimations (Figure 2.8). In addition, similar results were obtained with SVM-*Sd* (i.e., dynamic variables as inputs and without the SM_{t-1} series). Hence, it follows that the SVM method is not capable of accurately simulating the spatial dynamics of SM without previous information on SM. Nevertheless, when static variables are added to the SVM (*Sah*, *Ssh*), the results improve.

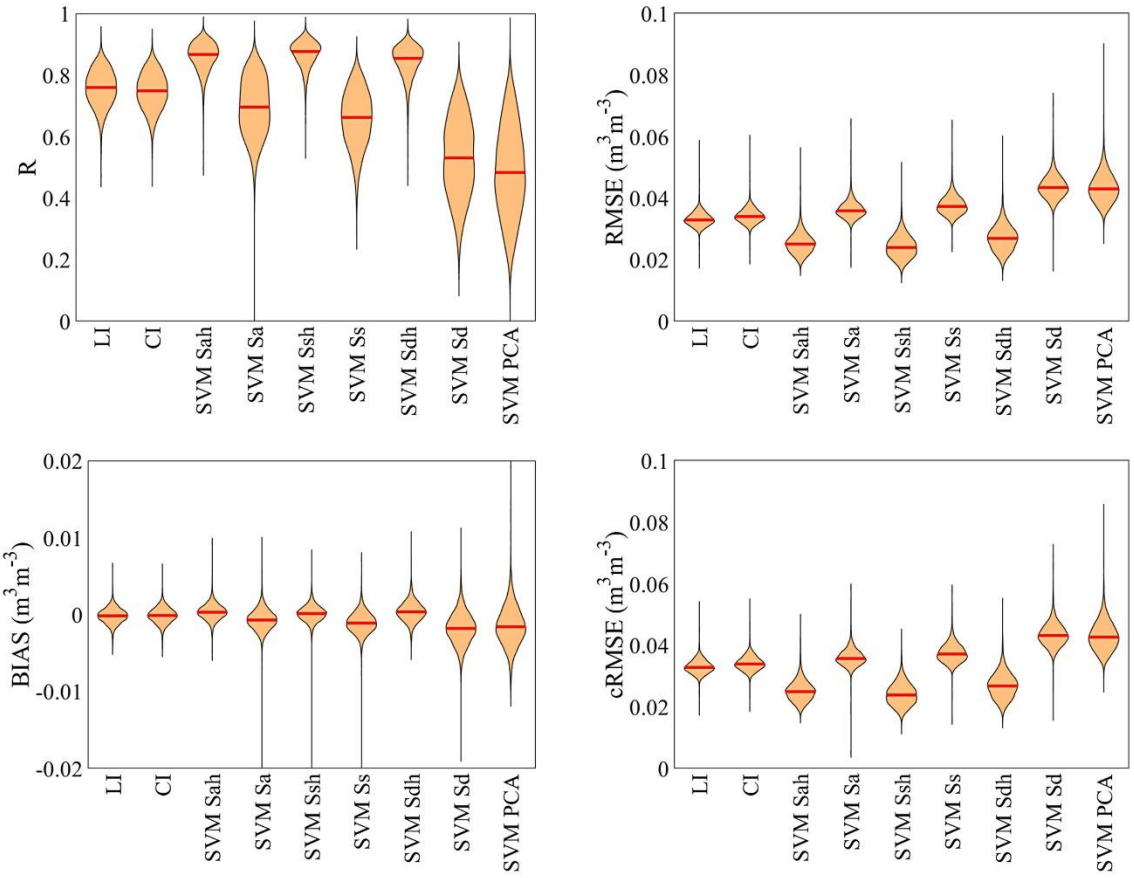

Figure 2.7 Statistical parameters of the cross-validation obtained for the nine approaches of the CCI SM gap-filling procedure in the spatial domain.

Table 2.5 Validation of the CCI SM series, original and reconstructed in the spatial domain, with in situ networks (ORA, ORACLE; TER, TERENO; REM, REMEDHUS; UMB, UMBRIA).

CCI SM	R				BIAS (m^3m^{-3})			
	ORA	TER	REM	UMB	ORA	TER	REM	UMB
Original	0.51	0.63	0.83	0.63	-0.014	0.019	-0.099	-0.004
LI	0.50	0.56	0.80	0.63	-0.015	0.021	-0.095	-0.003
CI	0.49	0.55	0.79	0.62	-0.015	0.021	-0.095	-0.002
SVM Sah	0.51	0.64	0.83	0.66	-0.012	0.019	-0.099	-0.001
SVM Sa	0.50	0.63	0.82	0.68	-0.014	0.020	-0.098	-0.008
SVM Ssh	0.51	0.64	0.83	0.66	-0.012	0.019	-0.099	-0.001
SVM Ss	0.51	0.62	0.82	0.67	-0.014	0.021	-0.098	-0.011
SVM Sdh	0.51	0.64	0.83	0.66	-0.012	0.019	-0.099	0.000
SVM Sd	0.50	0.64	0.82	0.70	-0.014	0.020	-0.098	-0.005
SVM PCA	0.51	0.65	0.81	0.63	-0.014	0.017	-0.096	-0.007

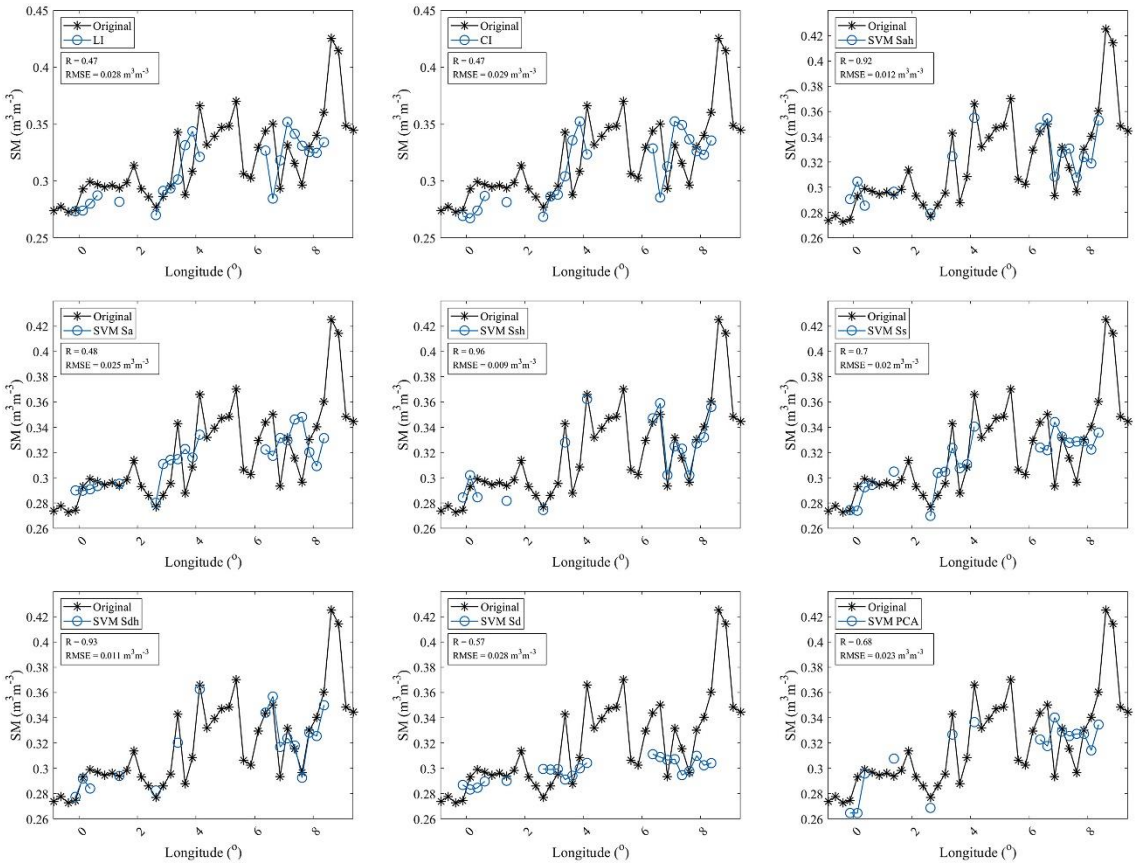

Figure 2.8 A transect for latitude 47.875° of the November 10, 2012, SM series reconstruction for each spatial approach. The original CCI SM series (black) and the reconstructed series according to a test set (blue).

These variables describe the soil properties and place SM values in space. SVM-*Ssh* obtained slightly better results than did SVM-*Sah*. Although differences in accuracy are small, SVM-*Ssh* has the advantage of using the lowest number of variables. Furthermore, the constraint of the availability of auxiliary databases with a coincident period with that of the CCI SM series disappears. To our knowledge, this is the first study that applies ML techniques in the spatial domain to estimate SM; therefore, we cannot compare our obtained results with those obtained using similar approaches. It should be noted that although the vast majority of gap-filling studies do not consider the use of only static layers, our results show that this could be a promising rapid and good approach to address this problem.

An analysis for assessing the relevance of the input variables was also carried out for SVM-*Ssh*, the best performing approach in the spatial domain. Six variables were combined and evaluated in groups, as was done for the temporal domain. In total, 32 combinations in 6 groups were studied, always using the SM_{t-1}. The best result obtained for each group was very similar in all cases (Table 2.6). Unlike the temporal study, the most accurate estimations were not obtained with the original combination of variables, that is, with the six variables, but with using only the geographic coordinates of each pixel and the sand content. This result implies that the SVM method could be simplified by reducing the number of input variables and reach comparable performances.

Table 2.6 Median values of the best combination for each group for the input variable combination analysis in the spatial domain.

Nº Variables	**Combination**	**R**	**bias** (m^3m^{-3})	**RMSE** (m^3m^{-3})	**cRMSE** (m^3m^{-3})
6	SM_{t-1}, sand, clay, silt, lat., lon.	0.875	0.000	0.024	0.024
5	SM_{t-1}, sand, silt, lat., lon.	0.878	0.000	0.024	0.024
4	SM_{t-1}, sand, lat., lon.	0.879	0.000	0.024	0.024
3	SM_{t-1}, lat., lon.	0.869	0.000	0.025	0.025
2	SM_{t-1}, lat.,	0.836	0.000	0.027	0.027
1	SM_{t-1}	0.818	0.000	0.029	0.029

2.3.3. Random forest with the best combination of input variables

The selection of the input variables to the SVM has been key to obtain good estimates of SM. To test the capacity of other non-linear approaches to estimating CCI SM missing values, RF was evaluated using the best combination of input variables obtained with SVMs for spatial and temporal domains. Thus, for the temporal domain, the variables of the SVM-*Tdh* approach were used and for the spatial, the coordinates and the sand content together with the SM_{t-1} series were used. The results (Figure 2.9) show that for the temporal domain the correlation is similar to that obtained with the SVM-*Tdh*, while the errors are slightly higher with a median of RMSE = 0.029 m^3m^{-3}. RF has proven to be a good tool

when estimating SM series in other studies (Long et al., 2019; Zhao et al., 2018) and results obtained here are in line with them. However, the SVM showed to be more accurate. On the contrary, the RF in spatial domain do not seem to be as accurate as SVM. The median of R obtained with RF is 0.76, while with SVM is 0.88. The bias and the errors obtained with RF are also higher, which indicates that RF in the spatial domain is not able to generalize as well as the SVM.

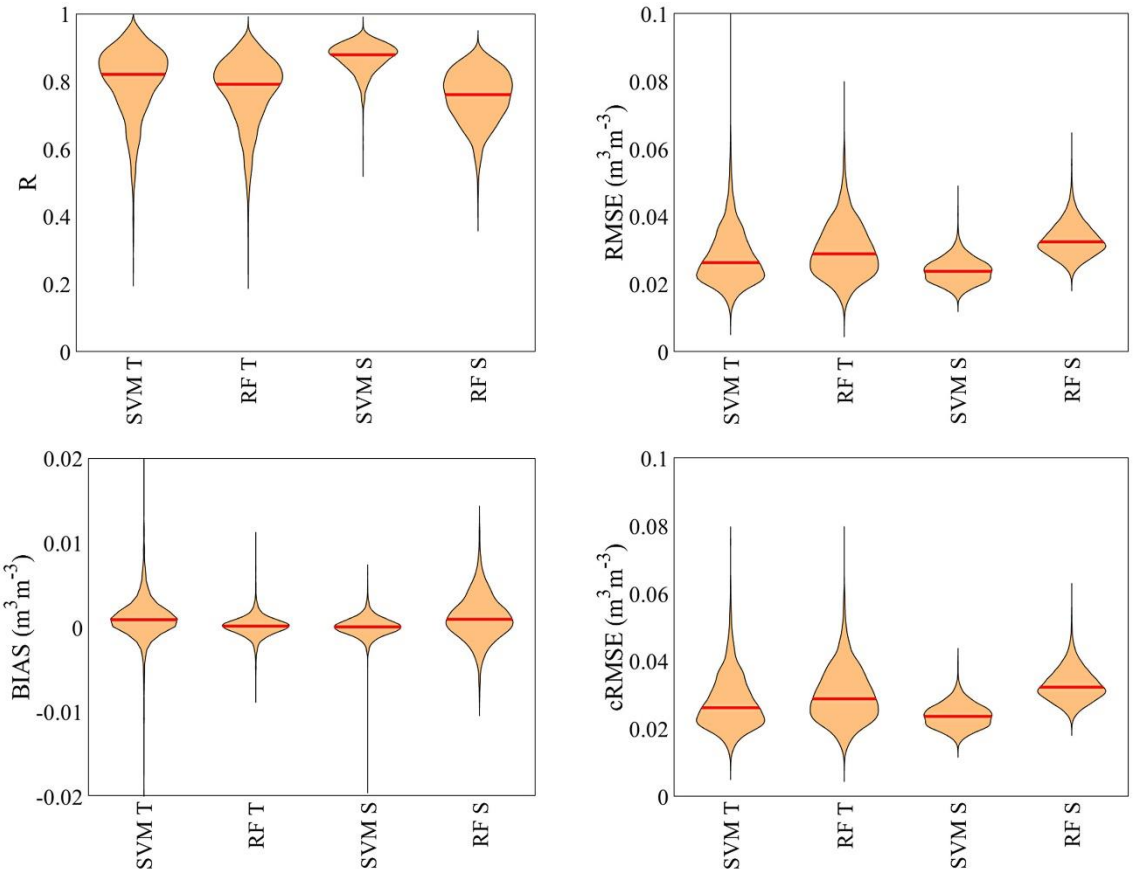

Figure 2.9 Statistical parameters of the cross-validation obtained for RF and SVM with best combination of input variables in the spatial (S) and temporal (T) domain.

2.3.4. Comparison of the most accurate spatial and temporal approaches

In general, all the methods and the different approaches studied in this work have proven to be valid gap-filling techniques for the CCI SM series. However, some of them reconstructed the time series with greater precision, specifically the SVM methods. For the temporal domain study, the SVM using all the dynamic auxiliary variables and the SMt-1 as inputs provided the best results. For the spatial domain study, the SVM with only the coordinates, sand content and SM of the day before as inputs was the most efficient. The percentiles of the parameters obtained in the cross-validation analysis were calculated with the aim of comparing the performances of the two approaches (Figure 2.10). The correlation was greater for the spatial approach in all of the cases, and the RMSE was

slightly lower. In addition, we observed that the temporal approach presented more outliers than the spatial approach. This result is possibly due its relationship with the uncertainty of the original CCI SM value in the temporal approach, while the spatial approach unifies all the pixels and, consequently, leads to more stable estimates. Despite being an uncommon approach, in terms of accuracy, the SVM applied in the spatial domain seems to be more appropriate to reconstruct CCI SM series.

Regarding the applicability of the methods, on the one hand, the temporal approach enables the completion of the series of each pixel, while the spatial approach depends on the availability of the SM value of the day before. Hence, it would be necessary to iteratively calculate the SM as is done in the temporal approach, but the quantification of the accuracy of each model would not be plausible since many SVM models would be mixed (one for each day). On the other hand, the spatial approach has the advantage of using only static auxiliary variables and could be used seamlessly to complete the 40 years of the CCI SM series. However, the precision of the method likely decreases in the early years of the series, where data availability is very low. This should be the subject of further research. Additionally, the spatial approach cannot be conducted on days where no SM value is available in an entire region, unlike the temporal approach where there will always be values for a given pixel. In summary, the performance of the two kinds of approaches may be linked to the data availability for a specific region and period, but the two are complementary and show great potential in terms of estimating the missing values in the CCI SM database.

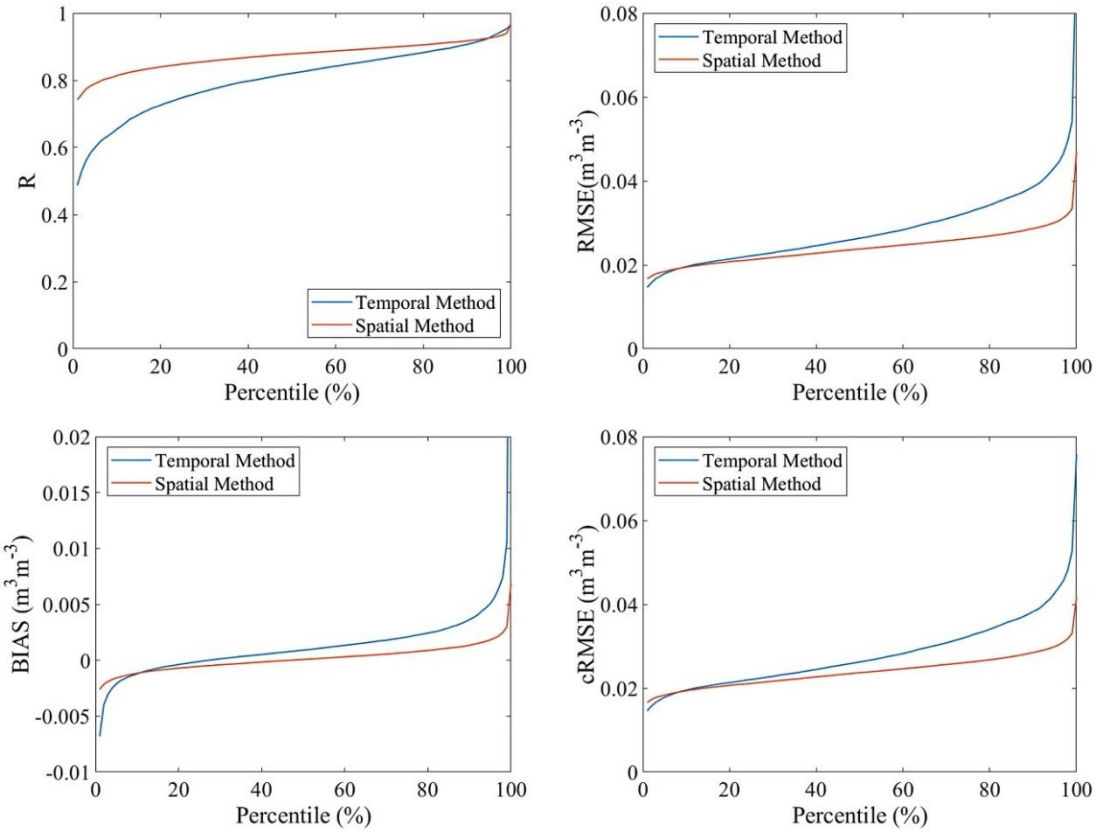

Figure 2.10 Percentiles of the cross-validation analysis parameters for the most accurate temporal (blue) and spatial (orange) approaches evaluated in this work.

2.4. Conclusions

The CCI SM database is currently the longest available data record of satellite soil moisture. However, its applicability is often compromised due to its spatiotemporal gaps, which depend mostly on the available satellites across its 40-year period. In this paper, gap-filling techniques of different complexities have been applied to ESA CCI SM data over Southern Europe for the period 2003–2015. Methods focused on the spatial and temporal domains have been explored and compared. Our results show that interpolation methods in both the temporal and the spatial domains have the advantage of being simple. However, when dealing with large spatial or temporal gaps, they failed. The autoregressive method in the temporal study somewhat improved the estimates obtained by the interpolations but could not address the large data gaps. In contrast, SVMs have proven to be a very robust technique for estimating missing values, especially in the spatial domain, and the accuracy of the estimates hardly depends on the gap length. The effectiveness of the SVMs had previously been tested on *in situ* SM databases but never on satellite databases. The choice of input variables for the SVM has been shown to have an impact on the method's performance. Using the SM_{t-1} series has proven to be key to obtaining good estimations in both temporal and spatial analysis. The application of PCA to input variables did not improve the performance and actually led to significantly worse results. In addition, the RF were not able to reproduce the spatial dynamics of the SM as well as the SVM did, and the obtained precision was slightly lower than the SVM when applied in the temporal domain.

For the temporal study, it was observed that the chosen variables were able to reproduce the SM dynamics. In particular, LST and precipitation proved to be a crucial variable since the accuracy always decreased when it was not incorporated. This result suggests that SVMs are able to capture the nonlinear relationship between the dynamics of the two variables. Interestingly, the variables used in the temporal approaches did not prove to be as useful in the spatial domain, where the best results were obtained with variables describing the spatial distribution of soil physical properties and antecedent SM. When evaluating the relevance of input variables, we obtained the best results when only the coordinates together with sand content and the SM one day before were incorporated into the SVM. This approach presents an advantage since the number of input variables is reduced, and therefore, the SVM model is simplified. However, it has been shown that the two approaches are complementary, so a combination of them could resolve some of their limitations. This assumption might be addressed in future studies.

The applicability of all the methods has been validated, and the results are satisfactory. We proved that, despite being an uncommon approach, the SVMs in the spatial domain, with the appropriate input variables, can be a suitable method used to fill the gaps in the CCI SM database. Thus, this approach can be used to obtain a long-term SM satellite-derived series with homogeneous coverage, meaning there are fewer limitations in applications where data gaps are a problem. Overall, our results demonstrate the applicability of ML approaches for gap-filling multidecadal soil moisture observational data records and highlight the value of exploiting both the temporal and the spatial domains.

CAPÍTVLO 3

ANALYSIS OF SOIL MOISTURE TRENDS IN EUROPE USING RANK-BASED AND EMPIRICAL DECOMPOSITION APPROACHES

Almendra-Martín, L., Martínez-Fernández, J., Piles, M., González-Zamora, Á., Benito-Verdugo, P., Gaona, J., 2022. Analysis of soil moisture trends in Europe using rank-based and empirical decomposition approaches. Glob Planet Change 215. https://doi.org/10.1016/j.gloplacha.2022.103868

Resumen

El impacto del cambio climático en la dinámica de la humedad del suelo (SM, *soil moisture*) es incierto. Durante las últimas décadas se han estudiado los cambios de la SM de la Tierra, de forma global y en diferentes regiones, pero Europa ha recibido poca atención. Además, la mayoría de los trabajos previos han evaluado solo el comportamiento monotónico de los cambios de la SM, algo que supone una asunción taxativa y que no siempre es válida. En este trabajo se argumenta que este hecho, junto con el uso de escalas temporales largas, ha dificultado la observación de patrones claros en las tendencias de la SM en el continente. En este trabajo, se estudian las tendencias de la SM de Europa en un periodo de 30 años, desde 1991 hasta 2020, usando dos bases de datos complementarias, una del proyecto de reanálisis ERA5-Land y otra del modelo LISFLOOD. Se consideraron y aplicaron dos enfoques basados en rangos y una descomposición empírica a las series de anomalías mensuales y anuales de SM. La clasificación de Köpen-Geiger ayudó a analizar la distribución de las tendencias de las anomalías de SM entre los diferentes climas europeos. Los resultados obtenidos con ambas bases de datos, métodos y escalas temporales fueron consistentes, siendo el método de descomposición empírica el que, generalmente, detectaba más tendencias significativas. Los resultados muestran una tendencia decreciente general de la SM, independientemente del tipo de clima, pero más intensa en Europa del este y central. Además, el método basado en rangos detectó menos tendencias positivas significativas, lo que sugiere que los cambios a condiciones más húmedas tienen un comportamiento no monotónico. Las diferencias más notables se obtuvieron con el método de descomposición empírica cuando se compararon las diferentes escalas temporales. Por esa razón, se realizó un análisis intra mensual para aclarar los diferentes patrones. Un aumento en tendencias significativas se observó en el mes de abril y en el otoño (septiembre-octubre-noviembre). Además, se realizó un análisis similar para estudiar las tendencias de las características sequías extremas (duración, intensidad y comienzo) y se obtuvieron resultados consistentes, siendo el método de descomposición empírica el que detectó más tendencias significativas. Esta investigación muestra un aumento general de la duración y la intensidad de las sequías extremas en el continente europeo, tendiendo a retrasarse unos pocos días por año en las zonas áridas y templadas.

Palabras clave: Humedad del suelo, Tendencias, Sequía, Duración, Intensidad, *Onset*, Mann-Kendall, *Empirical mode decomposition*

Abstract

The impact of climate change on soil moisture (SM) dynamics is uncertain. Changes in the Earth's SM during recent decades have been studied globally and in different regions, but little attention has been given to Europe. In addition, most previous works have just relied on a monotonic behavior of SM changes, which is a strong assumption and not always valid. We argue that this fact, together with the use of large temporal scales, has prevented the observation of clear patterns of SM trends over the continent. In this work, we study European SM trends for a 30-year period, from 1991 to 2020, using two complementary databases, one from reanalysis project ERA5-Land and the other from the model LISFLOOD. Both rank-based and empirical decomposition approaches have been considered and applied to monthly and annual series of SM anomalies. The Köppen-Geiger classification allowed us to analyze the distribution of SM anomaly trends in the separate European climates. The results obtained with both databases, methods and temporal scales were consistent, with the empirical decomposition method generally detecting more significant trends. Our results show a general decreasing trend of SM, regardless of climate type but more intense in Eastern and Central Europe. In addition, the rank-based method detected fewer positive trends, suggesting a non-monotonic behavior in changes to wetter conditions. The most notable differences were obtained with the empirical decomposition method when comparing the different temporal scales. Hence, an intramonthly analysis was conducted to provide insight into the different patterns. An increase in significant trends was observed in April and the autumn (September–October-November). Furthermore, we conducted a similar analysis to study trends in extreme drought characteristics (annual duration, intensity and onset) and we obtained consistent results, with the empirical decomposition method detecting more significant trends. Our investigations show a general increase in the duration and intensity of extreme droughts over the European continent, tending to be delayed a few days per year in arid and temperate regions.

Keywords: Soil moisture, Trends, Drought, Duration, Intensity, Onset, Mann-Kendall, Empirical mode decomposition

3.1. Introduction

Soil moisture (SM) is considered an essential climate variable (GCOS, 2010). It exerts control on the water and energy exchange between the soil and the atmosphere, as it behaves as a storage component for precipitation and induces persistence in the climate system (Martínez-Fernández et al., 2021; Piles et al., 2022; Seneviratne et al., 2010). Climate change is predicted to disrupt many environmental and, therefore, social and economic processes (Grillakis, 2019). Subsequently, it is likely that SM dynamics will also be affected and thereby alter the availability of water for plants (Kramer, 1944), the runoff yield (Merz and Plate, 1997) or the intensity and frequency of droughts (Martínez-Fernández et al., 2015). However, the magnitude and extent of these changes are still uncertain (Cheng et al., 2017).

There are several studies dedicated to the study of the SM trend, both on global (Albergel et al., 2013; Dorigo et al., 2012; Feng and Zhang, 2015; Piles et al., 2019; Sheffield and Wood, 2007) and regional scales (An et al., 2016; Li et al., 2015; Qiu et al., 2016; Rahmani et al., 2016; Trnka et al., 2009b; Zawadzki and Kędzior, 2014). Most of those studies just analyzed a monotonic trend, but SM, as many hydroclimatic variables, exhibits nonlinear and non-stationary changes (Bai et al., 2015). Additionally, the computed trends are known to strongly depend on the period of study (Hänsel et al., 2019; Sang et al., 2014) and the temporal scale analyzed (Gudmundsson and Seneviratne, 2015; Sang et al., 2021), especially when monotonic approaches are used. Hence, the extended use of methods that just account monotonic behavior to estimate SM changes has led in some cases to discrepancies between trends of series with different time scales or periods, which are difficult to interpret and reconcile (Dai, 2013). In particular, few trends have been observed in Europe when monotonic behavior is assumed (Albergel et al., 2013; Cammalleri et al., 2016; Dorigo et al., 2012; Zawadzki and Kędzior, 2014). In contrast, trends in drought indices, runoff, temperature, precipitation or evaporation have shown statistical significance in this region (Gudmundsson and Seneviratne, 2015; Hänsel et al., 2019; Jaagus et al., 2021; Masseroni et al., 2021; Song et al., 2020; Vautard et al., 2007), which suggests that the existence of similar trends in SM would be expected. Some studies have reported SM changes in recent decades throughout Europe. For example, Cammalleri et al. (2016) found differences between the year-average deficit water in most of the European soil surface. In regional studies, Almendra-Martín et al. (2021a) observed a general decreasing trend of SM in the Iberian Peninsula, and (Trnka et al., 2009a) analyzed SM derived by precipitation and temperature *in situ* series in the Czech Republic and found a larger number of climatic stations with significant trends.

Although some studies have analyzed nonlinear trends of hydroclimatic variables (Adarsh and Janga Reddy, 2019; Bordi et al., 2009; Carmona and Poveda, 2014; Wei et al., 2018), only a few are focused on SM series. Deng et al. (2020) found a change in the SM trend at the global scale in 2001 with a changing rate twice that of the previous period. Pan et al. (2019) proposed a nonlinear approach to estimate trends based on a polynomial fit. However, the general best fit they obtained was a first-degree polynomial, namely, a linear approach. Trend identification in hydrologic time series is not a trivial task (Bordi et al.,

2009; Sang et al., 2013), and many novel methods have been used to accurately identify components in its series (Sang et al., 2014), but very few of them have accounted for nonlinear SM behavior (Bueso et al., 2020a; Cheng and Huang, 2016; Piles et al., 2019).

Unlike other hydroclimatic variables, the study of SM trends has not received special attention until recent years due to a lack of long-term and continuous databases. For the stable records of climate, it is considered that a climatological-length series is needed (Merchant et al., 2014), and few databases of SM have that length. Remote sensing databases, such as the European Space Agency Climate Change Initiative (CCI) SM, provide spatial-temporal continuous series. However, some limitations are found in such databases, such as data gaps (Almendra-Martín et al., 2021b) or breaks due to its merging algorithm (Preimesberger et al., 2021). In contrast, the latest advances in land surface modelling and assimilation of observations in reanalysis ensure the completeness of separate variables at the global scale, such as SM, to enhance research in climate change studies (Muñoz-Sabater et al., 2021).

The main objective of this work is to study the trend of SM in Europe during the last three decades (1991 to 2020). The studies published thus far on the SM trend have been on a global scale, focusing the analysis on areas of special interest such as the Sahel, Australia, India or North America (Sheffield and Wood, 2007). However, too little attention has been given to Europe despite the expected increased risk of drought on the continent (Naumann et al., 2021). The second objective of the study is the comparison between a rank-based and an empirical decomposition approach in the analysis of SM trends. For these purposes, SM trends from two databases, one from modelling and the other from reanalysis, have been studied over Europe. Two methods were used: a widely used method based on monotonic behavior, the Mann-Kendall (MK), and a novel nonlinear method, the empirical mode decomposition (EMD). The statistical significance of trends and their signs were evaluated in the different types of climate, according to the Köppen-Geiger classification. In addition, the study was conducted at different time scales (monthly and annually) to gain a full understanding of the changes in temporal SM temporal dynamics that occurred in Europe during the last 30 years, from 1991 to 2020.

3.2. Material and methods

3.2.1. Soil moisture data

Two different SM databases were used, both provided by the Copernicus Climate Change Service (C3S) but with different sources and characteristics. On the one hand, the European Centre for Medium-Range Weather Forecasts (ECMWF) reanalysis project ERA5-Land provides several land variable series, including SM. The land surface reanalysis describes the water and energy cycles over land by using the Hydrology Tiled ECMWF Scheme for Surface Exchanges over Land (HTESSEL) (Balsamo et al., 2009), and derives the atmospheric forcing from ERA5 (Muñoz-Sabater et al., 2021). ERA5-Land (for simplicity, hereafter ERA5L) is indirectly influenced by several sources of assimilated observations, satellite and *in situ* (Hersbach et al., 2020), through the atmospheric forcing. The series are provided from 1981 to the present with hourly temporal resolution and a regular grid of 0.1°. SM is estimated in 4 depth layers from 0 to 289 cm. In this work, only surface (0–7 cm) SM was studied; thus, only the first layer of the product and the data at 12 am and 12 pm were used.

On the other hand, the SM series from the hydrological rainfall-runoff model LISFLOOD (LF) were also used. This model was developed by the floods group of the Natural Hazards Project of the Joint Research Centre (JRC) of the European Commission (van der Knijff et al., 2010) and is used in the Copernicus European Drought Observatory (EDO) (https://edo.jrc.ec.europa.eu) and the European Flood Awareness System (EFAS) (Smith et al., 2016). The model can simulate the long-term water balance by considering several processes such as snow melt, infiltration, interception of rainfall, evaporation or soil moisture exchange between the soil layers, among others Commission (van der Knijff et al., 2010). In this work, the dataset produced by EFAS was used, which was produced with gridded observational meteorological data (Smith et al., 2016). The SM series are provided daily since 1991 to present with a spatial resolution of 5 × 5 km (de Roo et al., 2000). SM is estimated for 3 depth layers, but only the first layer, which refers to the first 5 cm of the soil, was considered in this study.

Both databases have been validated (Laguardia and Niemeyer, 2008; Li et al., 2020) and widely used for several applications (González-Zamora et al., 2021; Zhang et al., 2021), including the study of SM trends (Almendra-Martín et al., 2021a; Cammalleri et al., 2016). Validation studies have shown accurate estimations of SM for both products in the region of study except for high latitudes and the Alps because of the poor performance in heterogeneous landscapes and topography regions, the presence of ice cover and the limited availability of satellite data (Laguardia and Niemeyer, 2008; Li et al., 2020). In this work, a comparison between both products was conducted (results not shown). The LF database was resampled into the ERA5L grid by calculating the spatial average, and the series were compared. A good correlation was obtained, with a median value of Pearson correlation coefficient of 0.67. The poorest values were obtained for the Alps and the Scandinavian

Peninsula, in line with previous works (Laguardia and Niemeyer, 2008; Li et al., 2020). Therefore, these regions were filtered using auxiliary databases.

Taking all of this into account, trends of SM anomaly series were evaluated for the study period, 1991–2020, and the monthly and annual temporal scales were analyzed. Thus, first, the daily series of both products were averaged into these scales. Then, anomalies were calculated by subtracting the monthly and annual mean calculated using the entire period of study for each pixel.

3.2.2. Auxiliary data and mask

Some regions were excluded from the study due to different factors, such as irrigation management, areas with permanent or seasonal ice cover or regions where estimations of SM are not such accurate. For this reason, ancillary databases were used to create a mask that filters these areas.

For the irrigated areas, the Digital Global Map of Irrigation Areas of the Food and Agriculture Organization (FAO) was used. It consists of a global map with a spatial resolution of 5 arc minutes that provides the percentage area irrigated (Siebert et al., 2005). In this study, pixels with >10% irrigation area were masked.

The Köppen-Geiger classification was used both to study the distribution of SM anomaly trends in the different European climates and to mask regions with less accurate SM values due to the presence of ice cover. This classification uses 3 categories to describe the various types of climates worldwide (Peel et al., 2007). The first category contains 5 main classes that are subdivided into 30 different types of climates. In this work, the map developed by Beck et al. (2018) with a spatial resolution of 1 km was used. This map was resampled into LF and ERA5L grids using a majority filter. The rest of the climate subdivisions were merged into their more general categories until each class represented at least 1% of the area of study.

Table 3.1 Percentages of coverage in Europe of each Köppen-Geiger climate type and the mask used in the study in both SM databases spatial resolution.

Köppen-Geiger	**LF (%)**	**ERA5L (%)**
Cold - without dry season - warm summer (Dfb)	44	46
Cold - without dry season - hot summer (Dfa)	3	3
Temperate - without dry season (Cf)	22	22
Temperate - dry summer (Cs)	9	8
Arid (B)	5	5
Mask	18	17

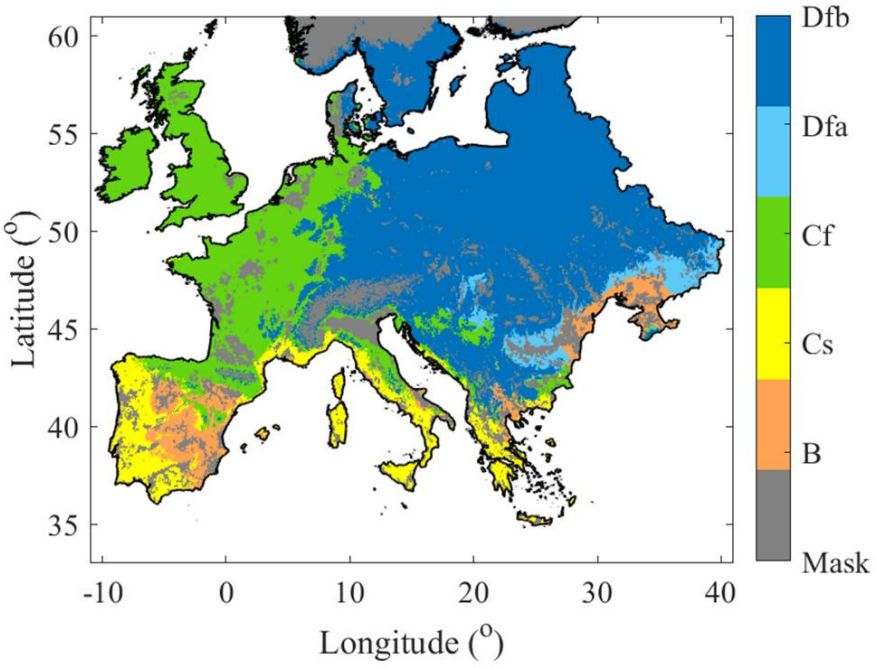

Figure 3.1 Spatial distribution of the Köppen-Geiger climate types and the mask used in the study.

Therefore, the mask was created by incorporating all the pixels considered irrigated areas and those with polar and cold – without dry season – very cold winter climate. In this way, those regions with low accuracy SM estimations for both products are excluded. The final classification used to study the SM trend distribution is shown in Table 3.1, and a map with the spatial distribution of each class is shown in Figure 3.1.

3.2.3. Drought attributes series

Since SM changes have a direct impact on the various types of droughts, their trends were also studied by analyzing the main attributes that characterize drought, namely, onset, duration and intensity. According to Sheffield and Wood (2007), a drought is defined as a period with SM quantile values below an arbitrary threshold. In this study, the threshold was set in the 10^{th} percentile (q_{10}) of the daily series of each pixel, corresponding to severe drought (Sheffield and Wood, 2008). Annual series were obtained for each attribute. Thus, duration (D) was calculated as the number of days in a year that SM had values below q_{10}. Onset series were calculated as the first day of the year on which SM presented a value below the threshold and was maintained for at least seven consecutive days. The 7-day criterium was chosen to avoid a flash drought occurring before the dry season from setting the representative onset of a specific year. Finally, intensity series were calculated as the mean magnitude over the drought duration of each year, with the magnitude of the deviation below the threshold.

3.2.4. Trend analysis

Hydrological trend identification is a challenging task usually investigated under the assumption of monotonic behavior in their interannual changes (Sang et al., 2013), but hydroclimatic series are known to change nonmonotonically. Linear trends can be heavily influenced by the period and the temporal scale of the study (Pan et al., 2019; Sang et al., 2018). Monotonic approximations, in turn, have also been proposed to study hydroclimatic series trends in the literature and have shown consistent results (Albergel et al., 2013; Dorigo et al., 2012; Li et al., 2015). In this work, two methodologies were considered to evaluate SM anomaly trends to consider both strategies, monotonic and nonmonotonic. Both methods were applied to the entire annual and monthly series of SM anomaly. In addition, interannual changes were computed for SM anomaly series by separately analyzing trends for each month.

3.2.4.1. Mann-Kendall test

The MK test (Kendall, 1948; Mann, 1945) is a nonparametric test widely used to detect trends. It identifies the monotonic upwards or downwards trend of a series and determines if it has statistical significance at a given level. The null hypothesis assumes that a given series has no trend, i.e., it is independently distributed. To accept or reject the null hypothesis, the statistic S, which determines the sign of the trend, is calculated of the following form:

$$S = \sum_{i=1}^{n-1} \sum_{j=i+1}^{n} sgn(x_j - x_i) \tag{3.1}$$

where x refers to the points of a series of lengths n, and $sgn()$ is the sign function that makes the test robust against outliers (Asfaw et al., 2018). The significance of the trend at a given significance level is given by the Z parameter obtained as follows:

$$Z = \begin{cases} \dfrac{S-1}{\sqrt{var(S)}} & S > 0 \\ 0 & S = 0 \\ \dfrac{S+1}{\sqrt{var(S)}} & S < 0 \end{cases} \tag{3.2}$$

where var refers to the variance. In this study, the significance level was set to 0.05, which implies that with absolute values of Z greater than 1.96, the null hypothesis is rejected, and the trend can be considered significant. One limitation of the MK is the chance of obtaining a significant trend with autocorrelated series (Hamed and Rao, 1998); however, we deal with this problem here by analyzing the anomalies of SM series, which is a common practice to avoid seasonal effects when analyzing SM trends (Albergel et al., 2013).

3.2.4.2. Empirical Mode Decomposition

The EMD is a method developed by Huang et al. (1998) for the analysis of nonlinear and nonstationary data. It allows the decomposition of a series into a number of intrinsic mode functions (IMFs) by empirically identifying the intrinsic oscillatory modes (Figure 3.2a). An IMF meets that (i) its number of extrema and its number of zero crossings must either be equal or differ at most by one, and that (ii) at any point, the mean value of the envelopes defined by the local maxima and by the local minima is zero (Narayanankutty et al., 2010). The decomposition is performed through a shifting process using only local extrema. For a signal $x(t)$, first, all the local extrema are identified. These local maxima and minima are connected with a suitable curve-fitting method. In this work, the piecewise-cubic Hermite interpolation polynomials method was used. The first component is obtained by subtracting the local mean curve of the upper and lower envelopes. The obtained component is treated as the original signal, and these steps are repeated until the envelopes are symmetric with respect to zero mean under certain criteria (Wu and Huang, 2009). The final component is designated as one IMF (C_i), and it is defined as follows: $r_0 = x(t) - C_i$. The shifting process is repeated using r_0 as the signal, and it is completed when the last component obtained becomes a monotonic function, the residual (R_n), from which no more IMF can be extracted. Thus, the EMD decomposes a signal $x(t)$ of the following form:

$$x(t) = \sum_{i}^{n} C_i + R_n \tag{3.3}$$

where the residual R_n represents the monotonic trend of the entire period of the series. This resulting trend is analyzed, as in the MK method, by its sign and its significance.

To differentiate the IMFs that provide a physically meaningful representation of the fundamental processes from those that represent the inherent noise in the data, characteristics of noise need first to be established (Wu and Huang, 2005). Wu and Huang (2005, 2004) studied the characteristics of white noise by using EMD and proposed a method to test the statistical significance based on deduced analytic expressions that describe the statistical characteristics of white noise. Thus, as the IMFs separate physical processes of a series at various time scales and give its temporal variation without a linear assumption, the mean period of the *n*th IMF (T_n) can be estimated as the ratio between the number of data (N) and the number of extrema of the series:

$$T_n = \frac{N}{N^{\underline{o}}\ extrema} \tag{3.4}$$

And the energy density (E_n) of the *n*th IMF (C_n) is defined as:

$$E_n = \frac{1}{N}\sum_{j=1}^{N}[C_n(j)]^2 \tag{3.5}$$

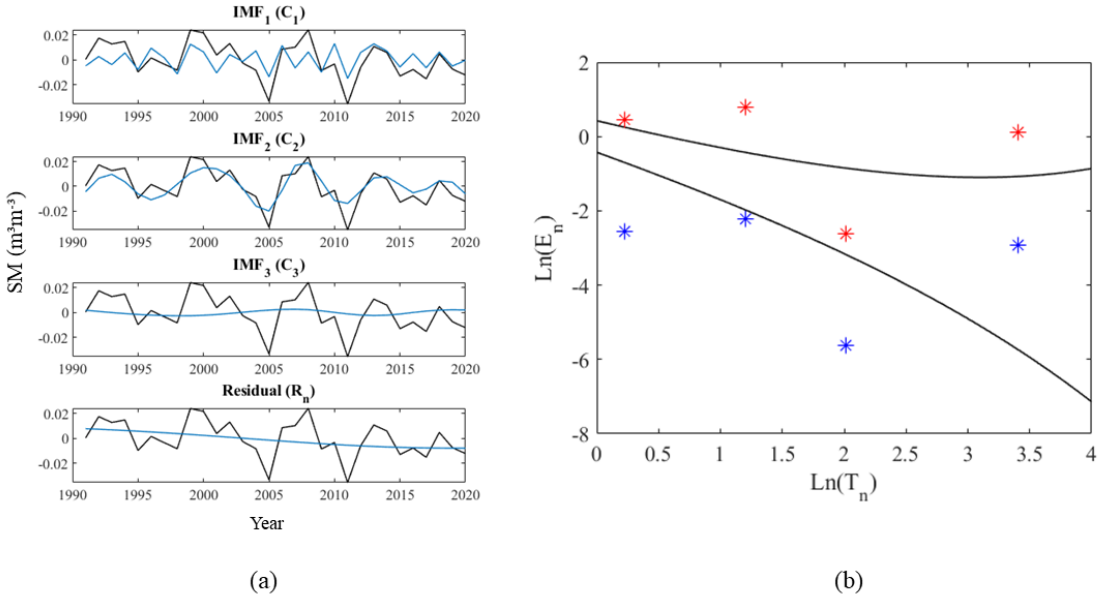

Figure 3.2 EMD is applied to an annual SM anomaly series as an example. (a) IMFs C1, C2 and C3 and the residual Rn (blue) obtained in the decomposition of a series *x* (black). (b) Representation of the a priori (blue stars) and a posteriori (red stars) significance tests with the spread lines at a 95% confidence level (black lines).

The authors established the spread of the energy densities of white noise by using the Monte Carlo method for different series of length (N). With this, they studied the relationship between the mean period (T_n) and the energy density (E_n) and defined its spread function. In this way, they designed a test to evaluate the significance of each IMF. First, the normalized series (between -1 and 1) is decomposed using EMD (Figure 3.2a), and the mean period and the energy density of each component is obtained. Then, the upper and lower lines of the spread function (black lines in Figure 3.2b) of the energy distribution at a confidence level are calculated using the analytical expressions defined in (Wu and Huang (2004). Finally, the energy density of the IMFs and the spread function are compared (blue stars in Figure 3.2b), if the energy is located between the upper and lower limits should be considered to contain just noise. However, this is an *a priori* test, in which the noise level of the data is unknown. For series in which it can be established that an IMF is just noise as it contains little useful information (IMF_1), its energy can be assigned to the 99% confidence upper line (Wu and Huang, 2005). With its energy, the energies of the other IMFs are rescaled (red stars in Figure 3.2b). In this *a posteriori* tests, the upper line of the spread function (upper black line in Figure 3.2b) sets the significance threshold. The IMFs with an energy above the threshold have physically meaningful representation. The *a posteriori* test has been verified and is widely used to lay the significance down when using the EMD (Adarsh and Janga Reddy, 2019; Lee and Ouarda, 2011; Wu and Huang, 2005). To evaluate the significance of the trend, this test was applied to the residual as in Sang et al. (2014).

3.3. Results and discussion

3.3.1. Annual and monthly soil moisture anomalies trends

The results for both trend analysis (MK and EMD) and SM products (ERA5L and LF) consistently agree on a general prevalence of negative trends, regardless of the type of climate, which implies a change to drier conditions in most parts of the European continent during the last 30 years (Figure 3.3, Figure 3.4). In general, the EMD method detects more significant trends than MK, and the increase in significant trends when using EMD is associated with an increase in positive trends. This fact could be related to the magnitude of these trends, since the MK does not have the power to detect small trends masked by other components of the series (Sang et al., 2014). This may imply that in regions showing an increase of SM with the EMD but not with MK, the components of the series with a nonmonotonic behavior have more weight than its long-term trend.

The spatial distribution of the obtained trends (Figure 3.3) indicates great consistency between the methods and temporal scales of the analysis. With both SM products, positive trends are mainly obtained in Scotland and northern Ireland, which implies a change to wetter conditions, similar to what Bordi et al. (2009) obtained. Changes to drier conditions are located in central and eastern Europe, in line with previous studies (Jaagus et al., 2021; Trnka et al., 2009b). Thus, regions that show a wetting trend are generally located at higher latitudes, in areas where the average moisture content is higher, and drying trends are generally located in central and southern Europe. This is in line with the "dry gets drier, wet gets wetter" trend paradigm studied by Feng and Zhang (2015). In contrast, very few and limited regions show distinct trends depending on the SM product used, such as Bulgaria, where a positive trend dominates with LF, and a negative trend with ERA5L or the Italian Peninsula, where a negative trend is observed in monthly series with LF but positive with ERA5L.

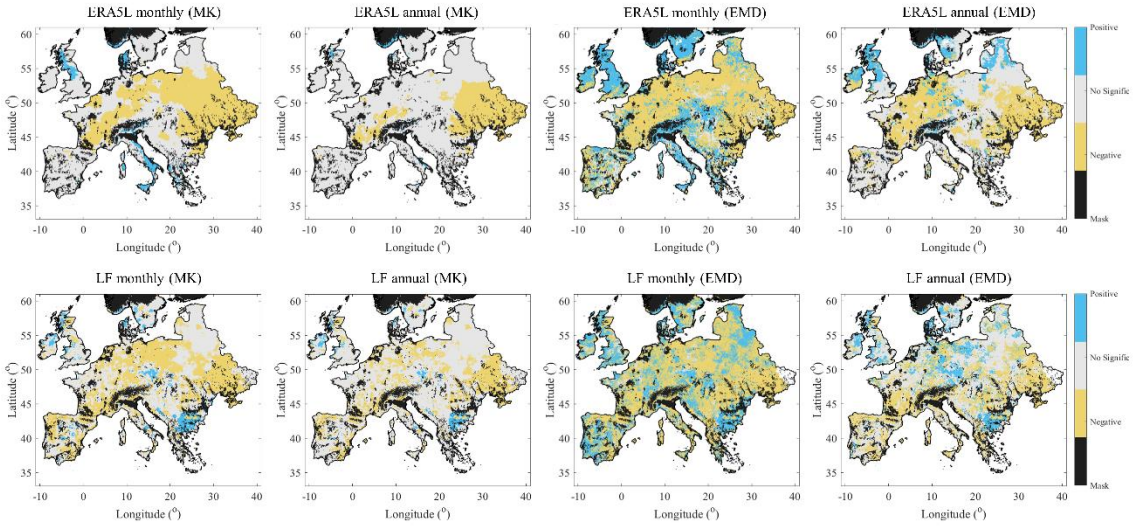

Figure 3.3 Spatial distribution of soil moisture anomaly trends obtained with ERA5L and LF for monthly and annual series using MK and EMD methods.

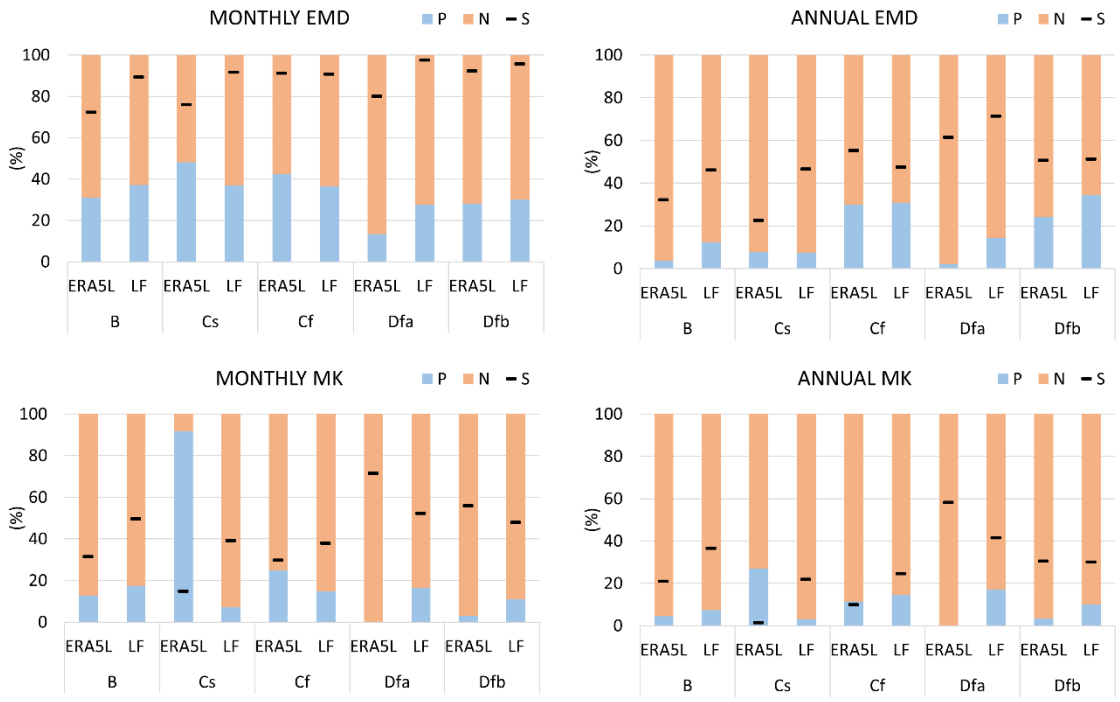

Figure 3.4 Percentage of pixels with significant trends (S, black line) and percentage of positive (P, blue bar) or negative (N, orange bar) trends regarding the significant ones, of each SM database and Köppen-Geiger climate regions in Table 3.1. The results are shown for the two methods, EMD and MK, and the two temporal scales, monthly and annual.

At temporal scales, the MK method shows more trends that are significant in monthly series than in annual series. This could be related to the fact that the MK depends on the sample size as well as on the magnitude of the trend to be identified (Adamowski et al., 2009; Sang et al., 2014). However, this difference is also observed when using EMD. This implies fewer interannual changes in this variable, similar to what (Piles et al., 2019) and what Vicente-Serrano et al. (2021) saw when they analyzed SM and droughts trends respectively. In the literature, trends have usually been analyzed at annual or seasonal scales and assuming monotonic behavior; thus, significant long-term trends have barely been observed in Europe (Albergel et al., 2013; Dorigo et al., 2012; Feng and Zhang, 2015).The distribution of trends according to the type of climate is quite similar. Although some patterns are observed, in all cases, they imply a change to drier conditions (Figure 3.4). In general, higher percentages of significant trends are located in regions with cold climates (Dfa and Dfb). When using MK, regions with temperate climates (Cs and Cf) present the lowest percentages of significant trends, while with the EMD, this pattern is not observed. Attending to products, higher percentages of significant trends in arid climate areas (B) and temperate with dry summer climate areas (Cs) are observed with LF. Finally, when comparing temporal scales, at monthly scale Cs region shows an abnormal positive trend percentage with ERA5L associated with positive trends obtained in Italy; however, although the number of significant trends is very low, a high percentage of positive trends are also obtained with this product at monthly scale with EMD.

Comparative tables were elaborated to quantify the differences between the results obtained with two methodologies (Table 3.2), temporal resolutions (Table 3.3), and products, similar to Qiu et al. (2016), but analyzing only pixels with a significant trend. The match rate is always higher than the discrepancies, with the negative trends being more consistent. On the one hand, when comparing both methods, it is observed that EMD tends to detect positive trends that MK considers negative (Table 3.2). Sang et al. (2014) obtained similar results when analyzing precipitation series, and they observed that the MK test underestimated the upwards trend. On the other hand, trends obtained with various temporal scales applying MK present no discrepancies; however, the number of coinciding significant trends is very low. In contrast, with EMD, higher values of significant trends are obtained, and therefore, discrepancies increase, with its total percentage being greater than that of positive coincident trends. These discrepancies again suggest that changes to wetter conditions are occurring slightly enough to be masked by nonmonotonic components of the series.

Table 3.2 Comparison of the percentage of trends obtained with the two methods, MK and EMD, for the two SM databases used at annual and monthly time scales. Sign "+" indicates positive and significant trends, and sign "-" indicates negative and significant trends.

		ERA5L		**LF**	
		MK +	**MK -**	**MK +**	**MK -**
Monthly	**EMD +**	9	7	11	11
	EMD -	1	83	1	77
Annual	**EMD +**	3	2	12	7
	EMD -	0	95	0	81

Table 3.3 Comparison in percentage of trends obtained for the two timescales, annual (A) and monthly (M), for the two methods and SM databases used. Sign "+" indicates positive and significant trends, and sign "-" indicates negative and significant trends.

		ERA5L		**LF**	
		M +	**M -**	**M +**	**M -**
EMD	**A +**	15	9	16	12
	A -	12	64	11	61
MK	**A +**	3	0	10	0
	A -	0	97	0	90

3.3.2. Monthly pattern of soil moisture anomalies trends

Despite the general consistency between results when using different approaches, some variations have been observed that deserve particular attention. The most notable ones were obtained when studying trends of the series with different temporal resolutions using the empirical decomposition method. To clarify these differences, a dedicated analysis of monthly changes and trends was performed. This approach revealed that most changes in SM are not uniform among the year. For simplicity, only results obtained with the EMD are shown (Figure 3.5, Figure 3.6), since very few significant trends were obtained with MK for this analysis.

Again, trends obtained with both SM products are consistent. An increase in significant negative trends is obtained in April over almost the entire continent with both products, which implies a general decrease in SM during this month. These results are in concordance with several studies that have detected drier springs in Europe over the last decades (Jaagus et al., 2021; Trnka et al., 2009b; Vautard et al., 2007). In contrast, an increasing trend of SM is obtained in the Iberian Peninsula for that same month, similar to what Almendra-Martín et al. (2021a) observed using a rank-based approach. The same wet pattern in the Iberian Peninsula (IP) and dry pattern elsewhere in Europe were obtained when analyzing precipitation trends of climatic research unit (CRU) monthly anomaly series (Figure 3.A1), which reinforces our obtained results with SM time series, i.e., a change in trend to wetter conditions in April and May in the IP.

In addition, the percentage of significant trends rises during autumn (September–October-November) for both products and in the winter (December–January-February) for the LF product (Figure 3.6). Between these months, there is a fluctuation in the sign of the trends obtained, which emphasizes the nonmonotonic behavior of SM at this temporal scale. November and January show a predominance of decreasing trends in most of the European territory, while for December and February, increasing trends in SM anomalies are mainly observed. However, a constant pattern of increase in SM trends is obtained for the winters in the northeastern region (Estonia, Latvia, Lithuania and Belarus), in concordance with what Cammalleri et al. (2016) obtained and with the increase in the winter precipitation observed by Jaagus et al. (2021) in this region. A decrease in significant trends is observed in the summer (June–July-August) months; however, there is a predominance of negative trends.

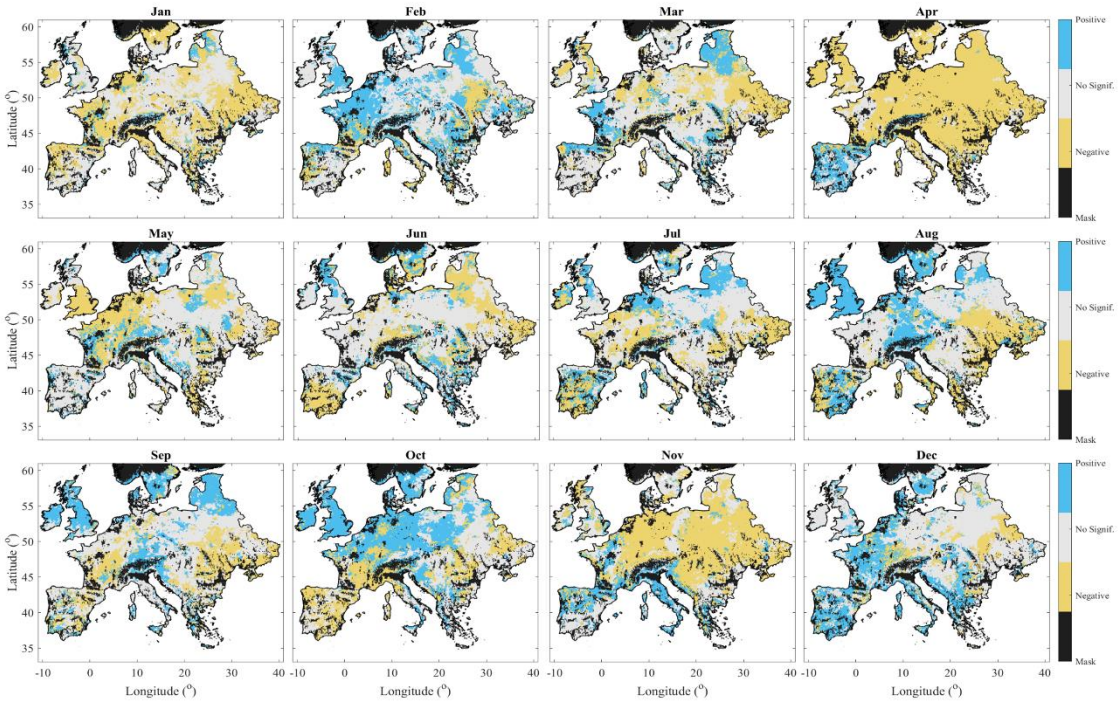

Figure 3.5 Spatial distribution of SM anomaly trends (EMD) obtained with monthly ERA5L series for each month.

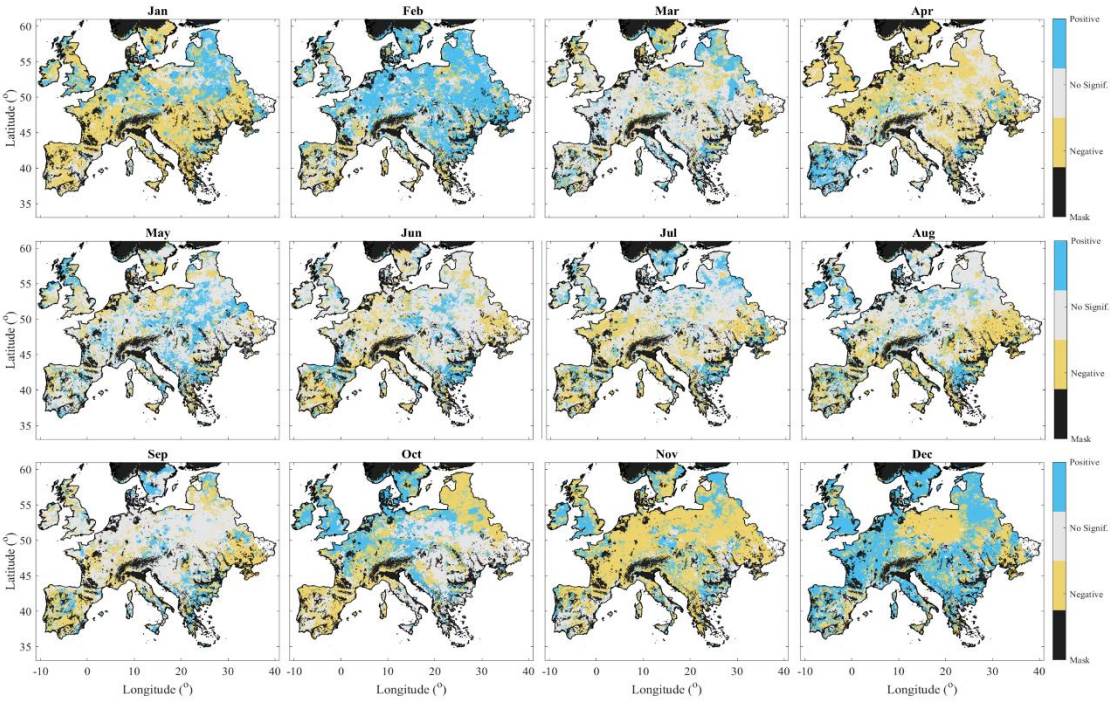

Figure 3.6 Spatial distribution of SM anomaly trends (EMD) obtained with monthly LF series for each month.

3.3.3. Drought attribute trends

Trends in SM anomaly series have been detected; thus, changes in related drought characteristics could be expected. To verify this, a similar analysis using MK and EMD was conducted on drought attributes annual series of ERA5L and LF to identify their changes during the last three decades. The EMD method also detected more significant trends than MK, but more importantly, our results obtained with both methods show a general increase in the duration and intensity of extreme droughts over the European continent (Figure 3.7). These results are in agreement with the expected evolution based on climate change models under different scenarios (Giorgi and Lionello, 2008; Grillakis, 2019; Spinoni et al., 2018). In addition, our results indicate that the onset of extreme drought events, in general, tends to be delayed a few days per year in some regions, especially with ERA5L in arid and temperate regions (Figure 3.A2).

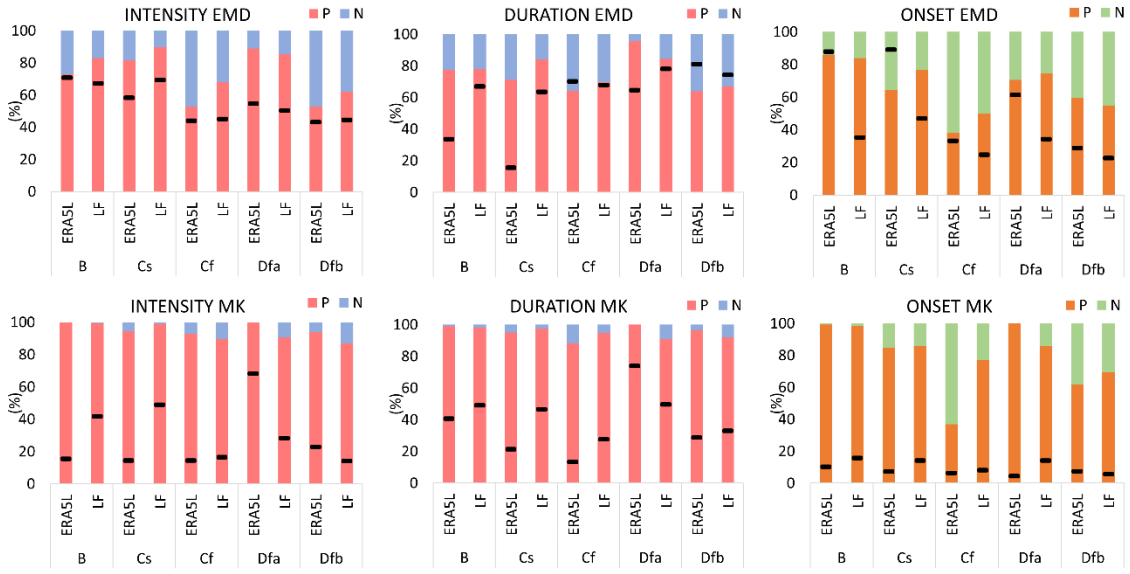

Figure 3.7 Percentage of pixels with significant trends (S, black line) and percentage of positive (P, blue bar) or negative (N, orange bar) trends regarding the significant ones, of duration, intensity and onset annual series of each SM database in each Köppen-Geiger type of climate. The results obtained with the two methods, EMD and MK.

In this analysis, the increase in significant trends when using EMD is associated with a slightly increase in negative trends for intensity and duration attributes, which implies a change to shorter and less intense droughts in some regions, mainly in Cf and Dfb climates. Again, we could only detect these changes with the empirical decomposition method and not with the MK approach, which suggests the convenience of using methods that account with nonmonotonic behavior to analyze the trend in soil moisture anomalies.

When each type of climate trend is analyzed, different patterns in drought trends are observed. Cf, Dfa and Dfb refer to climates without a dry season; therefore, lower changes in droughts should be expected. Indeed, the results obtained with the intensity series present the lowest percentages of significant trends, and almost half of them show a decreasing

trend in intensity with EMD in Cf and Dfb. However, there is a general increase in the duration of droughts in these regions, and the start of drought events tends to advance in temperate climate Cf and some regions with a Dfb climate. A clear pattern is observed in arid regions and regions with more intense, longer and increasingly delayed extreme droughts, although the number of significant results depends upon the SM product used, as LF detects more trends in duration series but less in onset than ERA5L. Similar results were obtained in regions with a Cs climate.

This general increase in the duration and intensity of extreme droughts is consistent with several changes observed in the precipitation behavior over Europe in prior studies (de Luis et al., 2011; Hänsel et al., 2019; Hynčica and Huth, 2019), alongside the rise of average temperature (Trenberth, 2011) and the consequent increase in potential evapotranspiration, which, in turn, causes an increase in extreme events such as droughts (Hänsel et al., 2019; Jaagus et al., 2021).

3.4. Conclusions

In this work, the trend of SM in Europe in the last three decades was investigated using rank-based and empirical decomposition approaches. For this, two SM databases, one from modelling (LF) and the other from reanalysis (ERA5L), were used. Anomaly series of SM were calculated at monthly and annual temporal scales and were analyzed using two approaches: monotonic (MK) and nonmonotonic (EMD). Strong consistency was observed between the results of both databases, methods and temporal scales. The distribution of SM anomaly trends in the different European climates was also studied, and no clear pattern was identified. The results showed a general change trend to drier conditions, mainly located in Central and Eastern Europe. Although the MK method has been widely used to study the trends of SM, the empirical decomposition approach detected more significant trends. The patterns in SM that could be identified only with EMD are in accordance with changes observed in other hydroclimatic variables on this continent during recent decades, such as temperature, precipitation or evaporation. Furthermore, many of the trends observed with EMD and not with MK are positive, while negative trends are more consistent with both methods. This suggests that changes to wetter conditions can be masked by a nonmonotonic behavior of the series.

The most notable differences in SM trends were obtained when comparing the results at monthly and annual scales, especially when using the EMD method. Less significant trends were observed at annual than at monthly scales, but significant ones showed in some regions different signs depending on the temporal scale. To further scrutinize this mismatch, interannual changes for each month series were analyzed using the EMD method. A general decreasing trend in SM anomalies was obtained in April over the entire continent, which implies a trend towards drier springs in Europe. Just the Iberian Peninsula showed the opposite behavior with an increasing trend of SM in April. Autumn and winter months showed a fluctuation in the sign of the trends, which emphasizes the nonmonotonic behavior of changes in this variable in the months when the average SM is the highest. In contrast, summer months showed fewer significant trends; however, the significant trends indicate a trend towards drier conditions.

As several changes were observed in the SM series, related changes in the characteristics of drought events could also be expected. To evaluate this hypothesis, the duration, intensity and onset annual trends of extreme droughts in Europe were studied. The results showed a prevalence of an increase in the duration and intensity of extreme droughts and a few days of delayed onset per year. However, some change patterns in the different climate regions of Europe could be observed only with the EMD method. Areas with climates without dry season (Cf, Dfa and Dfb) showed the lowest percentage of significant trends in intensity series, and almost half of the area showed a decreasing trend. However, the duration of extreme droughts showed a general increasing trend, especially in the coldest regions (Dfb). In arid regions, a clear pattern of increasingly longer, more intense and delayed extreme droughts was observed. In this analysis, the EMD method again detects more trends than MK, in particular, the negative (drier conditions) trends.

SM trends have been commonly studied through approaches that just account for the monotonic change and at large temporal scales. This has resulted in few to no changes in patterns being detected when analyzing this variable in Europe during recent decades. However, trends in related variables such as temperature or precipitation have been observed due to the impact of climate change, so changes could also be expected in SM. The empirical decomposition approach used in this work has revealed a large number of trends that show a general decreasing SM pattern in Europe, reconciling the results previously reported in the literature when analyzing the trends in intimately linked variables such as temperature, precipitation or evaporation. The results of this work prove that empirical decomposition approaches allow to account for the nonmonotonic behavior of the series and can be a suitable tool to understand the changes in SM dynamics, as well as the impact of climate change on this variable, which could be instrumental to better understand subsequent changes in the Earth's water cycle.

Appendix 3.A Supplementary data

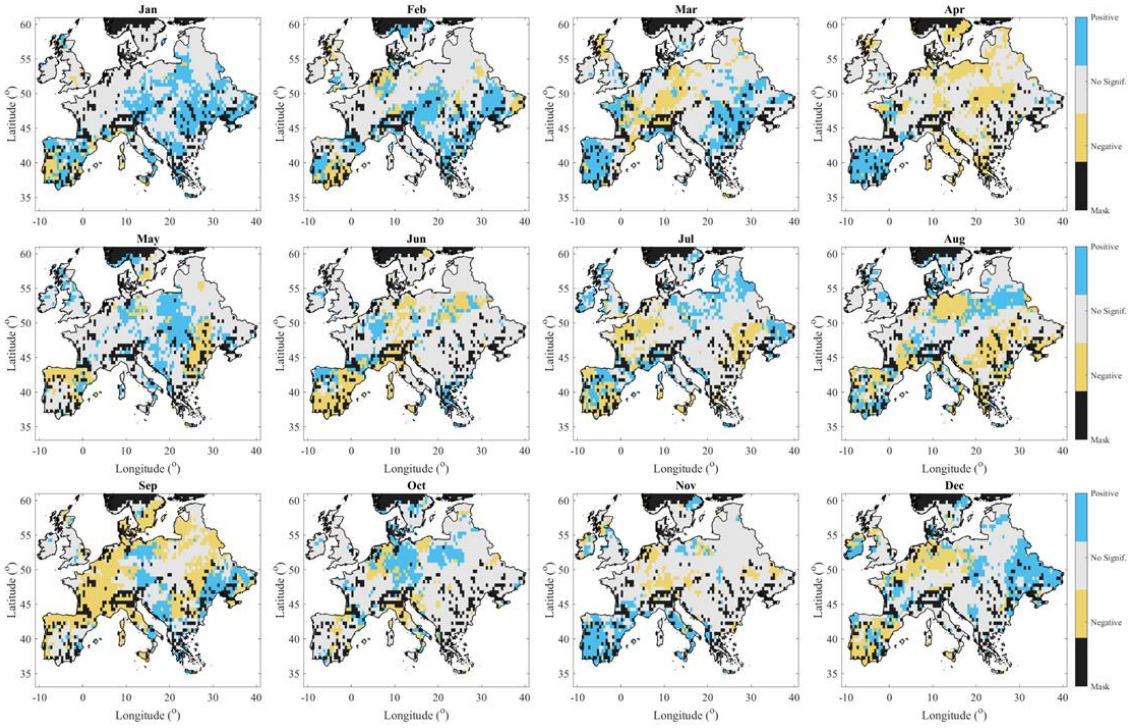

Figure 3. A1 Spatial distribution of precipitation anomaly trends obtained with monthly CRU series for each month.

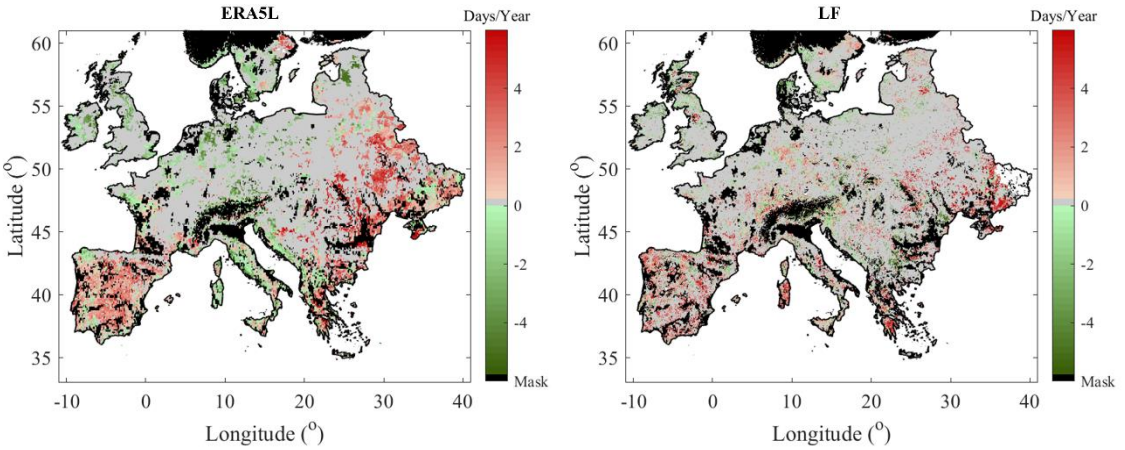

Figure 3. A2 Change in the extreme drought event onset trend expressed in days per year.

CAPÍTULO 4

INFLUENCE OF ATMOSPHERIC PATTERNS ON SOIL MOISTURE DYNAMICS IN EUROPE

Almendra-Martín, L., Martínez-Fernández, J., Piles, M., González-Zamora, Á., Benito-Verdugo, P., Gaona, J., 2022. Influence of atmospheric patterns on soil moisture dynamics in Europe. Science of The Total Environment 846, 157537. https://doi.org/10.1016/j.scitotenv.2022.157537

Resumen

La humedad del suelo (SM, *soil moisture*) juega un papel clave en el ciclo del agua, y su variabilidad está íntimamente ligada a los procesos acoplados entre la tierra y la atmósfera. Tener un buen conocimiento sobre las interacciones suelo-atmósfera es, por tanto, esencial para determinar el impacto del cambio climático en la SM. Sin embargo, muchos aspectos sobre los intercambios de agua y energía entre el suelo y la atmósfera son todavía inciertos. En particular, se sabe que los patrones de circulación atmosférica influyen en las condiciones climáticas de Europa, pero su impacto en la SM rara vez ha sido estudiado. Este estudio proporciona conocimiento sobre cómo los patrones atmosféricos influencian la dinámica de la SM en Europa, donde se espera un incremento de las temperaturas y la sequía agrícola como impacto del cambio climático. Para ello, se analizó la influencia de la *North Atlantic Oscillation* (NAO), la *Arctic Oscillation* (AO), y El Niño *Southern Oscillation* (ENSO) en la SM europea, incluyendo el desfase en la respuesta, para el periodo 1991-2020 a una escala mensual. Se emplearon dos métodos: el análisis *lagged-correlation* y un enfoque más sofisticado de análisis de causalidad usando el PCMCI (método PC combinado con el test *momentary conditional independence* (MCI)). Se consideraron series de SM de dos bases de datos diferentes: el modelo hidrológico LISFLOOD y el conjunto de datos de reanálisis ERA5-Land. Los resultados obtenidos del análisis *lagged-correlation* muestran relación significativa, predominantemente negativa, entre la SM y NAO y AO en la mayor parte de Europa, y ninguna relación significativa con ENSO. Con el análisis de causalidad, se encontraron patrones similares para NAO y AO, sin embargo, el análisis con PCMCI reveló patrones claros de influencia de ENSO en la SM con una respuesta retardada de uno o dos meses en Europa central y noroeste. Los resultados obtenidos en este trabajo ponen de manifiesto una relación causal entre los principales modos de oscilación climática interanual y la variación de SM en Europa, resaltando la importancia de contar con los patrones de circulación atmosférica para estudiar los actuales cambios regionales en los procesos relacionados con el agua del suelo.

Palabras clave: Humedad del suelo, *North Atlantic Oscillation*, *Arctic oscillation*, El Niño *Southern Oscillation*, Causalidad, Respuesta retrasada

Abstract

Soil moisture (SM) plays a key role in the water cycle, and its variability is intimately linked to coupled land-atmosphere processes. Having a good knowledge of soil-atmospheric interactions is thus essential to assess the impact of climate change on SM; however, many aspects of how water and energy exchanges occur in the soil-atmosphere continuum are still uncertain. In particular, it is known that atmospheric circulation patterns influence climate conditions over Europe but their impact on SM has only rarely been studied. This study provides insight into how atmospheric patterns influence soil moisture dynamics in Europe, where an increase in temperature and agricultural droughts are expected as an impact of climate change. To do so, we analysed the influence of the North Atlantic Oscillation (NAO), the Arctic Oscillation (AO), and the El Niño Southern Oscillation (ENSO) on European SM, including lagged responses, for the period 1991–2020 at a monthly scale. Two methods have been used: a lagged correlation analysis and a more sophisticated causality approach using the PCMCI (PC method combined with the momentary conditional independence (MCI) test). SM series from two different databases were considered: the hydrological model LISFLOOD and the reanalysis dataset ERA5-Land. The results from the correlation analysis showed a significant, predominantly negative relationships of SM with NAO and AO over almost all of Europe and no significant relation with ENSO. With the causality analysis, similar patterns are obtained for NAO and AO; however, the PCMCI analysis revealed clear patterns of ENSO influencing SM with a delayed response of one-to-two months in central and northwest Europe. The results obtained in this work highlight that there are causal relations between the main modes of interannual climate oscillations and SM variations in Europe, underlining the importance of accounting for global atmospheric circulations to study current changes in regional soil water-related processes.

Keywords: Soil moisture, North Atlantic Oscillation, Arctic oscillation, El Niño Southern Oscillation, Causality, Lagged response

4.1. Introduction

The study of climate change impacts on different environmental systems has motivated many works, especially on water-related systems (Arnell, 1999; Middelkoop et al., 2001). Soil moisture (SM) is a key variable involved in many climatic, geophysical and biological processes, so monitoring its dynamics and understanding its (causal) relations in these processes are crucial. In addition, SM plays a very important role in the hydrological cycle, as it modulates the water and energy exchanges within soil–atmosphere systems (Seneviratne et al., 2010). Thus, knowledge of the evolution of this variable can help to better understand the impact of climate change in these systems. SM dynamics and factors that influence its variability have been widely analysed from different perspectives (Daly and Porporato, 2005; Dorigo et al., 2012; Entekhabi et al., 1996; Martínez-Fernández et al., 2021; Piles et al., 2019). However, some issues about soil–atmosphere interactions are still uncertain (Boé, 2013).

It is well-known that different atmospheric circulation patterns highly influence climate conditions across the globe (Hurrell and van Loon, 1997; Lau and Yang, 2003). In particular, several teleconnection patterns dominate European climate variability (Hurrell, 1995; Thompson and Wallace, 1998). Thus, changes in atmospheric circulation can be related to changes in several climatic variables and the increase in extreme events during recent decades over this continent (Horton et al., 2015; Kostopoulou and Jones, 2007; Kyselý, 2007; Moberg and Jones, 2005). The dominant modes of climate variability in the Northern Hemisphere are the North Atlantic Oscillation (NAO) and the Arctic Oscillation (AO) (Simpkins, 2021). However, some other patterns also induce changes in European climate conditions, such as the El Niño Southern Oscillation (ENSO) (Fraedrich and Müller, 1992), the East Atlantic (EA) (Bastos et al., 2016) and the Scandinavian Pattern (SCAND) (Casanueva et al., 2014). They induce changes in precipitation and temperature (Hurrell et al., 2001; Ionita et al., 2020; Scaife et al., 2008; Toreti et al., 2010; Trigo et al., 2002) and, consequently, in related processes such as river flow (deCastro et al., 2006; Su et al., 2018) and vegetation growth (D'Odorico et al., 2002; Gordo and Sanz, 2010).

One of the most disturbing natural hazards is droughts, as they exert a great impact on human activities. They are complex phenomena influenced by several factors but they always have an atmospheric inception (Vicente-Serrano et al., 2011), hence understanding the atmospheric influence on droughts is crucial since it could help mitigating their damage spread. In this context, several works have focused on studying the influence of atmospheric circulation patterns on meteorological droughts in Europe (Ionita et al., 2015; Schubert et al., 2016; Vicente-Serrano et al., 2011). However, agricultural drought, defined by the SM deficit, represents a more direct and immediate impact (Almendra-Martín et al., 2021a; Salvia et al., 2021; Sánchez et al., 2018); thus, as a highly meaningful topic, this work focuses on exploring the influence that atmospheric fluctuation patterns exert on SM.

In the past, little attention has been given to the effect that some atmospheric patterns exert on SM, mainly because of the scarcity of long-term spatially continuous data series (de Luca et al., 2020; Wang et al., 2011). Diverse works have modelled SM data in certain

regions to perform this kind of analysis (Kurnik et al., 2015; Sheffield and Wood, 2008) or analyse the drivers of this variable to relate their dynamics (Hassan and Nayak, 2020; Ionita et al., 2015; Mühlbauer et al., 2016). Remote sensing databases have also been used to analyse this relationship. However, in such works, short study periods of only a few years were used (Bueso et al., 2020a; Piles et al., 2019) since available data are relatively recent and thus limited in time. Thus, the need for accurate long-term spatiotemporally continuous SM databases is highlighted to achieve rigorous assessments of climate change impacts (Thorne et al., 2018). Currently, there are SM databases available from modelling and reanalysis suitable for this type of analysis (Beck et al., 2020; Miralles et al., 2014).

Although relationships between atmospheric circulation patterns and general dryness or wetness conditions have been established in Europe, most are based on atmospheric teleconnections (Brönnimann, 2007; Hurrell et al., 2001). Furthermore, it is assumed that these relationships explain the variability of the different studied variables, but their causal relationships have rarely been analysed (Runge et al., 2019a). A causal relationship was found between ENSO, AO and NAO, and the streamflow of >30 % of the rivers in Europe (Su et al., 2018). Furthermore, in some regions, causality studies showed additional relationships between ENSO and climatic variables that were not detected with correlation analysis (Silva et al., 2021). Several methods have been proposed in the literature to study causality but are still rarely applied in Earth system science (Runge et al., 2019a).

Understanding the influence that atmospheric patterns exert on SM dynamics is key to assessing the impact of climate change on this variable and, therefore, on issues such as the occurrence of agricultural drought or groundwater recharge. This interest is highlighted in Europe, as the predicted changes in climatic conditions suggest an increase in temperature over all continents (Christensen et al., 2013), which can lead to an intensification of hydrological extremes such as floods (Dankers and Feyen, 2008) or agricultural droughts (Grillakis, 2019). Thus, the main objective of this work is to provide further knowledge of how SM responds to the main atmospheric patterns in Europe. The two atmospheric circulation patterns dominant in the Northern Hemisphere, the NAO and AO (Simpkins, 2021), and the phenomenon with more impact on global climate, ENSO (Brönnimann, 2007), were considered in this work. Two SM databases were used, for the period 1991–2020. We studied both the lagged influence that atmospheric patterns exert on SM and causation, i.e., whether there is a causal relationship between the climate modes and SM time series at a monthly time scale.

4.2. Methods and dataset

4.2.1. Soil moisture databases

Two SM databases were considered in this study, one from the ERA5-Land reanalysis (Muñoz-Sabater et al., 2021) and the other from the LISFLOOD hydrological model (van der Knijff et al., 2010). Both databases have been widely used for different purposes, such as flood forecasting (Wanders et al., 2014), growth vegetation studies (González-Zamora et al., 2021) and trend detection (Almendra-Martín et al., 2021a). The reanalysis database used in this study is the ERA5-Land (hereafter, ERA5L) from the European Centre for Medium-Range Weather Forecasts (ECMWF). It provides a global series of different land variables. These series are given on a regular grid of 0.1° with hourly time resolution from 1981 to the present (Muñoz-Sabater et al., 2021). As the surface SM is more demonstrative of the soil-atmosphere coupling (Santanello et al., 2011), only the first layer of the product, comprising the soil top 7 cm, was used. The second database used was the hydrological rainfall-runoff model LISFLOOD (hereafter, LF), developed by the Natural Hazards Project of the Joint Research Centre (JRC) of the European Commission (van der Knijff et al., 2010). It provides SM data over Europe with a spatial resolution of 5 × 5 km every 6 h from 1991 to the present (de Roo et al., 2000). These data are estimated for 3 depth layers, but for this study, only the surface layer (5 cm) was considered. In addition, this database has been rescaled to the ERA5L grid so that the study results are comparable.

Both databases have been validated in previous works, obtaining good results (Laguardia and Niemeyer, 2008; Muñoz-Sabater et al., 2021). However, in certain regions, the accuracy of their products is compromised due to constraints when estimating SM in areas with, for example, heterogeneous topography and permanent or seasonal ice cover (Laguardia and Niemeyer, 2008; Li et al., 2020). To gain a robust understanding of the similarity of these databases, a comparison was first performed between the LF and ERA5L SM products (Figure 4.1a). Good correlation was generally obtained between the two except in regions where the products show lower precision, such as high latitudes or great mountain ranges (Laguardia and Niemeyer, 2008; Li et al., 2020). Due to the great differences observed between products in these areas and the consequent uncertainty, we decided to exclude them from this study; pixels showing correlation values lower than 0.5 were not considered (Figure 4.1b). Similar thresholds have been used in other studies to ensure consistency in SM products and lower uncertainty (Preimesberger et al., 2021). Once these areas were masked, the SM time series were averaged to obtain monthly values for the study period, 1991–2020. Then, anomalies were computed for each pixel by subtracting the monthly mean calculated using the entire period of study.

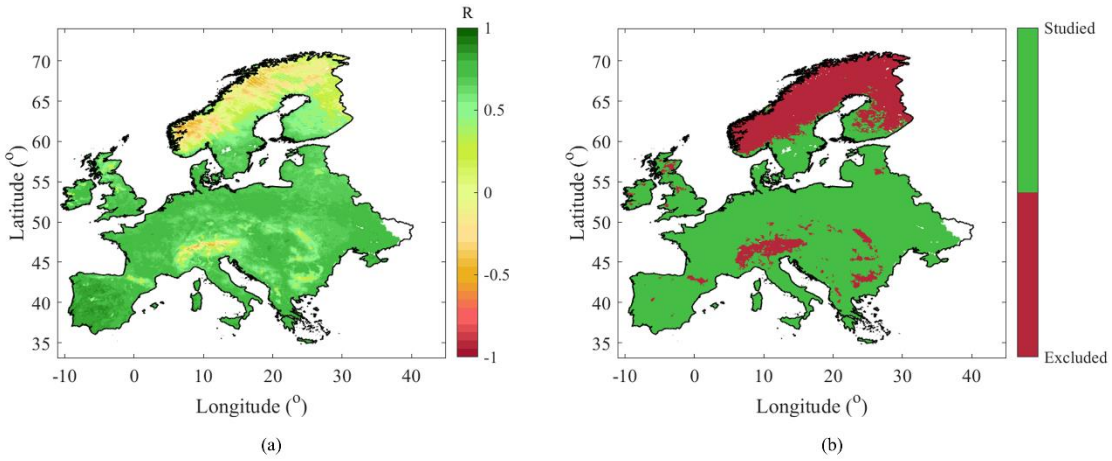

Figure 4.1(a) Pearson correlation coefficient between the LF and ERA5L SM series. (b) Mask applied to the SM products.

4.2.2. Teleconnection indices

The influence of three different atmospheric patterns on SM dynamics was studied, namely, the NAO, AO and ENSO.

The NAO refers to a circulation of atmospheric mass over the North Atlantic Ocean. It is typically monitored with the NAO index, defined as standardized differences in the surface sea-level pressure between both poles from the dipole Icelandic Low - Azores High (Hurrell et al., 2003). It entails a relevant source of interannual variability in the atmospheric circulation (Walker and Bliss, 1932) and exerts a great impact on climate conditions over most of the Northern Hemisphere, mainly in North America and Europe (Casanueva et al., 2014; Hurrell et al., 2001; Scaife et al., 2008; Trigo et al., 2002; Y. H. Wang et al., 2012), modulating patterns in wind, temperature and precipitation throughout the seasons but especially during boreal winter (Bastos et al., 2016). A positive phase of NAO is defined when low- and high-pressure anomalies exist over Iceland and Azores pressure centres, respectively (Visbeck et al., 2001). The pressure gradient over the North Atlantic during this phase is large, and an increase in west winds at midlatitudes is observed (Hurrell, 1995). This leads to colder and drier conditions in the Northwest Atlantic and Mediterranean regions and warmer and wetter conditions in northern Europe and the eastern United States (Visbeck et al., 2001). Conversely, a negative phase is defined by high- and low-pressure anomalies in Iceland and Azores, respectively, and leads to opposite climatic conditions. The NAO index has a high interseasonal variability; however, positive and negative phases can last several months (Wang et al., 2010).

The AO is defined as a fluctuation of atmospheric pressure involving an exchange of atmospheric mass between the Arctic and middle latitudes of the Northern Hemisphere (Thompson and Wallace, 1998). The AO index refers to the first empirical orthogonal function (EOF) of the atmospheric pressure anomalies between 20°N and 90°N latitudes (Thompson and Wallace, 1998). Similar to the NAO, it influences the climate conditions over most of the Northern Hemisphere, and both indices are highly correlated (Wanner et

al., 2001). Two phases are also distinguished: positive and negative (Hanna et al., 2015). During AO positive phases, lower atmospheric pressure anomalies over the Arctic and higher atmospheric pressure anomalies over the northern Pacific and Atlantic Oceans are observed. The mid-latitudes jet stream is located further north, steering ocean storms northwards (Lindsey, 2009). Thus, wetter and colder conditions occur in Alaska, Scotland, and Scandinavia, and drier and warmer conditions occur in North America, Europe, Siberia, and East Asia (Daoyi and Shaowu, 2003). The opposite conditions are seen during the AO negative phase.

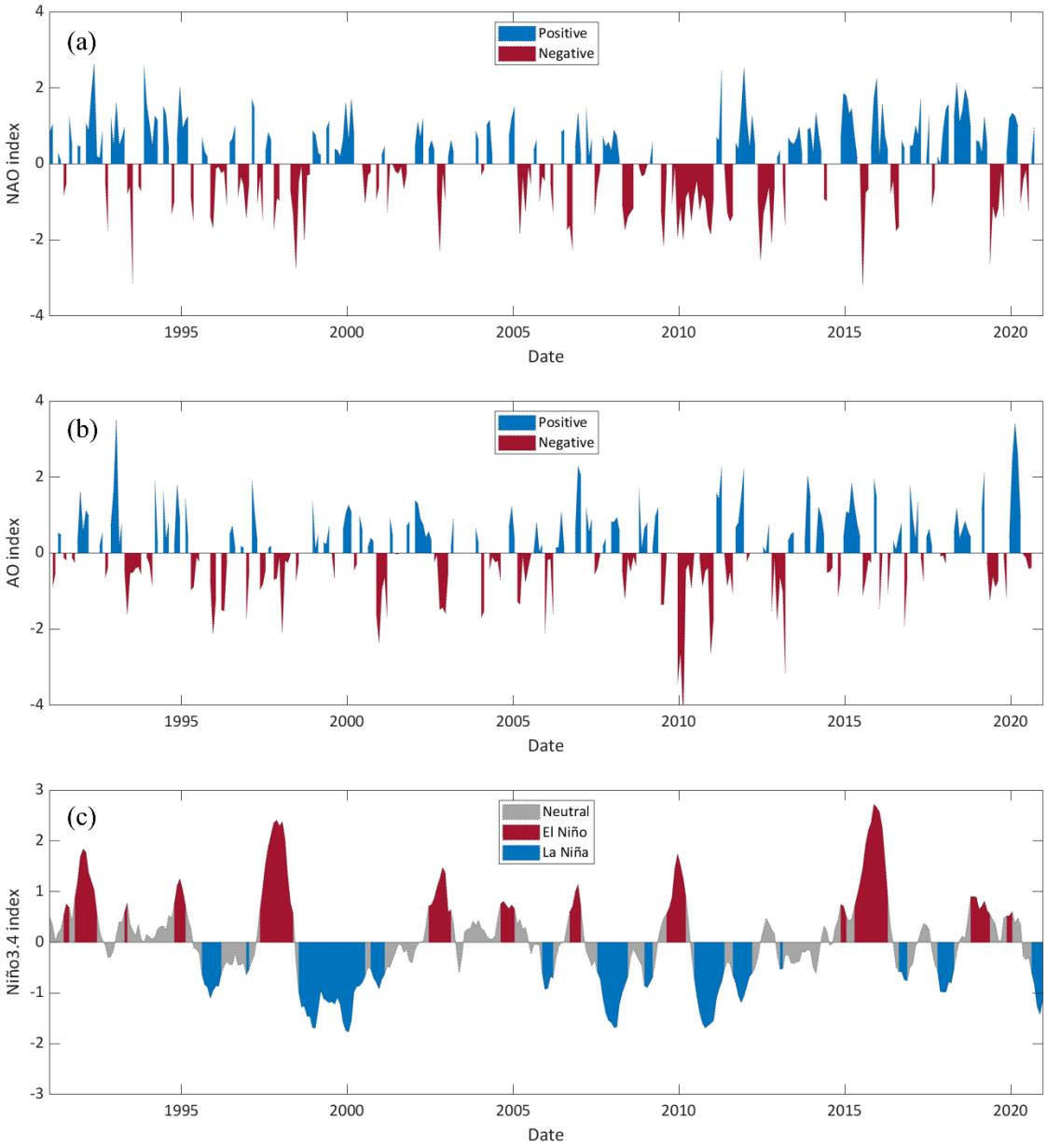

Figure 4.2 Time series of (a) NAO, (b) AO and (c) Niño 3.4 indices for the study period (1991–2020).

ENSO refers to a coupled mode of the ocean-atmosphere defined by periodic fluctuations in sea surface temperature (SST) and atmospheric circulation along the equator of the Pacific Ocean (McPhaden et al., 2006). It is the dominant mode of interannual climate variability on Earth (Brönnimann, 2007), as it directly or indirectly affects weather conditions over many regions of the planet. There are different ways of monitoring ENSO, depending on whether the atmospheric or the oceanic component is measured. On the one hand, the atmospheric part is measured by the Southern Oscillation index (SOI), a standardized index based on the difference between the sea level pressure at the Tahiti and Darwin, Australia (Ropelewski and Jones, 1987). For monitoring the oceanic component, SST is averaged over specific regions; thus, different indices and thresholds for ENSO are defined (L'Heureux et al., 2019). The NOAA CPC uses the Niño 3.4 region to define warm (El Niño) or cold (La Niña) events. This region comprises from 5°N–5°S to 120°–170°W, near the warm pool of the Pacific and main centres of convection (Trenberth, 1997). During El Niño events, SST anomalies above 0.5 °C are present in this region; thus, the ocean surface in the central and eastern tropical Pacific Ocean becomes warmer. Rainfall decreases over Indonesia and increases over the tropical Pacific (L'Heureux, 2014). Conversely, during La Niña events, SST anomalies below −0.5 °C are present. Easterly winds along the equator become stronger, and rainfall increases over Indonesia and decreases over the central tropical Pacific Ocean (L'Heureux, 2014). When the SST anomalies are between the upper and lower thresholds, ENSO is considered to be in the neutral phase.

This study used the monthly NAO, AO and Niño 3.4 teleconnection indices time series from the NOAA CPC [https://www.cpc.ncep.noaa.gov] for 1991–2020 (Figure 4.2).

4.2.3. Lagged-correlation and causality analysis

Correlation analysis is the most commonly used tool to study teleconnections (Anderson et al., 2017; Comas-Bru and Mcdermott, 2014; deCastro et al., 2006; Scaife et al., 2008). This analysis provides information about the strength of the relationship between two variables and whether it is direct (positive) or indirect (negative). The correlation between atmospheric patterns and SM could have a lagged effect due to decoupling between soil–atmosphere systems even at the monthly scale. For this reason, in this study, a lagged correlation analysis was carried out by computing the Pearson correlation coefficient between teleconnection indices and SM anomaly series (Benesty et al., 2009). The significance level was set at $p < 0.05$. This correlation analysis was computed iteratively introducing a lag (τ) from 0 to 6 months. Li et al. (2022) studied up to a 2-year lag between several teleconnection patterns and terrestrial water storage and observed an approximately 5-month lag for most surface components. However, in this study, a lagged effect of teleconnection indices on SM was considered for up to 6 months, as in similar studies (Runge et al., 2019b; Silva et al., 2021; van Oldenborgh et al., 2000). Once the 7 R values were obtained for each pixel, the maximum absolute value of R (R_{max}) was obtained, considering only those with statistical significance. In this way, a significant R_{max} for a

given τ can be obtained for each pixel. This kind of analysis has been widely used to study lagged effects between decoupled variables (Peng et al., 2019; Xie et al., 2020).

Although lagged correlation can be a suitable tool for this kind of study, the presence of correlation between variables does not have to imply causation (Runge et al., 2019a). Additionally, note that Pearson correlation only captures linear relationships. Causal discovery consists of estimating the causal parents from a given time series data, meaning statistically significant causal dependencies, their strength and lag (Runge et al., 2019b). Identifying causal relationships between NAO, AO, ENSO and SM can help to better understand soil–atmosphere system dynamics. The Granger causality method (Granger, 1969) has probably been the most widely used approach to study causal effects on Earth dynamical systems (Bueso et al., 2020b; Gupta and Jain, 2021; Kodra et al., 2011; Morata-Dolz et al., 2020; Zolghadr-Asli et al., 2021). However, Runge et al. (2019b) recently proposed a causality method with significantly higher detection power than previous methods. This method is called PCMCI since it combines the PC method (named after its creators Peter and Clark) and the momentary conditional independence (MCI) test and enables identification of both the existence of causal links and their strength (Runge et al., 2019a). The PC method (Spirtes and Glymour, 1991) estimates the causal parents from a series. This method uses a free parameter, the significance level αPC, to encompass the inclusion of both causal parents with a high probability and some false-positive links (Runge et al., 2019b). Then, the MCI test can remove irrelevant conditions even for highly autocorrelated data (Runge et al., 2019b). Both the PC and the MCI can be implemented with different conditional independence tests. In addition, to estimate time-lagged causal links, another free parameter must be chosen, the maximum time delay τmax (Runge et al., 2019b). To implement this method, the Python package Tigramite v4.2 (Kretschmer et al., 2018; Nowack et al., 2020; Runge et al., 2019b) was used with the PCMCI and the partial correlation conditional independence test. The resulting coefficient obtained by this test, ranging between −1 and 1, represents the strength of the link. In this study, the free parameter αPC, that ranges between 0 and 1, was chosen to be optimized for every pixel, and the time-lagged links were considered up to the previous 6 months; thus, τmax was set to 6. The causal links were computed considering the teleconnection indices independently together with the SM anomaly time series for each pixel. The strength of links (climate index → SM) and their significance (set to $p < 0.05$) were tracked and, for the lagged correlation analysis, the strongest significative causal links and the associated month were recorded for each pixel.

4.3. Results and discussion

4.3.1. Correlation analysis

The correlation between SM and teleconnection indices was calculated, and only R values with statistical significance ($p < 0.05$) were considered. The results obtained with the ERA5L database (Figure 4.3) showed an extensive significant relationship between SM anomalies and the NAO and AO indices over Europe. In addition, this relationship was, in general, negative, which means that drier soil conditions are given during positive phases of both NAO and AO, while wetter conditions are given during negative phases. As expected, the results obtained with both indices were quite similar, since they are highly linked patterns (Mares et al., 2002). However, there were exceptions. Direct relationships were observed with AO in some regions, such as the British Isles, south of Finland and the north coast of France, Netherlands and Germany, which are indirect with NAO. The opposite occurred in southern France and the northern coast of Spain, where direct relationships were obtained with NAO and indirect relationships were obtained with AO. In contrast to Tabari and Willems (2018), who reported a stronger influence of NAO in European precipitation than with AO, we obtained that, for SM, the strongest correlations are with AO, with R values over or around −0.3 in the Iberian Peninsula, northern Italy, the Great Hungarian Plain and the Black Sea coast. The NAO showed a more uniform pattern in the area of study with similar correlation values, between −0.2 and −0.3, and very few regions with direct relationships, mostly concentrated in areas of Scotland, around the Pyrenees, Italy and the Balkans. The positive correlation over southern France was consistent with those observed by Boé (2013). These results showed discrepancies with other studies, which detected a relationship between positive phases of NAO and wetness conditions in parts of central and northern Europe in winter (Schubert et al., 2016; Sheffield and Wood, 2008; van der Schrier et al., 2006) when NAO shows more influence on European climate. However, in summer, NAO exerts a great impact on northern Europe (Bladé et al., 2012) with an increase in temperature (Folland et al., 2009) and reduced precipitation during positive phases (Allan and Zveryaev, 2011), which agrees with the negative correlations we obtained with SM. The negative correlation we obtained in southern Europe is in line with the results of previous studies focused on the meteorological drought response in Mediterranean areas (Mariotti and Dell'Aquila, 2012; Mi Kim and Raible, 2021; Sheffield and Wood, 2008; Vicente-Serrano et al., 2011).

The results obtained with the LF database for AO and NAO were similar (Figure 4.4), although fewer significant correlation coefficients were observed. Interestingly, stronger correlation values were obtained with AO mainly in Mediterranean regions, with R values below −0.3. These results are aligned with those obtained by Hassan and Nayak (2020), who related the positive phases of AO with the appearance of droughts in the Mediterranean region.

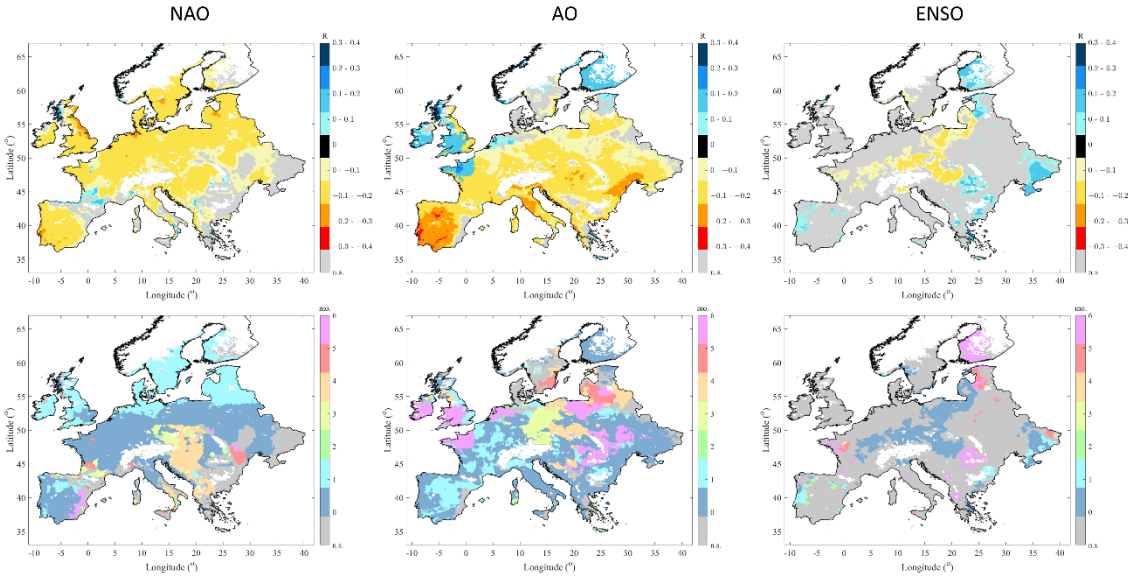

Figure 4.3 Results of the lagged correlation analysis between the ERA5L SM and teleconnection indices. The maps above show the maximum R-value and those below the lag in months in which these maxima occur. The area without statistical significance (n.s., $p < 0.05$) is in grey.

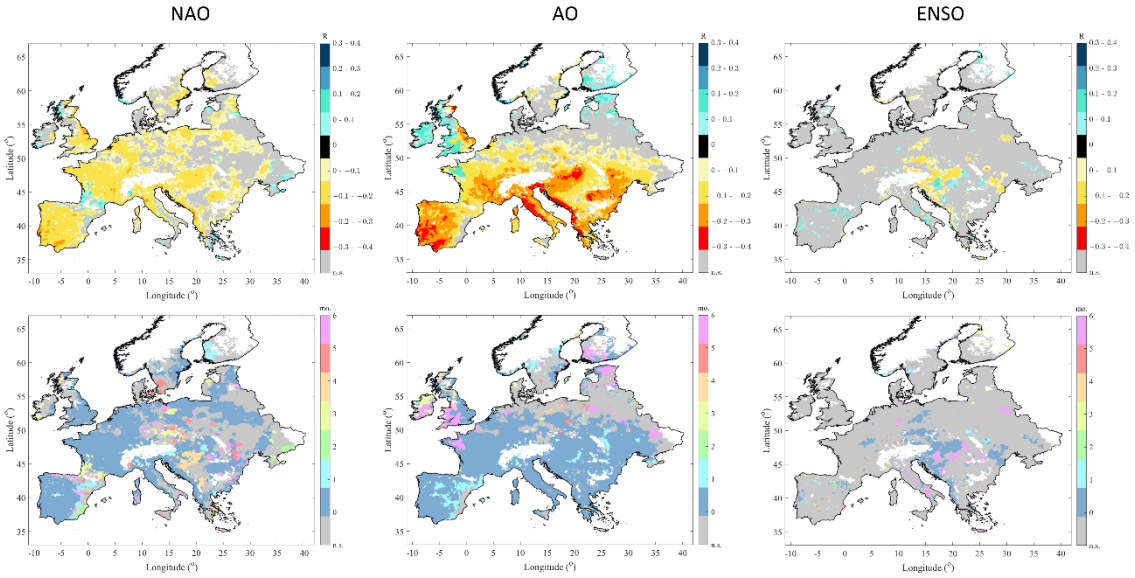

Figure 4.4 Results of the lagged correlation analysis between the LF SM and teleconnection indices. The maps above show the maximum R-value and those below the lag in months in which these maxima occur. The area without statistical significance (n.s., $p < 0.05$) is in grey.

Regarding the relationship of ENSO with both SM databases, only a few areas showed a significant correlation (Figure 4.3, Figure 4.4). These results can be explained by the fact that atmospheric changes in the El Niño region must be strong enough for this impact to be reflected in Europe (Brönnimann, 2007), and during our study period, only two strong El Niño events (1997–1998 and 2015–2016; Figure 4.2c) and no strong La Niña event occurred (Hardiman et al., 2019). Similarly, a previous study did not observe a significant relationship between modelled SM and the Southern Oscillation Index (SOI) in Europe for a similar period (Miralles et al., 2014). With ERA5L, indirect significant correlations were obtained in central Europe with R values between −0.1 and −0.2, which implies that, in that region, El Niño events lead to drier soils, while wetter conditions are given during La Niña events. Conversely, Brönnimann (2007) observed positive anomalies of precipitation during strong El Niño events and negative during strong La Niña for this region, but they only observed this during winter months. Direct correlations, meaning positive ENSO causes positive SM anomalies, were obtained in a few areas of eastern Europe, Finland and the Atlantic coast of the Iberian Peninsula. R values were, in general, lower than those obtained with AO and NAO; however, stronger correlations were obtained north of the Great Hungarian Plain, with R values below −0.2. The results obtained with the LF database matched in sign with those obtained with ERA5L, but the regions showing a significant correlation were reduced.

The R-values obtained with the three indices are relatively small in absolute value; however, it should be borne in mind that the influence of atmospheric anomalies in soil hydrology is being analysed and that there are many processes between the two systems that can dampen the strength of this relationship (Seneviratne et al., 2010). In addition, although several efforts have been made by many researchers to study teleconnections between atmospheric circulation and European climate (Brönnimann, 2007; Fraedrich and Müller, 1992), the results obtained in this study can be directly compared with only very few other results that targeted SM, either at regional or global scales (Le and Bae, 2022; Miralles et al., 2014; Sheffield and Wood, 2008). Although related variables in most cases present similar results, SM does not always behave as other water-related atmospheric variables, such as precipitation (Dai, 2011).

Some patterns could be observed when analysing the lag of maximum correlation obtained for the indices and SM anomalies (Figures 4.3, 4.4). With the NAO, few regions presented a lagged response of SM at a monthly scale for both databases. Nevertheless, more regions showed a delay in the SM anomalies with respect to teleconnection indices with ERA5L and not with LF. With ERA5L, a general one-month lag in Northern Europe was observed. A lag time of 4 months in southern Italy, the Great Hungarian Plain and the Balkans was found, while a later response (5–6 months lag) was observed in the east of the Iberian Peninsula and near the Danube mouth. For the AO, a prevalence of nonlagged effects also existed; however, the spatial distribution was less homogeneous with ERA5L. A one-month lag was mainly observed in western Europe, and a lag response of 3–4 months was observed in central Europe. In addition, it could be observed, with both products, that most regions with direct correlation presented a 6-month lag. Regarding ENSO, the lagged effects were seen mainly in regions with a direct relationship.

4.3.2. Causal discovery

A causality analysis was performed to investigate the existence of causal relationships between the NAO, AO and ENSO with SM anomalies. The PCMCI method was applied with a partial correlation conditional test and a maximum lag of 6 months. The results of causal link (climate index → SM) strength are shown in Figure 4.5, Figure 4.6 for ERA5L and LF, respectively. Both the AO and NAO results were quite similar to those obtained in the lagged correlation with both products, with similar strength magnitudes and signs, which indicates that the two indices are not only correlated to SM anomalies but are actually causing them. Thus, our obtained results reveal that negative phases of NAO and AO cause a general annual decrease in SM, beyond the broad presumption that winter (summer) positive NAO favours an increase (decrease) in precipitation and subsequently SM over central and northern Europe. According to this, the impact of climate change on atmospheric circulation patterns may ultimately induce changes in SM interannual variability. In this regard, an upwards trend in the AO has been reported since the 1960s (Delworth and Dixon, 2000) as well as a trend towards more positive NAO winters in the 1990s (Hurrell et al., 2003). Additionally, Hanna et al. (2015) reported a significant downwards trend in the summer NAO and an increase in variability in winter.

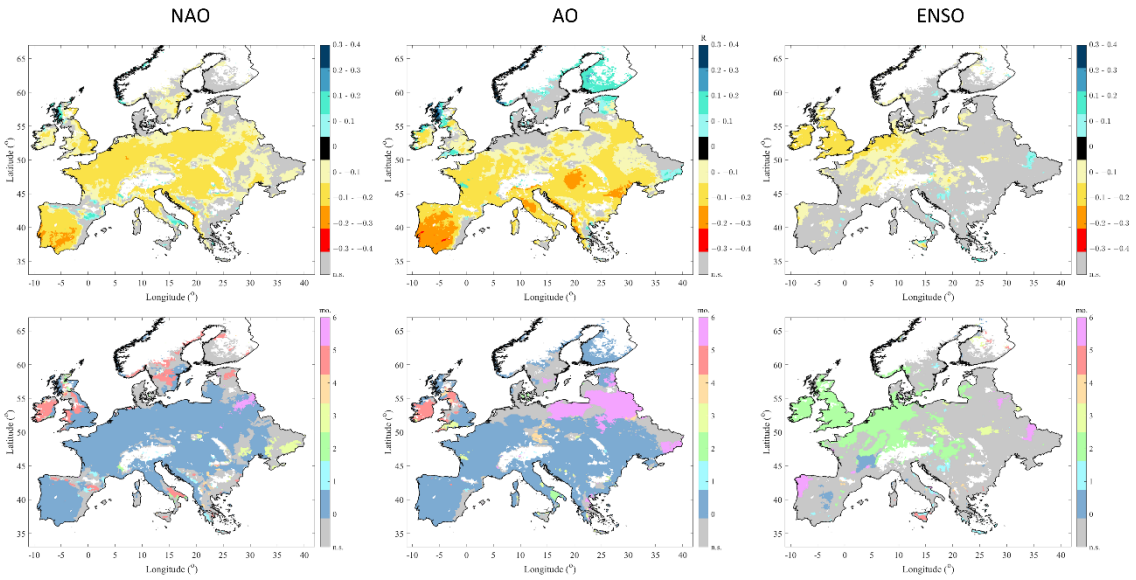

Figure 4.5 Results of the causality analysis between the ERA5L SM and teleconnection indices. The maps above show the highest causal strength (teleconnection index → SM) and those below the lag of those relations. The area without statistical significance (n.s., $p < 0.05$) is in grey.

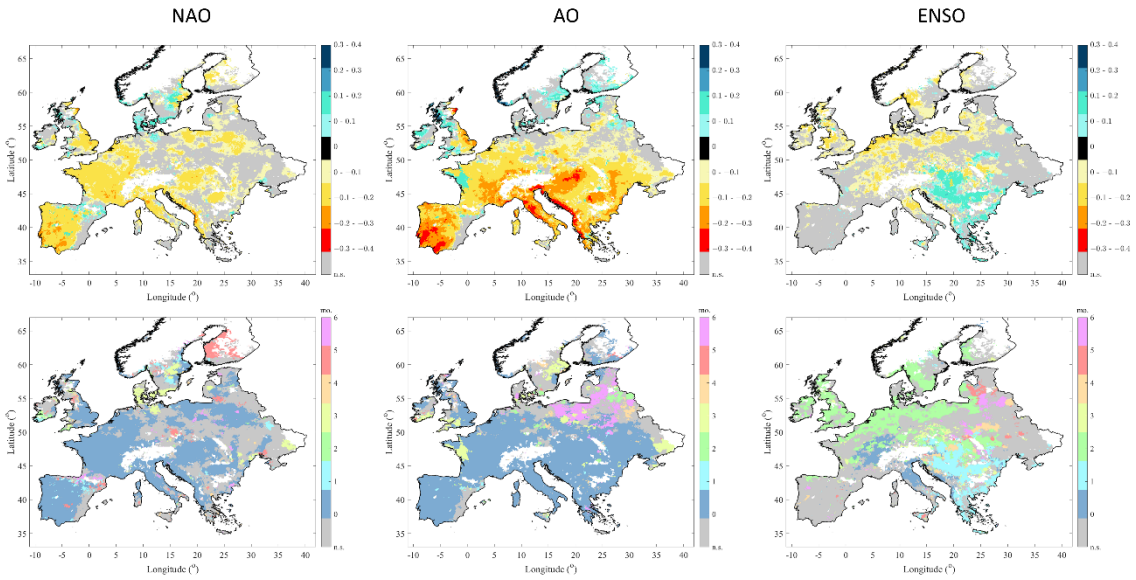

Figure 4.6 Results of the causality analysis between the LF SM and teleconnection indices. The maps above show the highest causal strength (teleconnection index → SM) and those below the lag of those relations. The area without statistical significance (n.s., $p < 0.05$) is in grey.

Causality and correlation do not necessarily have to coexist (Runge et al., 2019b), and this is precisely what we observed with ENSO and SM anomalies. Larger areas showed a significant causal relationship than in the lagged correlation analysis, especially with LF (see Figures 4.5, 4.6). Silva et al. (2021) also identified more response areas to ENSO with a causal method than with the correlation analysis. Negative causal relations appeared in the British Isles and the Atlantic coast, implying that an increase (decrease) in SST in the El Niño 3.4 region causes drier (wetter) soil conditions in these regions. This agrees with results found by Brönnimann (2007) during strong El Niño and La Niña events; he reported anomalies of low precipitation in those areas starting in Ireland during late autumn and extending to the continent in late winter, when they are combined with high temperature anomalies during El Niño and opposite conditions during La Niña. Positive causal relations were obtained (only with LF) in the Balkan region and the Great Hungarian Plain, which is also in agreement with that observed by Brönnimann (2007).

Regarding the lag of maximum causal strength, a similar pattern to that obtained with the lagged correlation analysis was observed. There is a predominance of nonlagged effects with the NAO and AO. Very few regions present a lagged response, especially with LF. For the NAO, lags were mainly observed when the relationships were positive, while for the AO, 6-month lagged causal relationships were located in the Baltic areas. With ENSO, a clear pattern was observed, consistent with both SM products: negative causal relationships showed a lag of 2 months, while positive ones showed a lag of 1 month. Longer lagged responses were obtained with this phenomenon than with AO and NAO, as could be expected, since different mechanisms occur between the equator of the Pacific Ocean and North Atlantic regions before seeing the impact in Europe (Brönnimann, 2007).

Bulić and Kucharski (2012) observed a lagged spring precipitation response to winter ENSO in Europe but also a contemporaneous response in spring, which agrees with the 1–2 month lag found here.

Causal discovery can help to better understand the processes interacting in the soil–atmosphere continuum. This methodology has shown that the correlations obtained with NAO and AO are indeed causal relationships and have allowed for a more in-depth analysis of the SM response to ENSO, which is probably nonlinear and hence was not fully captured by the correlation analysis. Nevertheless, the strength of the links obtained in this analysis refers to the evaluation of only two variables (teleconnection index and SM). These causal relationships could be analysed more precisely if more variables were incorporated, without increasing the dimensions of the analysis too much for the detection power to be affected (Runge et al., 2019b). However, performing this type of multivariable analysis would require a spatial aggregation of the information, and the spatial patterns would depend on the selected area and the method (Bueso et al., 2020a).

4.4. Conclusions

In this study, the influences that the NAO, AO and ENSO exert on European SM have been analysed. Monthly SM series were obtained from two different databases, one from the LF model and the other from reanalysis ERA5L. The results showed that both AO and NAO have a significant influence on European SM over almost the entire continent. The relationship was predominantly negative and maximum with no lag, which implies drier soil conditions in the positive phases and wetter conditions in the negative phases. The strongest correlations were obtained with AO in the Mediterranean regions. Whereas a direct relationship was expected with the NAO in Northern Europe, as NAO is traditionally assumed to increase precipitation and colder conditions in the north, this region only showed a direct relationship with AO with a lag of 6 months, while NAO showed a uniformly indirect response over almost the entire continent. With ENSO, hardly any correlation was observed, probably because ENSO influences the European climate indirectly and nonlinearly. Although the spatial patterns observed for SM were, in general, in line with those obtained in other works for water-related atmospheric variables, some differences have been observed, which highlights the need for focusing studies specifically on the SM response to atmospheric circulation patterns.

The analysis of causality between the teleconnection indices and SM was the second objective of this study. This type of analysis has been applied in only a few studies of Earth science. In this work, a novel method has been used, the PCMCI, which allows the incorporation of conditional independence tests such as partial correlation. In the causality study carried out, for AO and NAO, the results obtained have been very similar in strength, sign and lag to those obtained in the correlation study. This result showed the causal effect that both atmospheric patterns have on the SM dynamics, i.e., negative phases of NAO and AO will cause a decrease in SM. Stronger causal relations were obtained with AO in Mediterranean regions, which is important to consider due to the increasing risk of drought occurrence in this region. For ENSO, the causality analysis allowed finding SM response areas that were undetected by the correlation analysis. Direct links were observed in central and northwestern Europe with a delayed effect of two months, and indirect links were observed in the Balkan region with a delayed effect of 1 month.

Regarding both SM databases, the results obtained were very similar. However, slightly stronger correlations and causal relationships were observed with the LF database. Conversely, more surface area with significant correlations and more spatial patterns of delayed response of SM were observed with the ERA5L data.

From the results of the present study, causal discovery methods are powerful methods to help better understand soil–atmosphere interactions. However, the way of applying this methodology in this work shows some limitations, and the results should be taken with caution. In particular, only linear relationships and just two variables were considered here, the teleconnection index and SM, while incorporating more variables and apply no linear methods would probably enable a more precise evaluation of the causal relationships. Additionally, we are treating time series separately, while spatiotemporal methods could

also be considered. However, with a spatiotemporal approach, the spatial patterns would depend on the spatially aggregated area or the method used to analyse all information together.

This work highlights the importance of studies focused on SM dynamics and interactions, since most studies are centred on precipitation, but the atmosphere does not always impact all water-related variables in the same way, and SM is key to understanding its impact on issues such as agricultural drought, runoff yield, groundwater recharge and many other water-related processes. Undoubtedly, there is still work to be done to properly define the causal relationships between soil–atmosphere systems, but advances in this field are paramount to better understand the impact of climate change on SM dynamics and consequently on agricultural drought.

CAPÍTVLO 5

CONCLUSIONES Y LÍNEAS FUTURAS DE INVESTIGACIÓN

5.1. Conclusiones / Conclusions

Conclusiones

El trabajo desarrollado en esta tesis ha evaluado diferentes metodologías con el objeto de abordar asuntos que, hasta ahora, limitaban la comprensión de algunos aspectos sobre la SM y sus cambios como consecuencia del cambio climático en Europa. Esto se ha llevado a cabo a través de tres objetivos específicos basados tanto en la mejora de bases de datos de esta variable, como en el estudio de sus cambios y la interacción con los patrones atmosféricos. En este capítulo se presentan las conclusiones obtenidas, resaltando las principales contribuciones.

En primer lugar, en relación con la limitación que pueden suponer las lagunas de datos en las series satelitales de SM, esta tesis ha evaluado diferentes técnicas de *gap-filling* en la serie de datos satelital más larga disponible, la ESA CCI SM. Los resultados obtenidos han demostrado que, en general, los métodos más simples, es decir, las interpolaciones, son capaces de rellenar acertadamente las lagunas de datos, temporales o espaciales, siempre que éstas no sean muy grandes. De la misma forma, los métodos autorregresivos, aunque con mejor precisión, tampoco demostraron ser apropiados para rellenar lagunas de datos temporales de gran longitud. Esto no se observó con el método SVM, que, junto con una selección óptima de las variables de entrada, ha demostrado ser una herramienta capaz de estimar los datos ausentes en las series de CCI SM, independientemente de la longitud de las lagunas en los datos. Además, se ha observado que la aplicación de las SVM al dominio espacial puede ofrecer mejores resultados que aplicando este método al dominio temporal, y, que, en ambos casos, las estimaciones mejoran cuando se incorporan a los modelos las series de SM del día anterior. Por el contrario, el uso de un método de reducción de características (el PCA) junto con las SVM, empeoró en todos los casos las estimaciones de SM. Aunque se ha observado un gran potencial en las técnicas de ML para rellenar las lagunas, este trabajo demuestra que la selección de variables de entrada es asimismo clave para obtener buenas estimaciones. Las SVM demostraron poder reproducir la dinámica espacial o temporal de la SM mejor que otras técnicas ML más sencillas como los RF.

En segundo lugar, el análisis de la tendencia de la SM en Europa desarrollado en esta tesis ha permitido definir y cuantificar los patrones de cambio de esta variable durante los últimos 30 años. Los resultados obtenidos con los diferentes métodos, bases de datos y escalas temporales han mostrado una gran consistencia. Además, se ha observado que otros métodos, alternativos a aquellos más frecuentemente utilizados para el análisis de tendencias como es el test de MK, son capaces de determinar más patrones de cambio en variables con un comportamiento no lineal. En concreto, el EMD ha permitido identificar un patrón generalizado de cambio a condiciones más secas en los suelos europeos, siendo este cambio significativo en una gran extensión de territorio. Este resultado permite reconciliar los resultados obtenidos para otras variables estrechamente relacionadas con la SM como la precipitación, la evapotranspiración o la temperatura. Sin embargo, no se ha observado una dependencia de los patrones de cambio con los climas del continente. Asimismo, las tendencias observadas en los atributos de la sequía agrícola en Europa han

mostrado de forma predominante un incremento en su duración e intensidad, con un retraso de unos pocos días en su comienzo cada año.

Por último, se ha demostrado la necesidad de profundizar en la influencia que los patrones de circulación atmosférica pueden ejercer en la dinámica de la SM en Europa. Aunque, muchos de los resultados obtenidos en el trabajo desarrollado en esta tesis estén en consonancia con los obtenidos para otras variables hidro-climáticas, existen diferencias en la respuesta de esta variable. Las correlaciones estudiadas han mostrado una relación predominantemente inversa e inmediata entre la NAO y la AO con la SM en casi todo el continente. Por el contrario, apenas se observaron correlaciones significativas entre ENSO y SM. Complementariamente, el estudio de las relaciones causales realizado en este trabajo ha demostrado ser apropiado y de gran utilidad para definir la respuesta de la SM a NAO, AO y ENSO. En esta tesis, se evaluaron las relaciones causales empleando un método novedoso, el PCMCI, que no había sido utilizado antes en el contexto de las interacciones suelo-atmósfera. Aunque su aplicación puede presentar limitaciones al estudiar las relaciones lineales y únicamente entre dos variables, los resultados han permitido identificar relaciones causa-efecto entre NAO, AO, ENSO y la SM. Los resultados han demostrado un enorme interés, por un lado, porque han demostrado que las correlaciones obtenidas con NAO y AO implican una relación causal con la SM. Y, por otro lado, porque han permitido identificar regiones, no observadas en el análisis de correlación, donde la SM muestra una respuesta retrasada de uno o dos meses a ENSO.

Aunque su protagonismo ha estado en ocasiones enmascarado por otras variables hidrológicas más fáciles de monitorizar, como la precipitación, en esta tesis se ha puesto de manifiesto la importancia de poner el foco sobre la SM. El trabajo desarrollado ha contribuido a evaluar el uso de diferentes métodos y bases de datos aplicables tanto a la mejora de los mismos datos, como al estudio de sus cambios y sus interacciones con los patrones atmosféricos en una región de especial interés como es el continente europeo.

Conclusions

The work carried out in this thesis has evaluated different methodologies to address issues that, until now, have limited the understanding of some aspects of SM and its changes due to climate change in Europe. This has been done through three specific objectives based both on the improvement of databases of this variable and on the study of its changes and interaction with atmospheric patterns. This chapter reports the conclusions obtained, highlighting the main contributions.

First, in relation to the limitation that data gaps of satellite SM series may entail, this thesis has evaluated different gap-filling techniques in the longest satellite data series available, the ESA CCI SM. The results obtained have shown that, in general, the simplest methods, that is, interpolations, are capable of correctly filling the temporal and spatial data gaps if they are not very large. Likewise, autoregressive methods, although with better precision, did not prove to be appropriate for filling large temporal data gaps. This was not observed with the SVM method, which, together with optimal input variables, has been shown to be a suitable tool for estimating missing data in the CCI SM series, regardless of the gap length. In addition, it has been observed that the application of the SVM to the spatial domain can provide better results than applying this method in the temporal domain, and that, in both cases, the estimates improve when series of SM from the previous day are incorporated into the models. In contrast, the use of a feature reduction method (the PCA) together with the SVMs worsened the SM estimates in all cases. Although great potential has been observed in ML techniques to fill in the gaps, this work demonstrates that the selection of input variables is key to obtaining good estimates. SVMs proved to be able to reproduce the spatial or temporal dynamics of SM better than other simpler ML techniques such as RF.

Second, the analysis of SM trends in Europe carried out in this thesis has allowed us to define and quantify change patterns of this variable over the last 30 years. The results obtained with the different methods, databases, and time scales have shown great consistency. In addition, it has been observed that other methods, alternative to those most frequently used for trend analysis, such as the MK test, can identify more patterns of change in variables with non-linear behavior. Specifically, the EMD has allowed identifying a generalized pattern of change to drier conditions in European soils, being this change significant in a large area of the continent. This result allows us to reconcile other results obtained for variables closely related to SM such as precipitation, evapotranspiration, or temperature. However, differences between the change patterns in the different European climates has not been observed. Likewise, the trends observed in the agricultural drought attributes in Europe have predominantly shown an increase in its duration and intensity, with a delay of a few days in its onset each year.

Finally, it has been shown the need to explore the influence that atmospheric circulation patterns can have on the SM dynamics in Europe. Although many of the results obtained in the work developed in this thesis are consistent with those obtained for other hydro-climatic variables, there are differences in the response of this variable. The correlations obtained have shown a predominantly inverse and unlagged relationship between the NAO

and the AO with the SM in almost the entire continent. In contrast, hardly any significant correlations were observed between ENSO and SM. Besides, the study of the causal relationships carried out in this work has proven to be appropriate and very useful to define the response of the SM to NAO, AO, and ENSO. In this thesis, causal relationships were evaluated using a novel method, PCMCI, which had not been used before in the context of soil-atmosphere interactions. Although its application may have limitations when studying linear relationships and between only two variables, the results have allowed us to identify cause-effect relationships between NAO, AO and ENSO, and SM. The results have shown enormous interest, on the one hand, because they have shown that the correlations obtained with NAO and AO imply a causal relationship with SM. And, on the other hand, because it has allowed identifying regions where the SM shows a delayed response of one or two months to ENSO, which was not observed in the correlation analysis.

Although its role has sometimes been masked by other hydrological variables that are easier to monitor, such as precipitation, the importance of focusing on SM has been highlighted in this thesis. The work carried out has contributed to evaluating the use of different methods and databases applicable both to the improvement of the data and to the study of its changes and its interactions with atmospheric patterns in a region of special interest such as the European continent.

5.2. Líneas futuras de investigación

En esta tesis se han cumplido satisfactoriamente los objetivos planteados. No obstante, durante su desarrollo se han puesto de manifiesto diferentes incertidumbres, que posibilitan la definición de nuevos objetivos para abordar en futuras investigaciones.

En lo que respecta al relleno de las lagunas de datos en las series satelitales, se ha demostrado que las técnicas de ML junto con una buena selección de los datos de entrada poseen un enorme potencial para hacer frente a esta limitación. En particular los SVM han sido capaces de estimar las lagunas de datos espaciales de forma precisa, pero algunos aspectos pueden ser mejorados. Ejemplos de posibles mejoras pueden ser la optimización de los hiperparámetros del algoritmo o el uso de diferentes bases de datos de las variables de entrada para cuantificar y minimizar los errores generados por éstas. Además, existen diferentes técnicas de regresión de ML como los *Gaussian Processes* (GP) o las redes neuronales (*artificial neuronal networks*, ANNs), que podrían ofrecer estimaciones precisas de los valores ausentes de la SM. Durante el transcurso de la tesis, para una comunicación de congreso, se ha podido realizar una primera exploración de los GP aplicados al relleno de las lagunas de datos de la base de datos ESA CCI SM, y han ofrecido unos buenos resultados preliminares. Por último, aunque los resultados obtenidos en esta tesis se refieren únicamente a esta base de datos satelital, algunas de las técnicas evaluadas han demostrado un gran potencial y podrían ser aplicables a las series de SM más recientes como son las de SMOS o SMAP.

Por otro lado, en esta tesis se ha demostrado que tener en cuenta el comportamiento no monotónico es fundamental en el estudio de tendencias de la SM. Sin dejar de lado a los métodos clásicos como MK, se ha puesto de manifiesto la necesidad y utilidad de explorar nuevos métodos para la detección de tendencias. La EMD ha demostrado ser un método efectivo para identificar patrones de cambio no detectados por MK. Sin embargo, existen otros posibles métodos no monotónicos como la transformada *wavelet* o la transformada de Fourier que han mostrado un gran potencial al analizar las tendencias de otras variables hidroclimáticas. Para una correcta conciliación de resultados sería necesaria una comparación entre diferentes enfoques (test estadísticos, escalas temporales, bases de datos, etc.). Por lo que una posible vía de investigación podría ser evaluar los resultados obtenidos con otros métodos que tengan en cuenta la dinámica no monotónica. Además, en esta tesis se han estudiado las tendencias de la SM en la capa más superficial del suelo. Dado que los datos de los modelos también proporcionan series de SM a distintas profundidades, se podría analizar la tendencia de cambio en distintas capas del suelo y estudiar si existen diferencias en cuanto al signo, magnitud y/o linealidad entre las tendencias observadas en la capa más superficial y las de la zona radicular.

Por último, al estudiar la influencia que los patrones de circulación atmosférica ejercen en la variabilidad de la SM, se ha observado que los métodos de inferencia causal pueden ser una buena herramienta. En el análisis desarrollado en esta tesis, únicamente se han tenido en cuenta las relaciones lineales, sin embargo, el estudio de las relaciones no lineales podría ofrecer información adicional, sobre todo para las relaciones entre la ENSO y la SM en

Europa. Con respecto al análisis de causalidad, es sabido que la correlación no implica causalidad, y no se pueden fundamentar relaciones causales únicamente a través de asociaciones, ya que primero debe existir una suposición causal. Sin embargo, los resultados obtenidos en esta tesis han mostrado relaciones causales entre ENSO y SM sin haber observado previamente una asociación, por lo que estudiar en profundidad estas diferencias sería un interesante objetivo que abordar. Una forma de llevar esto a cabo sería la inclusión en el análisis de más variables que tengan una asociación con la dinámica de la SM, como la precipitación o la evapotranspiración, y estudiar las redes de relaciones causales que ofrece el PCMCI. Para este tipo de enfoque sería necesaria una agregación espacial de la información, por lo que sería más conveniente estudiar estas relaciones a una escala regional. También se podrían explorar otros métodos de causalidad no lineales que aprenden las relaciones directamente de las observaciones como el PCMCI junto con un test de independencia condicional no lineal o el método *kernel* para la causalidad de Granger.

REFERENCIAS

Abbott, M.B., Bathurst, J.C., Cunge, J.A., O'Connell, P.E., Rasmussen, J., 1986. An introduction to the European Hydrological System - Systeme Hydrologique Europeen, "SHE", 1: History and philosophy of a physically-based, distributed modelling system. J Hydrol (Amst) 87, 45–59. https://doi.org/10.1016/0022-1694(86)90114-9

Adamowski, K., Prokoph, A., Adamowski, J., 2009. Development of a new method of wavelet aided trend detection and estimation. Hydrol Process 23, 2686–2696. https://doi.org/10.1002/hyp.7260

Adarsh, S., Janga Reddy, M., 2019. Evaluation of trends and predictability of short-term droughts in three meteorological subdivisions of India using multivariate EMD-based hybrid modelling. Hydrol Process 33, 130–143. https://doi.org/10.1002/hyp.13316

Ahmad, A., Zhang, Y., Nichols, S., 2011. Review and evaluation of remote sensing methods for soil-moisture estimation. SPIE reviews 2, 028001.

Ahmad, S., Kalra, A., Stephen, H., 2010. Estimating soil moisture using remote sensing data: A machine learning approach. Adv Water Resour 33, 69–80. https://doi.org/10.1016/j.advwatres.2009.10.008

Albergel, C., Balsamo, G., de Rosnay, P., Muñoz-Sabater, J., Boussetta, S., 2012. A bare ground evaporation revision in the ECMWF land-surface scheme: Evaluation of its impact using ground soil moisture and satellite microwave data. Hydrol Earth Syst Sci 16, 3607–3620. https://doi.org/10.5194/hess-16-3607-2012

Albergel, C., Dorigo, W., Reichle, R.H., Balsamo, G., Derosnay, P., Muñoz-sabater, J., Isaksen, L., Dejeu, R., Wagner, W., 2013. Skill and global trend analysis of soil moisture from reanalyses and microwave remote sensing. J Hydrometeorol 14, 1259–1277. https://doi.org/10.1175/JHM-D-12-0161.1

Ali, I., Greifeneder, F., Stamenkovic, J., Neumann, M., Notarnicola, C., 2015. Review of Machine Learning Approaches for Biomass and Soil Moisture Retrievals from Remote Sensing Data. Remote Sens 7, 16398–16421. https://doi.org/10.3390/rs71215841

Allan, R.P., Zveryaev, I.I., 2011. Variability in the summer season hydrological cycle over the Atlantic-Europe region 1979-2007. Int J Climatol 31, 337–348. https://doi.org/10.1002/joc.2070

Almendra-Martín, L., Martínez-Fernández, J., González-Zamora, Á., Benito-Verdugo, P., Herrero-Jiménez, C.M., 2021a. Agricultural drought trends on the Iberian peninsula: An analysis using modeled and reanalysis soil moisture products. Atmosphere 12. https://doi.org/10.3390/atmos12020236

Almendra-Martín, L., Martínez-Fernández, J., Piles, M., González-Zamora, Á., 2021b. Comparison of gap-filling techniques applied to the CCI soil moisture database in Southern Europe. Remote Sens Environ 258. https://doi.org/10.1016/j.rse.2021.112377

Almendra-Martín, L., Martínez-Fernández, J., Piles, M., González-Zamora, Á., Benito-Verdugo, P., Gaona, J., 2022. Analysis of soil moisture trends in Europe using rank-based and empirical decomposition approaches. Glob Planet Change 215. https://doi.org/10.1016/j.gloplacha.2022.103868

Altese, E., Bolognani, O., Mancini, M., Troch, P.A., 1996. Retrieving Soil Moisture Over Bare Soil from ERS 1 Synthetic Aperture Radar Data: Sensitivity Analysis Based on a Theoretical Surface Scattering Model and Field Data. Water Resour Res 32, 653–661. https://doi.org/10.1029/95WR03638

Al-Yaari, A., Wigneron, J.-P., Dorigo, W., Colliander, A., Pellarin, T., Hahn, S., Mialon, A., Richaume, P., Fernandez-Moran, R., Fan, L., Kerr, Y.H., de Lannoy, G., 2019. Assessment and inter-comparison of recently developed/reprocessed microwave satellite soil moisture products using ISMN ground-based measurements. Remote Sens Environ 224, 289–303. https://doi.org/10.1016/j.rse.2019.02.008

An, R., Zhang, L., Wang, Z., Quaye-Ballard, J.A., You, J., Shen, X., Gao, W., Huang, L., Zhao, Y., Ke, Z., 2016. Validation of the ESA CCI soil moisture product in China. Int J Appl Earth Obs Geoinf 48, 28–36. https://doi.org/10.1016/j.jag.2015.09.009

Anderson, W., Seager, R., Baethgen, W., Cane, M., 2017. Life cycles of agriculturally relevant ENSO teleconnections in North and South America. Int J Climatol 37, 3297–3318. https://doi.org/10.1002/joc.4916

Archaux, F., Wolters, V., 2006. Impact of summer drought on forest biodiversity: what do we know? Ann For Sci 63, 645–652. https://doi.org/10.1051/forest:2006041

Arnell, N.W., 1999. The effect of climate change on hydrological regimes in Europe: A continental perspective. Glob Environ Change 9, 5–23. https://doi.org/10.1016/S0959-3780(98)00015-6

Asfaw, A., Simane, B., Hassen, A., Bantider, A., 2018. Variability and time series trend analysis of rainfall and temperature in northcentral Ethiopia: A case study in Woleka sub-basin. Weather Clim Extrem 19, 29–41. https://doi.org/10.1016/j.wace.2017.12.002

Bai, L., Xu, J., Chen, Z., Li, W., Liu, Z., Zhao, B., Wang, Z., 2015. The regional features of temperature variation trends over Xinjiang in China by the ensemble empirical mode decomposition method. Int J Climatol 35, 3229–3237. https://doi.org/10.1002/joc.4202

Ballabio, C., Panagos, P., Monatanarella, L., 2016. Mapping topsoil physical properties at European scale using the LUCAS database. Geoderma 261, 110–123. https://doi.org/10.1016/j.geoderma.2015.07.006

Balsamo, G., Albergel, C., Beljaars, A., Boussetta, S., Brun, E., Cloke, H., Dee, D., Dutra, E., Munõz-Sabater, J., Pappenberger, F., de Rosnay, P., Stockdale, T., Vitart, F., 2015. ERA-Interim/Land: A global land surface reanalysis data set. Hydrol Earth Syst Sci 19, 389–407. https://doi.org/10.5194/hess-19-389-2015

Balsamo, G., Viterbo, P., Beijaars, A., van den Hurk, B., Hirschi, M., Betts, A.K., Scipal, K., 2009. A revised hydrology for the ECMWF model: Verification from field site to terrestrial water storage and impact in the integrated forecast system. J Hydrometeorol 10, 623–643. https://doi.org/10.1175/2008JHM1068.1

Bannari, A., Morin, D., Bonn, F., Huete, A.R., 1995. A review of vegetation indices. Remote Sensing Reviews 13, 95–120. https://doi.org/10.1080/02757259509532298

Bao, Y., Lin, L., Wu, S., Kwal Deng, K.A., Petropoulos, G.P., 2018. Surface soil moisture retrievals over partially vegetated areas from the synergy of Sentinel-1 and Landsat 8 data using a modified water-cloud model. Int J Appl Earth Obs Geoinf 72, 76–85. https://doi.org/10.1016/j.jag.2018.05.026

Bartalis, Z., Wagner, W., Naeimi, V., Hasenauer, S., Scipal, K., Bonekamp, H., Figa, J., Anderson, C., 2007. Initial soil moisture retrievals from the METOP-A Advanced Scatterometer (ASCAT). Geophys Res Lett 34, L20401. https://doi.org/10.1029/2007GL031088

Bartsch, A., Balzter, H., George, C., 2009. The influence of regional surface soil moisture anomalies on forest fires in Siberia observed from satellites. Environ Res Lett 4, 045021. https://doi.org/10.1088/1748-9326/4/4/045021

Bastos, A., Janssens, I.A., Gouveia, C.M., Trigo, R.M., Ciais, P., Chevallier, F., Peñuelas, J., Rödenbeck, C., Piao, S., Friedlingstein, P., Running, S.W., 2016. European land CO2 sink influenced by NAO and East-Atlantic Pattern coupling. Nat Commun 7, 10315. https://doi.org/10.1038/ncomms10315

Beck, H.E., Pan, M., Miralles, D.G., Reichle, R.H., Dorigo, W.A., Hahn, S., Sheffield, J., Karthikeyan, L., Balsamo, G., Parinussa, R.M., van Dijk, A.I.J.M., Du, J., Kimball, J.S., Vergopolan, N., Wood, E.F., 2020. Evaluation of 18 satellite- and model-based soil moisture products using in situ measurements from 826 sensors. Hydrol Earth Syst Sci 1–35. https://doi.org/10.5194/hess-2020-184

Beck, H.E., Zimmermann, N.E., McVicar, T.R., Vergopolan, N., Berg, A., Wood, E.F., 2018. Present and future köppen-geiger climate classification maps at 1-km resolution. Sci Data 5, 1–12. https://doi.org/10.1038/sdata.2018.214

Benesty, J., Chen, J., Huang, Y., Cohen, I., 2009. Pearson correlation coefficient, in: Springer Topics in Signal Processing. Springer Science and Business Media B.V., pp. 1–4. https://doi.org/10.1007/978-3-642-00296-0_5

Bergström, S., 1976. Development and application of a conceptual runoff model for Scandinavian catchments. RHO, Hydrology and Oceanography.

Beven, K.J., Kirkby, M.J., 1979. A physically based, variable contributing area model of basin hydrology. Hydrological Sciences Bulletin 24, 43–69. https://doi.org/10.1080/02626667909491834

Bierkens, M.F.P., Bell, V.A., Burek, P., Chaney, N., Condon, L.E., David, C.H., de Roo, A., Döll, P., Drost, N., Famiglietti, J.S., Flörke, M., Gochis, D.J., Houser, P., Hut, R., Keune, J., Kollet, S., Maxwell, R.M., Reager, J.T., Samaniego, L., Sudicky, E., Sutanudjaja, E.H., van de Giesen, N., Winsemius, H., Wood, E.F., 2015. Hyper-resolution global hydrological modelling: what is next? Hydrol Process 29, 310–320. https://doi.org/10.1002/hyp.10391

Bindlish, R., Jackson, T., Cosh, M., Zhao, T., O'Neill, P., 2015. Global soil moisture from the aquarius/SAC-D satellite: Description and initial assessment. IEEE Geosci Remote Sens Lett 12, 923–927. https://doi.org/10.1109/LGRS.2014.2364151

Birkel, C., Barahona, A.C., 2019. Rainfall-Runoff Modeling: A Brief Overview, in: Reference Module in Earth Systems and Environmental Sciences. Elsevier. https://doi.org/10.1016/b978-0-12-409548-9.11595-7

Bladé, I., Liebmann, B., Fortuny, D., van Oldenborgh, G.J., 2012. Observed and simulated impacts of the summer NAO in Europe: Implications for projected drying in the Mediterranean region. Clim Dyn 39, 709–727. https://doi.org/10.1007/s00382-011-1195-x

Boé, J., 2013. Modulation of soil moisture-precipitation interactions over France by large scale circulation. Clim Dyn 40, 875–892. https://doi.org/10.1007/s00382-012-1380-6

Boni, G., Entekhabi, D., Castelli, F., 2001. Land data assimilation with satellite measurements for the estimation of surface energy balance components and surface control on evaporation. Water Resour Res 37, 1713–1722. https://doi.org/10.1029/2001WR900020

Bordi, I., Fraedrich, K., Sutera, A., 2009. Observed drought and wetness trends in Europe: An update. Hydrol Earth Syst Sci 13, 1519–1530. https://doi.org/10.5194/hess-13-1519-2009

Botter, G., Peratoner, F., Porporato, A., Rodriguez-Iturbe, I., Rinaldo, A., 2007. Signatures of large-scale soil moisture dynamics on streamflow statistics across U.S. climate regimes. Water Resour Res 43, 1–10. https://doi.org/10.1029/2007WR006162

Breiman, L., 2001. Random Forests. Mach Learn 45, 5–32. https://doi.org/10.1023/A:1010933404324

Brocca, L., Camici, S., Melone, F., Moramarco, T., Martínez-Fernández, J., Didon-Lescot, J.-F., Morbidelli, R., 2014. Improving the representation of soil moisture by using a semi-analytical infiltration model. Hydrol Process 28, 2103–2115. https://doi.org/10.1002/hyp.9766

Brocca, L., Ciabatta, L., Massari, C., Camici, S., Tarpanelli, A., 2017. Soil Moisture for Hydrological Applications: Open Questions and New Opportunities. Water 9, 140. https://doi.org/10.3390/w9020140

Brocca, L., Melone, F., Moramarco, T., 2011. Distributed rainfall-runoff modelling for flood frequency estimation and flood forecasting. Hydrol Process 25, 2801–2813. https://doi.org/10.1002/hyp.8042

Brocca, L., Melone, F., Moramarco, T., 2008. On the estimation of antecedent wetness conditions in rainfall–runoff modelling. Hydrol Process 22, 629–642. https://doi.org/10.1002/hyp.6629

Brocca, L., Melone, F., Moramarco, T., Morbidelli, R., 2010. Spatial - temporal variability of soil moisture and its estimation across scales. Water Resour Res 46, 1–14. https://doi.org/10.1029/2009WR008016

Brocca, L., Moramarco, T., Melone, F., Wagner, W., Hasenauer, S., Hahn, S., 2012. Assimilation of Surface- and Root-Zone ASCAT Soil Moisture Products Into Rainfall-Runoff Modeling. IEEE Trans Geosci Remote Sens 50, 2542–2555. https://doi.org/10.1109/TGRS.2011.2177468

Brocca, L., Tarpanelli, A., Filippucci, P., Dorigo, W., Zaussinger, F., Gruber, A., Fernández-Prieto, D., 2018. How much water is used for irrigation? A new approach exploiting coarse resolution satellite soil moisture products. Int J Appl Earth Obs Geoinf 73, 752–766. https://doi.org/10.1016/j.jag.2018.08.023

Brönnimann, S., 2007. Impact of El Niño-Southern Oscillation on European climate. Reviews of Geophysics 45. https://doi.org/10.1029/2006RG000199

Browne, M.W., 2000. Cross-Validation Methods. J Math Psychol 44, 108–132. https://doi.org/10.1006/jmps.1999.1279

Bueso, D., Piles, M., Camps-Valls, G., 2020a. Nonlinear PCA for Spatio-Temporal Analysis of Earth Observation Data. IEEE Trans Geosci Remote Sens 58, 5752–5763. https://doi.org/10.1109/TGRS.2020.2969813

Bueso, D., Piles, M., Camps-Valls, G., 2020b. Explicit Granger causality in kernel Hilbert spaces. Phys Rev E 102, 062201. https://doi.org/10.1103/PhysRevE.102.062201

Bulić, I.H., Kucharski, F., 2012. Delayed ENSO impact on spring precipitation over North/Atlantic European region. Clim Dyn 38, 2593–2612. https://doi.org/10.1007/s00382-011-1151-9

Caloiero, T., Caloiero, P., Frustaci, F., 2018. Long-term precipitation trend analysis in Europe and in the Mediterranean basin. Water Environ J 32, 433–445. https://doi.org/10.1111/wej.12346

Cammalleri, C., Micale, F., Vogt, J., 2016. Recent temporal trend in modelled soil water deficit over Europe driven by meteorological observations. Int J Climatol 36, 4903–4912. https://doi.org/10.1002/joc.4677

Camps-Valls, G., Gómez-Chova, L., Calpe-Maravilla, J., Martín-Guerrero, J.D., Soria-Olivas, E., Alonso-Chordá, L., Moreno, J., 2004. Robust support vector method for hyperspectral data classification and knowledge discovery. IEEE Trans Geosci Remote Sens 42, 1530–1542. https://doi.org/10.1109/TGRS.2004.827262

Carmona, A.M., Poveda, G., 2014. Detection of long-term trends in monthly hydro-climatic series of Colombia through Empirical Mode Decomposition. Clim Change 123, 301–313. https://doi.org/10.1007/s10584-013-1046-3

Casanueva, A., Rodríguez-Puebla, C., Frías, M.D., González-Reviriego, N., 2014. Variability of extreme precipitation over Europe and its relationships with teleconnection patterns. Hydrol Earth Syst Sci 18, 709–725. https://doi.org/10.5194/hess-18-709-2014

Champagne, C., White, J., Berg, A., Belair, S., Carrera, M., 2019. Impact of Soil Moisture Data Characteristics on the Sensitivity to Crop Yields Under Drought and Excess Moisture Conditions. Remote Sens 11, 372. https://doi.org/10.3390/rs11040372

Chan, S.K., Bindlish, R., O'Neill, P.E., Njoku, E., Jackson, T., Colliander, A., Chen, F., Burgin, M., Dunbar, S., Piepmeier, J., Yueh, S., Entekhabi, D., Cosh, M.H., Caldwell, T., Walker, J., Wu, X., Berg, A., Rowlandson, T., Pacheco, A., McNairn, H., Thibeault, M., Martínez-Fernández, J., González-Zamora, Á., Seyfried, M., Bosch, D., Starks, P., Goodrich, D., Prueger, J., Palecki, M., Small, E.E., Zreda, M., Calvet, J.-C., Crow, W.T., Kerr, Y., 2016. Assessment of the SMAP Passive Soil Moisture Product. IEEE Trans Geosci Remote Sens 54, 4994–5007. https://doi.org/10.1109/TGRS.2016.2561938

Chaubell, J., Yueh, S., Dunbar, R.S., Colliander, A., Entekhabi, D., Chan, S.K., Chen, F., Xu, X., Bindlish, R., Oaneill, P., Asanuma, J., Berg, A.A., Bosch, D.D., Caldwell, T., Cosh, M.H., Collins, C.H., Jensen, K.H., Martínez-Fernández, J., Seyfried, M., Starks, P.J., Su, Z., Thibeault, M., P. Walker, J., 2022. Regularized Dual-Channel Algorithm for the Retrieval of Soil Moisture and Vegetation Optical Depth from SMAP Measurements. IEEE J Sel Top Appl Earth Obs Remote Sens 15, 102–114. https://doi.org/10.1109/JSTARS.2021.3123932

Cheng, S., Huang, J., 2016. Enhanced soil moisture drying in transitional regions under a warming climate. J Geophys Res Atmos 121, 2542–2555. https://doi.org/10.1002/2015JD024559

Cheng, S., Huang, J., Ji, F., Lin, L., 2017. Uncertainties of soil moisture in historical simulations and future projections. J Geophys Res 122, 2239–2253. https://doi.org/10.1002/2016JD025871

Christensen, J.H., Kanikicharla, K.K., Aldrian, E., An, S. il, Albuquerque Cavalcanti, I.F., de Castro, M., Dong, W., Goswami, P., Hall, A., Kanyanga, J.K., Kitoh, A., Kossin, J., Lau, N.C., Renwick, J., Stephenson, D.B., Xie, S.P., Zhou, T., Abraham, L., Ambrizzi, T., Anderson, B., Arakawa, O., Arritt, R., Baldwin, M., Barlow, M., Barriopedro, D., Biasutti, M., Biner, S., Bromwich, D., Brown, J., Cai, W., Carvalho, L. v., Chang, P., Chen, X., Choi, J., Christensen, O.B., Deser, C., Emanuel, K., Endo,

H., Enfield, D.B., Evan, A., Giannini, A., Gillett, N., Hariharasubramanian, A., Huang, P., Jones, J., Karumuri, A., Katzfey, J., Kjellström, E., Knight, J., Knutson, T., Kulkarni, A., Kundeti, K.R., Lau, W.K., Lenderink, G., Lennard, C., Leung, L. yung R., Lin, R., Losada, T., Mackellar, N.C., Magaña, V., Marshall, G., Mearns, L., Meehl, G., Menéndez, C., Murakami, H., Nath, M.J., Neelin, J.D., van Oldenborgh, G.J., Olesen, M., Polcher, J., Qian, Y., Ray, S., Reich, K.D., de Fonseca, B.R., Ruti, P., Screen, J., Sedláček, J., Solman, S., Stendel, M., Stevenson, S., Takayabu, I., Turner, J., Ummenhofer, C., Walsh, K., Wang, B., Wang, C., Watterson, I., Widlansky, M., Wittenberg, A., Woollings, T., Yeh, S.W., Zhang, C., Zhang, L., Zheng, X., Zou, L., 2013. Climate phenomena and their relevance for future regional climate change, in: Climate Change 2013 the Physical Science Basis: Working Group I Contribution to the Fifth Assessment Report of the Intergovernmental Panel on Climate Change. Cambridge University Press, pp. 1217–1308. https://doi.org/10.1017/CBO9781107415324.028

Chuvieco, E., 1990. Fundamentos de teledetection espacial. Ed. Rialp, Madrid.

Ciabatta, L., Massari, C., Brocca, L., Gruber, A., Reimer, C., Hahn, S., Paulik, C., Dorigo, W., Kidd, R., Wagner, W., 2018. SM2RAIN-CCI: a new global long-term rainfall data set derived from ESA CCI soil moisture. Earth Syst Sci Data 10, 267–280. https://doi.org/10.5194/essd-10-267-2018

Civeira, G., 2019. Introductory Chapter: Soil Moisture, in: Civeira, G. (Ed.), Soil Moisture. IntechOpen, London, pp. 3–5. https://doi.org/10.5772/intechopen.83603

Comas-Bru, L., Mcdermott, F., 2014. Impacts of the EA and SCA patterns on the European twentieth century NAO-winter climate relationship. Q J R Meteorol Soc 140, 354–363. https://doi.org/10.1002/qj.2158

Coulibaly, P., Baldwin, C.K., 2005. Nonstationary hydrological time series forecasting using nonlinear dynamic methods. J Hydrol (Amst) 307, 164–174. https://doi.org/10.1016/j.jhydrol.2004.10.008

Cui, Y., Long, D., Hong, Y., Zeng, C., Zhou, J., Han, Z., Liu, R., Wan, W., 2016. Validation and reconstruction of FY-3B/MWRI soil moisture using an artificial neural network based on reconstructed MODIS optical products over the Tibetan Plateau. J Hydrol (Amst) 543, 242–254. https://doi.org/10.1016/j.jhydrol.2016.10.005

Cui, Y., Zeng, C., Zhou, J., Xie, H., Wan, W., Hu, L., Xiong, W., Chen, X., Fan, W., Hong, Y., 2019. A spatio-temporal continuous soil moisture dataset over the Tibet Plateau from 2002 to 2015. Sci Data 6, 247. https://doi.org/10.1038/s41597-019-0228-x

Dai, A., 2013. Increasing drought under global warming in observations and models. Nat Clim Chang 3, 52–58. https://doi.org/10.1038/nclimate1633

Dai, A., 2011. Drought under global warming: A review. Wiley Interdiscip Rev Clim Change 2, 45–65. https://doi.org/10.1002/wcc.81

Dalal, R.C., Henry, R.J., 1986. Simultaneous Determination of Moisture, Organic Carbon, and Total Nitrogen by Near Infrared Reflectance Spectrophotometry. Soil Sci Soc Am J 50, 120–123. https://doi.org/10.2136/sssaj1986.03615995005000010023x

Daly, E., Porporato, A., 2005. A review of soil moisture dynamics: From rainfall infiltration to ecosystem response. Environ Eng Sci 22, 9–24. https://doi.org/10.1089/ees.2005.22.9

Dankers, R., Feyen, L., 2008. Climate change impact on flood hazard in Europe: An assessment based on high-resolution climate simulations. J Geophys Res Atmos 113, 1–17. https://doi.org/10.1029/2007JD009719

Daoyi, G., Shaowu, W., 2003. Influence of Arctic Oscillation on winter climate over China. Dili Xuebao/Acta Geographica Sinica 58, 568–575. https://doi.org/10.1007/bf02837460

de Berg, M., Cheong, O., van Kreveld, M., Overmars, M., 2008. Delaunay Triangulations, in: Computational Geometry. Springer Berlin Heidelberg, Berlin, Heidelberg, pp. 191–218. https://doi.org/10.1007/978-3-540-77974-2_9

de Jeu, R.A.M., Wagner, W., Holmes, T.R.H., Dolman, A.J., van de Giesen, N.C., Friesen, J., 2008. Global Soil Moisture Patterns Observed by Space Borne Microwave Radiometers and Scatterometers. Surv Geophys 29, 399–420. https://doi.org/10.1007/s10712-008-9044-0

de Luca, P., Messori, G., Wilby, R.L., Mazzoleni, M., di Baldassarre, G., 2020. Concurrent wet and dry hydrological extremes at the global scale. Earth Syst Dyn 11, 251–266. https://doi.org/10.5194/esd-11-251-2020

de Luis, M., González-Hidalgo, J.C., Brunetti, M., Longares, L.A., 2011. Precipitation concentration changes in Spain 1946-2005. Nat Hazards Earth Sys Sci 11, 1259–1265. https://doi.org/10.5194/nhess-11-1259-2011

de Roo, A.P.J., Wesseling, C.G., van Deursen, W.P.A., 2000. Physically based river basin modelling within a GIS: The LISFLOOD model. Hydrol Process 14, 1981–1992. https://doi.org/10.1002/1099-1085(20000815/30)14:11/12<1981::aid-hyp49>3.0.co;2-f

deCastro, M., Lorenzo, N., Taboada, J.J., Sarmiento, M., Alvarez, I., Gomez-Gesteira, M., 2006. Influence of teleconnection patterns on precipitation variability and on river flow regimes in the Miño River basin (NW Iberian Peninsula). Handbook of Environmental Chemistry, Volume 5: Water Pollution 32, 63–73. https://doi.org/10.3354/cr032063

Delworth, T.L., Dixon, K.W., 2000. Implications of the recent trend in the Arctic/North Atlantic oscillation for the North Atlantic thermohaline circulation. J Clim 13, 3721–3727. https://doi.org/10.1175/1520-0442(2000)013<3721:IOTRTI>2.0.CO;2

Deng, Y., Wang, S., Bai, X., Luo, G., Wu, L., Cao, Y., Li, H., Li, C., Yang, Y., Hu, Z., Tian, S., 2020. Variation trend of global soil moisture and its cause analysis. Ecol Indic 110, 105939. https://doi.org/10.1016/j.ecolind.2019.105939

Dibike, Y.B., Velickov, S., Solomatine, D., Abbott, M.B., 2001. Model Induction with Support Vector Machines: Introduction and Applications. J Comput Civ Eng 15, 208–216. https://doi.org/10.1061/(ASCE)0887-3801(2001)15:3(208)

Didan, K., Munoz, A.B., Solano, R., Huete, A., 2015. MODIS Vegetation Index User 's Guide (Collection 6) 2015, 31. https://doi.org/10.5067/MODIS/MOD13A2.006

Dirmeyer, P.A., Tan, L., 2001. A Multi-Decadal Global Land-Surface Data Set of State Variables and Fluxes. COLA Technical Report.

Dobson, M., Ulaby, F., 1986. Active Microwave Soil Moisture Research. IEEE Trans Geosci Remote Sens GE-24, 23–36. https://doi.org/10.1109/TGRS.1986.289585

Dobson, M., Ulaby, F., Hallikainen, M., El-rayes, M., 1985. Microwave Dielectric Behavior of Wet Soil-Part II: Dielectric Mixing Models. IEEE Trans Geosci Remote Sens GE-23, 35–46. https://doi.org/10.1109/TGRS.1985.289498

D'Odorico, P., Yoo, J.C., Jaeger, S., 2002. Changing seasons: An effect of the North Atlantic Oscillation? J Clim 15, 435–445. https://doi.org/10.1175/1520-0442(2002)015<0435:CSAEOT>2.0.CO;2

Dominguez, F., Kumar, P., Liang, X.Z., Ting, M., 2006. Impact of atmospheric moisture storage on precipitation recycling. J Clim 19, 1513–1530. https://doi.org/10.1175/JCLI3691.1

Dorigo, W., Bauer-marschallinger, B., Depoorter, M., Miralles, D., 2016. Assessing the impact of the 2015 / 2016 El Niño event on multi-satellite soil moisture over the Southern Hemisphere. Geophysical Research Abstracts 18, EGU2016-15476.

Dorigo, W., de Jeu, R., Chung, D., Parinussa, R., Liu, Y., Wagner, W., Fernández-Prieto, D., 2012. Evaluating global trends (1988-2010) in harmonized multi-satellite surface soil moisture. Geophys Res Lett 39, 3–9. https://doi.org/10.1029/2012GL052988

Dorigo, W., Himmelbauer, I., Aberer, D., Schremmer, L., Petrakovic, I., Zappa, L., Preimesberger, W., Xaver, A., Annor, F., Ardö, J., Baldocchi, D., Bitelli, M., Blöschl, G., Bogena, H., Brocca, L., Calvet, J., Camarero, J.J., Capello, G., Choi, M., Cosh, M.C., van de Giesen, N., Hajdu, I., Ikonen, J., Jensen, K.H., Kanniah, K.D., de Kat, I., Kirchengast, G., Kumar Rai, P., Kyrouac, J., Larson, K., Liu, S., Loew, A., Moghaddam, M., Martínez Fernández, J., Mattar Bader, C., Morbidelli, R., Musial, J.P., Osenga, E., Palecki, M.A., Pellarin, T., Petropoulos, G.P., Pfeil, I., Powers, J., Robock, A., Rüdiger, C., Rummel, U., Strobel, M., Su, Z., Sullivan, R., Tagesson, T., Varlagin, A., Vreugdenhil, M., Walker, J., Wen, J., Wenger, F., Wigneron, J.P., Woods, M., Yang, K., Zeng, Y., Zhang, X., Zreda, M., Dietrich, S., Gruber, A., van Oevelen, P., Wagner, W., Scipal, K., Drusch, M., Sabia, R., 2021. The International Soil Moisture Network: serving Earth system science for over a decade. Hydrol Earth Syst Sci 25, 5749–5804. https://doi.org/10.5194/hess-25-5749-2021

Dorigo, W., Wagner, W., Albergel, C., Albrecht, F., Balsamo, G., Brocca, L., Chung, D., Ertl, M., Forkel, M., Gruber, A., Haas, E., Hamer, P.D., Hirschi, M., Ikonen, J., de Jeu, R., Kidd, R., Lahoz, W., Liu, Y.Y., Miralles, D., Mistelbauer, T., Nicolai-Shaw, N., Parinussa, R., Pratola, C., Reimer, C., van der Schalie, R., Seneviratne, S.I., Smolander, T., Lecomte, P., 2017. ESA CCI Soil Moisture for improved Earth system understanding: State-of-the art and future directions. Remote Sens Environ 203, 185–215. https://doi.org/10.1016/j.rse.2017.07.001

Dorigo, W.A., Gruber, A., de Jeu, R.A.M., Wagner, W., Stacke, T., Loew, A., Albergel, C., Brocca, L., Chung, D., Parinussa, R.M., Kidd, R., 2015. Evaluation of the ESA CCI soil moisture product using ground-based observations. Remote Sens Environ 162, 380–395. https://doi.org/10.1016/j.rse.2014.07.023

Dorigo, W.A., Wagner, W., Hohensinn, R., Hahn, S., Paulik, C., Xaver, A., Gruber, A., Drusch, M., Mecklenburg, S., van Oevelen, P., Robock, A., Jackson, T., 2011. The International Soil Moisture Network: a data hosting facility for global in situ soil moisture measurements. Hydrol Earth Syst Sci 15, 1675–1698. https://doi.org/10.5194/hess-15-1675-2011

Dubois, P.C., Zyl, J. Van, Engman, T., 1995. Measuring Soil Moisture with Imaging Radars. IEEE Trans Geosci Remote Sens 33, 915–926. https://doi.org/10.1109/36.406677

Duguay–Tetzlaff, A., Stöckli, R., Bojanowski, J., Hollmann, R., Fuchs, P., Werscheck, M., 2017. CM SAF Land SUrface Temperature dataset from METeosat First and Second Generation - Edition 1 (SUMET Ed. 1). Satellite Application Facility on Climate Monitoring (CM SAF). https://doi.org/10.5676/EUM_SAF_CM/LST_METEOSAT/V001

Dumedah, G., Coulibaly, P., 2011. Evaluation of statistical methods for infilling missing values in high-resolution soil moisture data. J Hydrol (Amst) 400, 95–102. https://doi.org/10.1016/j.jhydrol.2011.01.028

Dumedah, G., Walker, J.P., Chik, L., 2014. Assessing artificial neural networks and statistical methods for infilling missing soil moisture records. J Hydrol (Amst) 515, 330–344. https://doi.org/10.1016/j.jhydrol.2014.04.068

Eagleman, J.R., Lin, W.C., 1976. Remote sensing of soil moisture by a 21-cm passive radiometer. J Geophys Res 81, 3660–3666. https://doi.org/10.1029/JC081i021p03660

Eichler, M., 2012. Causal Inference in Time Series Analysis, in: Causality: Wiley Series in Probability and Statistics. pp. 327–354. https://doi.org/10.1002/9781119945710.ch22

Ek, M.B., 2018. Land Surface Hydrological Models, in: Handbook of Hydrometeorological Ensemble Forecasting. Springer Berlin Heidelberg, Berlin, Heidelberg, pp. 1–42. https://doi.org/10.1007/978-3-642-40457-3_24-1

Engman, E.T., 1990. Progress in Microwave Remote Sensing of Soil Moisture. Can J Remote Sens 16, 6–14. https://doi.org/10.1080/07038992.1990.11487620

Entekhabi, D., Njoku, E.G., O'Neill, P.E., Kellogg, K.H., Crow, W.T., Edelstein, W.N., Entin, J.K., Goodman, S.D., Jackson, T.J., Johnson, J., Kimball, J., Piepmeier, J.R., Koster, R.D., Martin, N., McDonald, K.C., Moghaddam, M., Moran, S., Reichle, R., Shi, J.C., Spencer, M.W., Thurman, S.W., Tsang, L., Van Zyl, J., 2010a. The Soil Moisture Active Passive (SMAP) Mission. Proc IEEE 98, 704–716. https://doi.org/10.1109/JPROC.2010.2043918

Entekhabi, D., Reichle, R.H., Koster, R.D., Crow, W.T., 2010b. Performance Metrics for Soil Moisture Retrievals and Application Requirements. J Hydrometeorol 11, 832–840. https://doi.org/10.1175/2010JHM1223.1

Entekhabi, D., Rodriguez-Iturbe, I., Castelli, F., 1996. Mutual interaction of soil moisture state and atmospheric processes. J Hydrol (Amst) 184, 3–17. https://doi.org/10.1016/0022-1694(95)02965-6

Entekhabi, D., Yueh, S., O'Neill, P.E., Kellogg, K.H., Allen, A., Bindlish, R., Brown, M., Chan, S., Colliander, A., Crow, W.T., Das, N., De Lannoy, G., Dunbar, R.S., Edelstein, W.N., Entin, J.K., Escobar, V., Goodman, S.D., Jackson, T.J., Jai, B., Johnson, J., Kim, E., Kim, S., Kimball, J., Koster, R.D., Leon, A., McDonald, K.C., Moghaddam, M., Mohammed, P., Moran, S., Njoku, E.G., Piepmeier, J.R., Reichle, R., Rogez, F., Shi, J., Spencer, M.W., Thurman, S.W., Tsang, L., Van Zyl, J., Weiss, B., West, R., 2014. SMAP Handbook–Soil Moisture Active Passive: Mapping Soil Moisture and Freeze/Thaw from Space. JPL Publication, Pasadena, CA.

Entin, J.K., Robock, A., Vinnikov, K.Y., Hollinger, S.E., Liu, S., Namkhai, A., 2000. Temporal and spatial scales of observed soil moisture variations in the extratropics. J Geophys Res Atmos 105, 11865–11877. https://doi.org/10.1029/2000JD900051

Feldman, A., Gianotti, D., Dong, J., Akbar, R., Crow, W., McColl, K., Nippert, J., Tumber-Dávila, S.J., Holbrook, N.M., Rockwell, F., Scott, R., Reichle, R., Chatterjee, A., Joiner, J., Poulter, B., Entekhabi, D., 2022. Satellites capture soil moisture dynamics deeper than a few centimeters and are relevant to plant water uptake. [*preprint*] https://doi.org/10.1002/ESSOAR.10511280.1

Feng, H., 2016. Individual contributions of climate and vegetation change to soil moisture trends across multiple spatial scales. Sci Rep 6, 1–6. https://doi.org/10.1038/srep32782

Feng, H., Zhang, M., 2015. Global land moisture trends: Drier in dry and wetter in wet over land. Sci Rep 5, 1–6. https://doi.org/10.1038/srep18018

Fernandez-Moran, R., Al-Yaari, A., Mialon, A., Mahmoodi, A., al Bitar, A., de Lannoy, G., Rodriguez-Fernandez, N., Lopez-Baeza, E., Kerr, Y., Wigneron, J.-P., 2017. SMOS-IC: An Alternative SMOS Soil Moisture and Vegetation Optical Depth Product. Remote Sens 9, 457. https://doi.org/10.3390/rs9050457

Fidal, J., Kjeldsen, T.R., 2020. Accounting for soil moisture in rainfall-runoff modelling of urban areas. J Hydrol (Amst) 589, 125122. https://doi.org/10.1016/j.jhydrol.2020.125122

Fisher, R.A., Koven, C.D., 2020. Perspectives on the Future of Land Surface Models and the Challenges of Representing Complex Terrestrial Systems. J Adv Model Earth Syst. https://doi.org/10.1029/2018MS001453

Folland, C.K., Knight, J., Linderholm, H.W., Fereday, D., Ineson, S., Hurrel, J.W., 2009. The summer North Atlantic oscillation: Past, present, and future. J Clim 22, 1082–1103. https://doi.org/10.1175/2008JCLI2459.1

Ford, T.W., Quiring, S.M., 2014. Comparison and application of multiple methods for temporal interpolation of daily soil moisture. Int J Climatol 34, 2604–2621. https://doi.org/10.1002/joc.3862

Fraedrich, K., Müller, K., 1992. Climate anomalies in Europe associated with ENSO extremes. Int J Climatol 12, 25–31. https://doi.org/10.1002/joc.3370120104

Fritsch, F.N., Carlson, R.E., 1980. Monotone Piecewise Cubic Interpolation. SIAM J Numer Anal 17, 238–246.

Gaona, J., Benito-Verdugo, P., Martínez-Fernández, J., González-Zamora, Á., Almendra-Martín, L., Herrero-Jiménez, C.M., 2022. Soil Moisture Outweighs Climatic Factors in Critical Periods for Rainfed Cereal Yields: An Analysis in Spain. Agriculture 12, 533. https://doi.org/10.3390/agriculture12040533

Garcia, D., 2010. Robust smoothing of gridded data in one and higher dimensions with missing values. Comput Stat Data Anal 54, 1167–1178. https://doi.org/10.1016/j.csda.2009.09.020

GCOS, 2016. The Global Observing System for Climate: Implementation Needs. Guayaquil, Ecuador.

GCOS, 2010. Implementation Plan for the Global Observing System for Climate in support of the UNFCCC: (2010 update). Geneva, Switzerland.

Georgakakos, K.P., Baumer, O.W., 1996. Measurement and utilization of on-site soil moisture data. J Hydrol (Amst) 184, 131–152. https://doi.org/10.1016/0022-1694(95)02971-0

Gill, M.K., Asefa, T., Kemblowski, M.W., McKee, M., 2006. SOIL MOISTURE PREDICTION USING SUPPORT VECTOR MACHINES. J Am Water Resour Assoc 42, 1033–1046. https://doi.org/10.1111/j.1752-1688.2006.tb04512.x

Gillies, R.R., Carlson, T.N., 1995. Thermal Remote Sensing of Surface Soil Water Content with Partial Vegetation Cover for Incorporation into Climate Models. J Appl Meteorol Climatol 34, 745–756. https://doi.org/10.1175/1520-0450(1995)034<0745:TRSOSS>2.0.CO;2

Giorgi, F., Lionello, P., 2008. Climate change projections for the Mediterranean region. Glob Planet Change 63, 90–104. https://doi.org/10.1016/j.gloplacha.2007.09.005

Gloersen, P., Barath, F., 1977. A scanning multichannel microwave radiometer for Nimbus-G and SeaSat-A. IEEE J Ocean Eng 2, 172–178. https://doi.org/10.1109/JOE.1977.1145331

Gocic, M., Trajkovic, S., 2013. Analysis of changes in meteorological variables using Mann-Kendall and Sen's slope estimator statistical tests in Serbia. Glob Planet Change 100, 172–182. https://doi.org/10.1016/j.gloplacha.2012.10.014

Gómez-Chova, L., Camps-Valls, G., Bruzzone, L., Calpe-Maravilla, J., 2010. Mean map kernel methods for semisupervised cloud classification. IEEE Trans Geosci Remote Sens 48, 207–220. https://doi.org/10.1109/TGRS.2009.2026425

González-Zamora, Á., 2017. Análisis y validación de nuevos productos SMOS de interés en agricultura e hidrología. Tesis doctoral Universidad de Salamanca.

González-Zamora, Á., Almendra-Martín, L., de Luis, M., Martínez-Fernández, J., 2021. Influence of soil moisture vs. Climatic factors in pinus halepensis growth variability in spain: A study with remote sensing and modeled data. Remote Sens 13, 1–20. https://doi.org/10.3390/rs13040757

González-Zamora, Á., García-Barreda, S., Martínez-Fernández, J., Almendra-Martín, L., Gaona, J., Benito-Verdugo, P., 2022. Soil Moisture and Black Truffle Production Variability in the Iberian Peninsula. Forests 13, 819. https://doi.org/10.3390/f13060819

González-Zamora, Á., Sánchez, N., Martínez-Fernández, J., 2016. Validation of Aquarius Soil Moisture Products Over the Northwest of Spain: A Comparison With SMOS. IEEE J Sel Top Appl Earth Obs Remote Sens 9, 2763–2769. https://doi.org/10.1109/JSTARS.2016.2517401

González-Zamora, Á., Sánchez, N., Pablos, M., Martínez-Fernández, J., 2019. CCI soil moisture assessment with SMOS soil moisture and in situ data under different environmental conditions and spatial scales in Spain. Remote Sens Environ 225, 469–482. https://doi.org/10.1016/j.rse.2018.02.010

Gordo, O., Sanz, J.J., 2010. Impact of climate change on plant phenology in Mediterranean ecosystems. Glob Chang Biol 16, 1082–1106. https://doi.org/10.1111/j.1365-2486.2009.02084.x

Granger, C.W.J., 1969. Investigating Causal Relations by Econometric Models and Cross-spectral Methods. Econometrica 37, 424. https://doi.org/10.2307/1912791

Grillakis, M.G., 2019. Increase in severe and extreme soil moisture droughts for Europe under climate change. Sci Total Environ 660, 1245–1255. https://doi.org/10.1016/j.scitotenv.2019.01.001

Gruber, A., Dorigo, W.A., Crow, W., Wagner, W., 2017. Triple Collocation-Based Merging of Satellite Soil Moisture Retrievals. IEEE Trans Geosci Remote Sens 55, 6780–6792. https://doi.org/10.1109/TGRS.2017.2734070

Gruber, A., Scanlon, T., van der Schalie, R., Wagner, W., Dorigo, W., 2019. Evolution of the ESA CCI Soil Moisture climate data records and their underlying merging methodology. Earth Syst Sci Data 11, 717–739. https://doi.org/10.5194/essd-11-717-2019

Gudmundsson, L., Seneviratne, S.I., 2015. European drought trends. Proceedings of the Int Assoc Hydrol Sci 369, 75–79. https://doi.org/10.5194/piahs-369-75-2015

Gupta, V., Jain, M.K., 2021. Unravelling the teleconnections between ENSO and dry/wet conditions over India using nonlinear Granger causality. Atmos Res 247, 105168. https://doi.org/10.1016/j.atmosres.2020.105168

Hamed, K.H., Rao, R.A., 1998. A modified Mann-Kendall trend test for autocorrelated data. J Hydrol (Amst) 204, 182–196. https://doi.org/10.1016/S0022-1694(97)00125-X

Hanna, E., Cropper, T.E., Jones, P.D., Scaife, A.A., Allan, R., 2015. Recent seasonal asymmetric changes in the NAO (a marked summer decline and increased winter variability) and associated changes in the AO and Greenland Blocking Index. Int J Climatol 35, 2540–2554. https://doi.org/10.1002/joc.4157

Hänsel, S., Ustrnul, Z., Łupikasza, E., Skalak, P., 2019. Assessing seasonal drought variations and trends over Central Europe. Adv Water Resour 127, 53–75. https://doi.org/10.1016/j.advwatres.2019.03.005

Hardiman, S.C., Dunstone, N.J., Scaife, A.A., Smith, D.M., Ineson, S., Lim, J., Fereday, D., 2019. The Impact of Strong El Niño and La Niña Events on the North Atlantic. Geophys Res Lett 46, 2874–2883. https://doi.org/10.1029/2018GL081776

Hassan, W.U., Nayak, M.A., 2020. Global teleconnections in droughts caused by oceanic and atmospheric circulation patterns. Environ Res Lett 16. https://doi.org/10.1088/1748-9326/abc9e2

Hausman, D.M., Woodward, J., 1999. Independence, invariance and the Causal Markov condition. Br J Philos Sci 50, 521–583. https://doi.org/10.1093/bjps/50.4.521

Hayes, M., Svoboda, M., Wall, N., Widhalm, M., 2011. The Lincoln declaration on drought indices: universal meteorological drought index recommended. Bull Am Meteorol Soc 94, 485–488. https://doi.org/10.1175/2010BAMS3103.1

Heim, R.R., 2002. A Review of Twentieth-Century Drought Indices Used in the United States. Bull Am Meteorol Soc 83, 1149–1166. https://doi.org/10.1175/1520-0477-83.8.1149

Hersbach, H., Bell, B., Berrisford, P., Hirahara, S., Horányi, A., Muñoz-Sabater, J., Nicolas, J., Peubey, C., Radu, R., Schepers, D., Simmons, A., Soci, C., Abdalla, S., Abellan, X., Balsamo, G., Bechtold, P., Biavati, G., Bidlot, J., Bonavita, M., de Chiara, G., Dahlgren, P., Dee, D., Diamantakis, M., Dragani, R., Flemming, J., Forbes, R., Fuentes, M., Geer, A., Haimberger, L., Healy, S., Hogan, R.J., Hólm, E., Janisková, M., Keeley, S., Laloyaux, P., Lopez, P., Lupu, C., Radnoti, G., de Rosnay, P., Rozum, I., Vamborg, F., Villaume, S., Thépaut, J.N., 2020. The ERA5 global reanalysis. Q J R Meteorol Soc 146, 1999–2049. https://doi.org/10.1002/qj.3803

Hillel, D., 2003. Soil Physics and Soil Physical Characteristics, in: Introduction to Environmental Soil Physics. Academic Press, pp. 3–17. https://doi.org/10.1016/B978-012348655-4/50002-2

Hillel, D., 1998. Environmental Soil Physics, No. of pages: 771 Language: English Copyright: © Academic Press 1998 Published: 31st August 1998 Imprint: Academic Press Hardcover ISBN: 9780123485250 eBook ISBN: 9780080544151. Academic Press, San Diego, CA.

Holgate, C.M., De Jeu, R.A.M., van Dijk, A.I.J.M., Liu, Y.Y., Renzullo, L.J., Vinodkumar, Dharssi, I., Parinussa, R.M., Van Der Schalie, R., Gevaert, A., Walker, J., McJannet, D., Cleverly, J., Haverd, V., Trudinger, C.M., Briggs, P.R., 2016. Comparison of remotely sensed and modelled soil moisture data sets across Australia. Remote Sens Environ 186, 479–500. https://doi.org/10.1016/j.rse.2016.09.015

Hollmann, R., Merchant, C.J., Saunders, R., Downy, C., Buchwitz, M., Cazenave, A., Chuvieco, E., Defourny, P., Leeuw, G. de, Forsberg, R., Holzer-Popp, T., Paul, F., Sandven, S., Sathyendranath, S., Roozendael, M. van, Wagner, W., 2013. The ESA Climate Change Initiative: Satellite Data Records for Essential Climate Variables. Bull Am Meteorol Soc 94, 1541–1552. https://doi.org/https://doi.org/10.1175/BAMS-D-11-00254.1

Horton, D.E., Johnson, N.C., Singh, D., Swain, D.L., Rajaratnam, B., Diffenbaugh, N.S., 2015. Contribution of changes in atmospheric circulation patterns to extreme temperature trends. Nature 522, 465–469. https://doi.org/10.1038/nature14550

Huang, N.E., Shen, Z., Long, S.R., Wu, M.C., Shih, H.H., Zheng, Q., Yen, N.-C., Tung, C.C., Liu, H.H., 1998. The empirical mode decomposition and the Hilbert spectrum for nonlinear and non-stationary time series analysis. Proc Math Phys Eng Sci 454, 903–995. https://doi.org/10.1098/rspa.1998.0193

Huffman, G.J., Bolvin, D.T., Braithwaite, D., Hsu, K.-L., Joyce, R.J., Kidd, C., Nelkin, E.J., Sorooshian, S., Stocker, E.F., Tan, J., Wolff, D.B., Xie, P., 2020. Integrated Multi-satellite Retrievals for the Global Precipitation Measurement (GPM) Mission (IMERG) 343–353. https://doi.org/10.1007/978-3-030-24568-9_19

Hunt, E.D., Hubbard, K.G., Wilhite, D.A., Arkebauer, T.J., Dutcher, A.L., 2009. The development and evaluation of a soil moisture index. Int J Climatol 29, 747–759. https://doi.org/10.1002/joc.1749

Hurrell, J.W., 1995. Decadal Trends in the North Atlantic Oscillation: Regional Temperatures and Precipitation. Science (1979) 269, 676–679. https://doi.org/10.1126/science.269.5224.676

Hurrell, J.W., Kushnir, Y., Ottersen, G., Visbeck, M., 2003. An overview of the north atlantic oscillation. Geophys Monogr Ser 134, 1–35. https://doi.org/10.1029/134GM01

Hurrell, J.W., Kushnir, Y., Visbeck, M., 2001. The North Atlantic oscillation. Science (1979). https://doi.org/10.1126/science.1058761

Hurrell, J.W., van Loon, H., 1997. Decadal Variations in Climate Associated with the North Atlantic Oscillation. Climatic Change at High Elevation Sites 69–94. https://doi.org/10.1007/978-94-015-8905-5_4

Hynčica, M., Huth, R., 2019. Long-term changes in precipitation phase in Europe in cold half year. Atmos Res 227, 79–88. https://doi.org/10.1016/j.atmosres.2019.04.032

Igor Shiklomanov, 1993. World fresh water resources, in: Gleick, P.H. (Ed.), Water in Crisis: A Guide to the World's Fresh Water Resources. Oxford University Press, New York.

Ikonen, J., Smolander, T., Rautiainen, K., Cohen, J., Lemmetyinen, J., Salminen, M., Pulliainen, J., 2018. Spatially Distributed Evaluation of ESA CCI Soil Moisture Products in a Northern Boreal Forest Environment. Geosciences 8, 51. https://doi.org/10.3390/geosciences8020051

Ionita, M., Boroneanț, C., Chelcea, S., 2015. Seasonal modes of dryness and wetness variability over Europe and their connections with large scale atmospheric circulation and global sea surface temperature. Clim Dyn 45, 2803–2829. https://doi.org/10.1007/s00382-015-2508-2

Ionita, M., Nagavciuc, V., Kumar, R., Rakovec, O., 2020. On the curious case of the recent decade, mid-spring precipitation deficit in central Europe. NPJ Clim Atmos Sci 3, 1–10. https://doi.org/10.1038/s41612-020-00153-8

IPCC, 2022. Climate Change 2022 Mitigation of Climate Change. Working Group III contribution to the Sixth Assessment Report of the Intergovernmental Panel on Climate Change. Cambridge University Press, Cambridge, United Kingdom and New York, NY, USA.

Iturria, I., Campo-Bescós, M.A., Gómez, U., López, M., Giménez, R., 2019. Evaluación de 24 sondas de humedad: calibración y volumen de influencia. Estudios en la Zona No Saturada XIV, 69–74.

Jaagus, J., Aasa, A., Aniskevich, S., Boincean, B., Bojariu, R., Briede, A., Danilovich, I., Castro, F.D., Dumitrescu, A., Labuda, M., Labudová, L., Lõhmus, K., Melnik, V., Mõisja, K., Pongracz, R., Potopová, V., Řezníčková, L., Rimkus, E., Semenova, I., Stonevičius, E., Štěpánek, P., Trnka, M., Vicente-Serrano, S.M., Wibig, J., Zahradníček, P., 2021. Long-term changes in drought indices in eastern and central Europe. Int J Climatol 1–25. https://doi.org/10.1002/joc.7241

Jackson, T.J., 2005. Estimation of Surface Soil Moisture Using Microwave Sensors. Encyclopedia of Hydrological Sciences. https://doi.org/10.1002/0470848944.hsa060

Jackson, T.J., 1997. Soil moisture estimation using special satellite microwave/imager satellite data over a grassland region. Water Resour Res 33, 1475–1484. https://doi.org/10.1029/97WR00661

Jackson, T.J., 1993. III. Measuring surface soil moisture using passive microwave remote sensing. Hydrol Process 7, 139–152. https://doi.org/10.1002/hyp.3360070205

Jackson, T.J., Le Vine, D.M., Swift, C.T., Schmugge, T.J., Schiebe, F.R., 1995. Large area mapping of soil moisture using the ESTAR passive microwave radiometer in Washita'92. Remote Sens Environ 54, 27–37. https://doi.org/10.1016/0034-4257(95)00084-E

Jackson, T.J., O'Neill, P., 1987. Temporal observations of surface soil moisture using a passive microwave sensor. Remote Sens Environ 21, 281–296. https://doi.org/10.1016/0034-4257(87)90013-7

Jiang, H., Cotton, W.R., 2004. Soil moisture estimation using an artificial neural network: a feasibility study. Can J Remote Sens 30, 827–839. https://doi.org/10.5589/m04-041

Jiménez Cisneros, B.E., Oki, T., Arnell, N.W., Benito, G., Cogley, J.G., Döll, P., Jiang, T., Mwakalila, S.S., 2014. Freshwater resources, in: Field, C.B., Barros, V.R., Dokken, D.J., Mach, K.J., Mastrandrea, M.D., Bilir, T.E., Chatterjee, M., Ebi, K.L., Estrada, Y.O., Genova, R.C., Girma, B., Kissel, E.S., Levy, A.N., MacCracken, S., Mastrandrea, P.R., White, L.L. (Eds.), Climate Change 2014: Impacts, Adaptation, and Vulnerability. Part A: Global and Sectoral Aspects. Contribution of Working Group II to the Fifth Assessment Report of the Intergovernmental Panel on Climate Change. Cambridge University Press, Cambridge, United Kingdom and New York, NY, USA, pp. 229–269.

Karl, T.R., Trenberth, K.E., 2003. Modern Global Climate Change. Science (1979) 302, 1719–1723. https://doi.org/10.1126/science.1090228

Kawanishi, T., Sezai, T., Ito, Y., Imaoka, K., Takeshima, T., Ishido, Y., Shibata, A., Miura, M., Inahata, H., Spencer, R.W., 2003. The Advanced Microwave Scanning Radiometer for the Earth Observing System (AMSR-E), NASDA's contribution to the EOS for global energy and water cycle studies. IEEE Trans Geosci Remote Sens 41, 184–194. https://doi.org/10.1109/TGRS.2002.808331

Kendall, M.G., 1948. Rank Correlation Methods. Griffin, London, UK.

Kerr, Y.H., 2007. Soil moisture from space : Where are we ? 117–120. https://doi.org/10.1007/s10040-006-0095-3

Kerr, Y.H., Waldteufel, P., Richaume, P., Wigneron, J.P., Ferrazzoli, P., Mahmoodi, A., Al Bitar, A., Cabot, F., Gruhier, C., Juglea, S.E., Leroux, D., Mialon, A., Delwart, S., 2012. The SMOS Soil Moisture Retrieval Algorithm. IEEE Trans Geosci Remote Sens 50, 1384–1403. https://doi.org/10.1109/TGRS.2012.2184548

Kerr, Y.H., Waldteufel, P., Wigneron, J.-P., Delwart, S., Cabot, F., Boutin, J., Escorihuela, M.-J., Font, J., Reul, N., Gruhier, C., Juglea, S.E., Drinkwater, M.R., Hahne, A., Martín-Neira, M., Mecklenburg, S., 2010. The SMOS Mission: New Tool for Monitoring Key Elements ofthe Global Water Cycle. Proc IEEE 98, 666–687. https://doi.org/10.1109/JPROC.2010.2043032

Kerr, Y.H., Waldteufel, P., Wigneron, J.-P., Martinuzzi, J., Font, J., Berger, M., 2001. Soil moisture retrieval from space: the Soil Moisture and Ocean Salinity (SMOS) mission. IEEE Trans Geosci Remote Sens 39, 1729–1735. https://doi.org/10.1109/36.942551

Kerr, Y.H., Wigneron, J., Bitar, A. al, Mialon, A., Srivastava, P.K., 2016. Soil Moisture from Space : Techniques and Limitations, Satellite Soil Moisture Retrieval. Elsevier Inc. https://doi.org/10.1016/B978-0-12-803388-3.00001-2

Khellouk, R., Barakat, A., Jazouli, A. el, Boudhar, A., Lionboui, H., Rais, J., Benabdelouahab, T., 2019. An integrated methodology for surface soil moisture estimating using remote sensing data approach. Geocarto Int. https://doi.org/10.1080/10106049.2019.1655797

Kodra, E., Chatterjee, S., Ganguly, A.R., 2011. Exploring Granger causality between global average observed time series of carbon dioxide and temperature. Theor Appl Climatol 104, 325–335. https://doi.org/10.1007/s00704-010-0342-3

Kornelsen, K., Coulibaly, P., 2014. Comparison of interpolation, statistical, and data-driven methods for imputation of missing values in a distributed soil moisture dataset. J Hydrol Eng 19, 26–43. https://doi.org/10.1061/(ASCE)HE.1943-5584.0000767

Korres, W., Reichenau, T.G., Schneider, K., 2013. Patterns and scaling properties of surface soil moisture in an agricultural landscape: An ecohydrological modeling study. J Hydrol (Amst) 498, 89–102. https://doi.org/10.1016/j.jhydrol.2013.05.050

Kostopoulou, E., Jones, P.D., 2007. Comprehensive analysis of the climate variability in the eastern Mediterranean. Part II: relationships between atmospheric circulation patterns and surface climatic elements. Int J Climatol 27, 1351–1371. https://doi.org/10.1002/joc.1466

Kramer, P.J., 1944. Soil moisture in relation to plant growth. The Botanical Review 10, 525–559. https://doi.org/10.1007/BF02861165

Kretschmer, M., Cohen, J., Matthias, V., Runge, J., Coumou, D., 2018. The different stratospheric influence on cold-extremes in Eurasia and North America. NPJ Clim Atmos Sci 1, 1–10. https://doi.org/10.1038/s41612-018-0054-4

Kumar, V., Panu, U., 1997. PREDICTIVE ASSESSMENT OF SEVERITY OF AGRICULTURAL DROUGHTS BASED ON AGRO-CLIMATIC FACTORS. J Am Water Resour Assoc 33, 1255–1264. https://doi.org/10.1111/j.1752-1688.1997.tb03550.x

Kurnik, B., Kajfež-Bogataj, L., Horion, S., 2015. An assessment of actual evapotranspiration and soil water deficit in agricultural regions in Europe. Int J Climatol 35, 2451–2471. https://doi.org/10.1002/joc.4154

Kyselý, J., 2007. Implications of enhanced persistence of atmospheric circulation for the occurrence and severity of temperature extremes. Int J Climatol 27, 689–695. https://doi.org/10.1002/joc.1478

Laguardia, G., Niemeyer, S., 2008. On the comparison between the LISFLOOD modelled and the ERS/SCAT derived soil moisture estimates. Hydrol Earth Syst Sci 12, 1339–1351. https://doi.org/10.5194/hess-12-1339-2008

Lary, D.J., Alavi, A.H., Gandomi, A.H., Walker, A.L., 2016. Machine learning in geosciences and remote sensing. Geosci Front 7, 3–10. https://doi.org/10.1016/j.gsf.2015.07.003

Lau, K.-M., Yang, S., 2003. Walker Circulation, in: Encyclopedia of Atmospheric Sciences. Elsevier, pp. 2505–2510. https://doi.org/10.1016/b0-12-227090-8/00450-4

Le, T., Bae, D., 2022. Causal Impacts of El Niño–Southern Oscillation on Global Soil Moisture Over the Period 2015–2100. Earths Future 10, e2021EF002522. https://doi.org/10.1029/2021EF002522

Lee, T., Ouarda, T.B.M.J., 2011. Prediction of climate nonstationary oscillation processes with empirical mode decomposition. J Geophys Res Atmos 116, 1–15. https://doi.org/10.1029/2010JD015142

Leone, A.P., Sommer, S., 2000. Multivariate analysis of laboratory spectra for the assessment of soil development and soil degradation in the southern Apennines (Italy). Remote Sens Environ 72, 346–359. https://doi.org/10.1016/S0034-4257(99)00110-8

L'Heureux, M., 2014. What is the El Niño–Southern Oscillation (ENSO) in a nutshell? | NOAA Climate.gov [WWW Document]. URL https://www.climate.gov/news-features/blogs/enso/what-el-ni%C3%B1o%E2%80%93southern-oscillation-enso-nutshell (accessed 10-21-2022).

L'Heureux, M.L., Tippett, M.K., Takahashi, K., Barnston, A.G., Becker, E.J., Bell, G.D., di Liberto, T.E., Gottschalck, J., Halpert, M.S., Hu, Z.Z., Johnson, N.C., Xue, Y., Wang, W., 2019. Strength outlooks for the El Niño-Southern Oscillation. Weather Forecast 34, 165–175. https://doi.org/10.1175/WAF-D-18-0126.1

Li, M., Wu, P., Ma, Z., 2020. A comprehensive evaluation of soil moisture and soil temperature from third-generation atmospheric and land reanalysis data sets. Int J Climatol 40, 5744–5766. https://doi.org/10.1002/joc.6549

Li, P., Zha, Y., Shi, L., Zhong, H., Tso, C.H.M., Wu, M., 2022. Assessing the Global Relationships Between Teleconnection Factors and Terrestrial Water Storage Components. Water Resour Manag 36, 119–133. https://doi.org/10.1007/s11269-021-03015-x

Li, X., Gao, X., Wang, J., Guo, H., 2015. Microwave soil moisture dynamics and response to climate change in Central Asia and Xinjiang Province, China, over the last 30 years. J Appl Remote Sens 9, 096012. https://doi.org/10.1117/1.jrs.9.096012

Li, Z.-L., Leng, P., Zhou, C., Chen, K.-S., Zhou, F.-C., Shang, G.-F., 2021. Soil moisture retrieval from remote sensing measurements: Current knowledge and directions for the future. Earth Sci Rev 218, 103673. https://doi.org/10.1016/j.earscirev.2021.103673

Lindsey, R., 2009. Climate Variability: Arctic Oscillation | NOAA Climate.gov [WWW Document]. URL https://www.climate.gov/news-features/understanding-climate/climate-variability-arctic-oscillation (accessed 10-21-2022).

Liu, X., Zhu, X., Pan, Y., Li, S., Liu, Y., Ma, Y., 2016. Agricultural drought monitoring: Progress, challenges, and prospects. J Geogr Sci 26, 750–767. https://doi.org/10.1007/s11442-016-1297-9

Liu, Y., Yang, Y., Jing, W., 2020. Potential Applicability of SMAP in ECV Soil Moisture Gap-Filling: A Case Study in Europe. IEEE Access 8, 133114–133127. https://doi.org/10.1109/ACCESS.2020.3009977

Liu, Yongwei, Liu, Yuanbo, Wang, W., 2019. Inter-comparison of satellite-retrieved and Global Land Data Assimilation System-simulated soil moisture datasets for global drought analysis. Remote Sens Environ 220, 1–18. https://doi.org/10.1016/j.rse.2018.10.026

Liu, Z., Wang, Y., Xu, Z., Duan, Q., 2017. Conceptual Hydrological Models, in: Handbook of Hydrometeorological Ensemble Forecasting. Springer Berlin Heidelberg, Berlin, Heidelberg, pp. 1–23. https://doi.org/10.1007/978-3-642-40457-3_22-1

Llamas, R.M., Guevara, M., Rorabaugh, D., Taufer, M., Vargas, R., 2020. Spatial Gap-Filling of ESA CCI Satellite-Derived Soil Moisture Based on Geostatistical Techniques and Multiple Regression. Remote Sens 12, 665. https://doi.org/10.3390/rs12040665

Lobell, D.B., Asner, G.P., 2002. Moisture Effects on Soil Reflectance. Soil Sci Soc Am J 66, 722–727. https://doi.org/10.2136/sssaj2002.7220

Loew, A., Bell, W., Brocca, L., Bulgin, C.E., Burdanowitz, J., Calbet, X., Donner, R. V., Ghent, D., Gruber, A., Kaminski, T., Kinzel, J., Klepp, C., Lambert, J.C., Schaepman-Strub, G., Schröder, M., Verhoelst, T., 2017. Validation practices for satellite-based Earth observation data across communities. Reviews of Geophysics 55, 779–817. https://doi.org/10.1002/2017RG000562

Long, D., Bai, L., Yan, L., Zhang, C., Yang, W., Lei, H., Quan, J., Meng, X., Shi, C., 2019. Generation of spatially complete and daily continuous surface soil moisture of high spatial resolution. Remote Sens Environ 233, 111364. https://doi.org/10.1016/j.rse.2019.111364

Luterbacher, J., Dietrich, D., Xoplaki, E., Grosjean, M., Wanner, H., 2004. European Seasonal and Annual Temperature Variability, Trends, and Extremes Since 1500. Science (1979) 303, 1499–1503. https://doi.org/10.1126/science.1093877

Mann, H.B., 1945. Nonparametric Tests Against Trend. Econometrica 13, 245. https://doi.org/10.2307/1907187

Manzoni, S., Schimel, J.P., Porporato, A., 2012. Responses of soil microbial communities to water stress: results from a meta-analysis. Ecology 93, 930–938. https://doi.org/10.1890/11-0026.1

Mares, I., Mares, C., Mihailescu, M., 2002. NAO impact on the summer moisture variability across Europe. Phys Chem Earth 27, 1013–1017. https://doi.org/10.1016/S1474-7065(02)00135-3

Mariotti, A., Dell'Aquila, A., 2012. Decadal climate variability in the Mediterranean region: Roles of large-scale forcings and regional processes. Clim Dyn 38, 1129–1145. https://doi.org/10.1007/s00382-011-1056-7

Martens, B., Miralles, D.G., Lievens, H., van der Schalie, R., de Jeu, R.A.M., Fernández-Prieto, D., Beck, H.E., Dorigo, W.A., Verhoest, N.E.C., 2017. GLEAM v3: satellite-based land evaporation and root-zone soil moisture. Geosci Model Dev 10, 1903–1925. https://doi.org/10.5194/gmd-10-1903-2017

Martin, D.L., Gilley, J.R., Skaggs, R.W., 2015. Soil Water Balance and Management, in: Managing Nitrogen for Groundwater Quality and Farm Profitability. Soil Science Society of America, Madison, WI, USA, pp. 199–235. https://doi.org/10.2136/1991.managingnitrogen.c10

Martínez-Fernández, J., Almendra-Martín, L., de Luis, M., González-Zamora, A., Herrero-Jiménez, C., 2019. Tracking tree growth through satellite soil moisture monitoring: A case study of Pinus halepensis in Spain. Remote Sens Environ 235, 111422. https://doi.org/10.1016/j.rse.2019.111422

Martínez-Fernández, J., Ceballos, A., 2003. Temporal Stability of Soil Moisture in a Large-Field Experiment in Spain. Soil Sci Soc Am J 67, 1647–1656. https://doi.org/10.2136/sssaj2003.1647

Martínez-Fernández, J., González-Zamora, A., Almendra-Martín, L., 2021. Soil moisture memory and soil properties: An analysis with the stored precipitation fraction. J Hydrol (Amst) 593. https://doi.org/10.1016/j.jhydrol.2020.125622

Martínez-Fernández, J., González-Zamora, A., Sánchez, N., Gumuzzio, A., 2015. A soil water based index as a suitable agricultural drought indicator. J Hydrol (Amst) 522, 265–273. https://doi.org/10.1016/j.jhydrol.2014.12.051

Martínez-Fernández, J., González-Zamora, A., Sánchez, N., Gumuzzio, A., Herrero-Jiménez, C.M., 2016. Satellite soil moisture for agricultural drought monitoring: Assessment of the SMOS derived Soil Water Deficit Index. Remote Sens Environ 177, 277–286. https://doi.org/10.1016/j.rse.2016.02.064

Mascaro, G., Vivoni, E.R., Deidda, R., 2011. Soil moisture downscaling across climate regions and its emergent properties. J Geophys Res 116. https://doi.org/10.1029/2011JD016231

Masseroni, D., Camici, S., Cislaghi, A., Vacchiano, G., Massari, C., Brocca, L., 2021. The 63-year changes in annual streamflow volumes across Europe with a focus on the Mediterranean basin. Hydrol Earth Syst Sci 25, 5589–5601. https://doi.org/10.5194/hess-25-5589-2021

Maxwell, R.M., Chow, F.K., Kollet, S.J., 2007. The groundwater–land-surface–atmosphere connection: Soil moisture effects on the atmospheric boundary layer in fully-coupled simulations. Adv Water Resour 30, 2447–2466. https://doi.org/10.1016/j.advwatres.2007.05.018

McColl, K.A., Alemohammad, S.H., Akbar, R., Konings, A.G., Yueh, S., Entekhabi, D., 2017. The global distribution and dynamics of surface soil moisture. Nat Geosci 10, 100–104. https://doi.org/10.1038/ngeo2868

McNally, A., Shukla, S., Arsenault, K.R., Wang, S., Peters-Lidard, C.D., Verdin, J.P., 2016. Evaluating ESA CCI soil moisture in East Africa. Int J Appl Earth Obs Geoinf 48, 96–109. https://doi.org/10.1016/j.jag.2016.01.001

McPhaden, M.J., Zebiak, S.E., Glantz, M.H., 2006. ENSO as an integrating concept in earth science. Science (1979) 314, 1740–1745. https://doi.org/10.1126/science.1132588

Medina-González, H., Hernández-Pereira, Y., Santiago-Piloto, A.B., Lau-Quan, A., 2015. Modelación de perfil de humedad de suelos empleando un filtro de Kalman de Monte-Carlo. Revista Ciencias Técnicas Agropecuarias 24, 31–37.

Merchant, C.J., Embury, O., Roberts-Jones, J., Fiedler, E., Bulgin, C.E., Corlett, G.K., Good, S., McLaren, A., Rayner, N., Morak-Bozzo, S., Donlon, C., 2014. Sea surface temperature datasets for climate applications from Phase 1 of the European Space Agency Climate Change Initiative (SST CCI) . Geosci Data J 1, 179–191. https://doi.org/10.1002/gdj3.20

Merz, B., Plate, E.J., 1997. An analysis of the effects of spatial variability of soil and soil moisture on runoff. Water Resour Res 33, 2909–2922. https://doi.org/10.1029/97WR02204

Mi Kim, W., Raible, C.C., 2021. Dynamics of the Mediterranean droughts from 850 to 2099 CE in the Community Earth System Model. Climate of the Past 17, 887–911. https://doi.org/10.5194/cp-17-887-2021

Middelkoop, H., Daamen, K., Gellens, D., Grabs, W., Kwadijk, J.C.J., Lang, H., Parmet, B.W.A.H., Schädler, B., Schulla, J., Wilke, K., 2001. Impact of climate change on hydrological regimes and water resources management in the Rhine basin. Clim Change 49, 105–128. https://doi.org/10.1023/A:1010784727448

Militino, A.F., Ugarte, M.D., Montesino, M., 2019. Filling missing data and smoothing altered data in satellite imagery with a spatial functional procedure. Stochastic Environmental Research and Risk Assessment 33, 1737–1750. https://doi.org/10.1007/s00477-019-01711-0

Miralles, D.G., Holmes, T.R.H., de Jeu, R.A.M., Gash, J.H., Meesters, A.G.C.A., Dolman, A.J., 2011. Global land-surface evaporation estimated from satellite-based observations. Hydrol Earth Syst Sci 15, 453–469. https://doi.org/10.5194/hess-15-453-2011

Miralles, D.G., van den Berg, M.J., Gash, J.H., Parinussa, R.M., de Jeu, R.A.M., Beck, H.E., Holmes, T.R.H., Jiménez, C., Verhoest, N.E.C., Dorigo, W.A., Teuling, A.J., Johannes Dolman, A., 2014. El Niño-La Niña cycle and recent trends in continental evaporation. Nat Clim Chang 4, 122–126. https://doi.org/10.1038/nclimate2068

Mladenova, I.E., Bolten, J.D., Crow, W., Sazib, N., Reynolds, C., 2020. Agricultural Drought Monitoring via the Assimilation of SMAP Soil Moisture Retrievals Into a Global Soil Water Balance Model. Front Big Data 3, 1–16. https://doi.org/10.3389/fdata.2020.00010

Moberg, A., Jones, P.D., 2005. Trends in indices for extremes in daily temperature and precipitation in central and western Europe, 1901-99. Int J Climatol 25, 1149–1171. https://doi.org/10.1002/joc.1163

Morata-Dolz, M., Bueso, D., Piles, M., Camps-Valls, G., 2020. Understanding Climate Impacts on Vegetation with Gaussian Processes in Granger Causality.

Mountrakis, G., Im, J., Ogole, C., 2011. Support vector machines in remote sensing: A review. ISPRS J Photogramm Remote Sens 66, 247–259. https://doi.org/10.1016/j.isprsjprs.2010.11.001

Mühlbauer, S., Costa, A.C., Caetano, M., 2016. A spatiotemporal analysis of droughts and the influence of North Atlantic Oscillation in the Iberian Peninsula based on MODIS imagery. Theor Appl Climatol 124, 703–721. https://doi.org/10.1007/s00704-015-1451-9

Muñoz-Carpena, R., Ritter, A., Bosch, D.D., 2004. Field methods for monitoring soil water status, in: Soil–Water–Solute Process Characterization. pp. 167–195.

Muñoz-Sabater, J., Dutra, E., Agustí-Panareda, A., Albergel, C., Arduini, G., Balsamo, G., Boussetta, S., Choulga, M., Harrigan, S., Hersbach, H., Martens, B., Miralles, D., Piles, M., Rodríguez-Fernández, N., Zsoter, E., Buontempo, C., Thépaut, J.-N., 2021. ERA5-Land: A state-of-the-art global reanalysis dataset for land applications. Earth System Science Data Discussions 1–50. https://doi.org/10.5194/essd-2021-82

Mutanga, O., Adam, E., Cho, M.A., 2012. High density biomass estimation for wetland vegetation using worldview-2 imagery and random forest regression algorithm. Int J Appl Earth Obs Geoinf 18, 399–406. https://doi.org/10.1016/j.jag.2012.03.012

Narasimhan, B., Srinivasan, R., 2005. Development and evaluation of Soil Moisture Deficit Index (SMDI) and Evapotranspiration Deficit Index (ETDI) for agricultural drought monitoring. Agric For Meteorol 133, 69–88. https://doi.org/10.1016/j.agrformet.2005.07.012

Narayanan, R.M., Hegde, M.S., 1995. Soil moisture inversion algorithms using ERS-1, JERS-1, and ALMAZ SAR data, in: International Geoscience and Remote Sensing Symposium, IGARSS '95. Quantitative Remote Sensing for Science and Applications. IEEE, pp. 504–506. https://doi.org/10.1109/IGARSS.1995.520321

Narayanankutty, K.A., Nair, A.A., Soori, D., Pradeep, D., Teja, V.R., K.B., V., 2010. Cognitive Radio Sensing Using Hilbert Huang Transform. Wireless Engineering and Technology 01, 36–40. https://doi.org/10.4236/wet.2010.11006

Naumann, G., Cammalleri, C., Mentaschi, L., Feyen, L., 2021. Increased economic drought impacts in Europe with anthropogenic warming. Nat Clim Chang 11, 485–491. https://doi.org/10.1038/s41558-021-01044-3

Nicolai-Shaw, N., Zscheischler, J., Hirschi, M., Gudmundsson, L., Seneviratne, S.I., 2017. A drought event composite analysis using satellite remote-sensing based soil moisture. Remote Sens Environ 203, 216–225. https://doi.org/10.1016/j.rse.2017.06.014

Njoku, E.G., Entekhabi, D., 1996. Passive microwave remote sensing of soil moisture. J Hydrol (Amst) 184, 101–129. https://doi.org/10.1016/0022-1694(95)02970-2

Nowack, P., Runge, J., Eyring, V., Haigh, J.D., 2020. Causal networks for climate model evaluation and constrained projections. Nat Commun 11, 1–11. https://doi.org/10.1038/s41467-020-15195-y

Orth, R., Seneviratne, S.I., 2012. Analysis of soil moisture memory from observations in Europe. J Geophys Res Atmos 117, n/a-n/a. https://doi.org/10.1029/2011JD017366

Overgaard, J., Rosbjerg, D., Butts, M.B., 2006. Land-surface modelling in hydrological perspective – a review. Biogeosciences 3, 229–241. https://doi.org/10.5194/bg-3-229-2006

Owe, M., de Jeu, R., Holmes, T., 2008. Multisensor historical climatology of satellite-derived global land surface moisture. J Geophys Res 113, F01002. https://doi.org/10.1029/2007JF000769

Pal, M., 2006. Support vector machine-based feature selection for land cover classification: a case study with DAIS hyperspectral data. Int J Remote Sens 27, 2877–2894. https://doi.org/10.1080/01431160500242515

Pal, M., 2005. Random forest classifier for remote sensing classification. Int J Remote Sens 26, 217–222. https://doi.org/10.1080/01431160412331269698

Paloscia, S., Pampaloni, P., Pettinato, S., Santi, E., 2008. A Comparison of Algorithms for Retrieving Soil Moisture from ENVISAT/ASAR Images. IEEE Trans Geosci Remote Sens 46, 3274–3284. https://doi.org/10.1109/TGRS.2008.920370

Pan, N., Wang, S., Liu, Y., Zhao, W., Fu, B., 2019. Global surface soil moisture dynamics in 1979-2016 observed from ESA CCI SM dataset. Water 11. https://doi.org/10.3390/w11050883

Panciera, R., Walker, J.P., Jackson, T.J., Gray, D.A., Tanase, M.A., Ryu, D., Monerris, A., Yardley, H., Rüdiger, C., Wu, X., Gao, Y., Hacker, J.M., 2014. The soil moisture active passive experiments (SMAPEx): Toward soil moisture retrieval from the SMAP mission. IEEE Trans Geosci Remote Sens 52, 490–507. https://doi.org/10.1109/TGRS.2013.2241774

Parajka, J., Naeimi, V., Blöschl, G., Wagner, W., Merz, R., Scipal, K., 2006. Assimilating scatterometer soil moisture data into conceptual hydrologic models at the regional scale. Hydrol Earth Syst Sci 10, 353–368. https://doi.org/10.5194/hess-10-353-2006

Pearl, J., 2009. Causal inference in statistics: An overview. Stat Surv 3, 96–146. https://doi.org/10.1214/09-SS057

Pearl, J., 1995. Causal diagrams for empirical research. Biometrika 82, 669–688. https://doi.org/10.1093/biomet/82.4.669

Peel, M.C., Finlayson, B.L., McMahon, T.A., 2007. Updated world map of the Köppen-Geiger climate classification. Hydrol Earth Syst Sci 11, 1633–1644. https://doi.org/10.5194/hess-11-1633-2007

Peng, J., Albergel, C., Balenzano, A., Brocca, L., Cartus, O., Cosh, M.H., Crow, W.T., Dabrowska-Zielinska, K., Dadson, S., Davidson, M.W.J., de Rosnay, P., Dorigo, W., Gruber, A., Hagemann, S., Hirschi, M., Kerr, Y.H., Lovergine, F., Mahecha, M.D., Marzahn, P., Mattia, F., Musial, J.P., Preuschmann, S., Reichle, R.H., Satalino, G., Silgram, M., van Bodegom, P.M., Verhoest, N.E.C., Wagner, W., Walker, J.P., Wegmüller, U., Loew, A., 2021. A roadmap for high-resolution satellite soil moisture applications – confronting product characteristics with user requirements. Remote Sens Environ. https://doi.org/10.1016/j.rse.2020.112162

Peng, J., Loew, A., Merlin, O., Verhoest, N.E.C., 2017. A review of spatial downscaling of satellite remotely sensed soil moisture. Reviews of Geophysics 55, 341–366. https://doi.org/10.1002/2016RG000543

Peng, J., Wu, C., Zhang, X., Wang, X., Gonsamo, A., 2019. Satellite detection of cumulative and lagged effects of drought on autumn leaf senescence over the Northern Hemisphere. Glob Chang Biol 25, 2174–2188. https://doi.org/10.1111/gcb.14627

Pérez-Planells, L., Delegido, J., Rivera-Caicedo, J.P., Verrelst, J., 2015. Análisis de métodos de validación cruzada para la obtención robusta de parámetros biofísicos. Revista de Teledetección 44, 55–65. https://doi.org/10.4995/raet.2015.4153

Petropoulos, G.P., Ireland, G., Barrett, B., 2015. Surface soil moisture retrievals from remote sensing: Current status, products & future trends. Phys Chem Earth 83–84, 36–56. https://doi.org/10.1016/j.pce.2015.02.009

Piles, M., Ballabrera-Poy, J., Muñoz-Sabater, J., 2019. Dominant features of global surface soil moisture variability observed by the SMOS satellite. Remote Sens 11, 1–21. https://doi.org/10.3390/rs11010095

Piles, M., Camps, A., Vall-llossera, M., Corbella, I., Panciera, R., Rudiger, C., Kerr, Y.H., Walker, J., 2011. Downscaling SMOS-Derived Soil Moisture Using MODIS Visible/Infrared Data. IEEE Trans Geosci Remote Sens 49, 3156–3166. https://doi.org/10.1109/TGRS.2011.2120615

Piles, M., Fernandez-Moran, R., Gómez-Chova, L., Camps-Valls, G., Entekhabi, D., Baur, M., Jagdhuber, T., Wigneron, J.-P., Prigent, C., Donlon, C., 2021. The CIMR mission and its unique capabilities for soil moisture sensing, in: EGU General Assembly 2021. online, 19–30 Apr 2021. https://doi.org/10.5194/egusphere-egu21-9484

Piles, M., Muñoz-Mari, J., Guerrero-Curieses, A., Camps-Valls, G., Rojo-Alvarez, J.L., 2022. Autocorrelation Metrics to Estimate Soil Moisture Persistence From Satellite Time Series: Application to Semiarid Regions. IEEE Trans Geosci Remote Sens 60, 1–17. https://doi.org/10.1109/TGRS.2021.3057928

Piles, M., Petropoulos, G.P., Sánchez, N., González-Zamora, Á., Ireland, G., 2016. Towards improved spatio-temporal resolution soil moisture retrievals from the synergy of SMOS and MSG SEVIRI spaceborne observations. Remote Sens Environ 180, 403–417. https://doi.org/10.1016/j.rse.2016.02.048

Piles, M., Sánchez, N., Vall-llossera, M., Camps, A., Martínez-Fernández, J., Martínez, J., González-Gambau, V., 2014. A Downscaling Approach for SMOS Land Observations: Evaluation of High-Resolution Soil Moisture Maps Over the Iberian Peninsula. IEEE J Sel Top Appl Earth Obs Remote Sens 7, 3845–3857. https://doi.org/10.1109/JSTARS.2014.2325398

Preimesberger, W., Scanlon, T., Su, C.H., Gruber, A., Dorigo, W., 2021. Homogenization of Structural Breaks in the Global ESA CCI Soil Moisture Multisatellite Climate Data Record. IEEE Trans Geosci Remote Sens 59, 2845–2862. https://doi.org/10.1109/TGRS.2020.3012896

Price, J.C., 1980. The potential of remotely sensed thermal infrared data to infer surface soil moisture and evaporation. Water Resour Res 16, 787–795. https://doi.org/10.1029/WR016i004p00787

Qiu, J., Gao, Q., Wang, S., Su, Z., 2016. Comparison of temporal trends from multiple soil moisture data sets and precipitation: The implication of irrigation on regional soil moisture trend. Int J Appl Earth Obs Geoinf 48, 17–27. https://doi.org/10.1016/j.jag.2015.11.012

Qu, Y., Zhu, Z., Chai, L., Liu, S., Montzka, C., Liu, J., Yang, X., Lu, Z., Jin, R., Li, X., Guo, Z., Zheng, J., 2019. Rebuilding a Microwave Soil Moisture Product Using Random Forest Adopting AMSR-E/AMSR2 Brightness Temperature and SMAP over the Qinghai–Tibet Plateau, China. Remote Sens 11, 683. https://doi.org/10.3390/rs11060683

Quesney, A., 2000. Estimation of Watershed Soil Moisture Index from ERS/SAR Data. Remote Sens Environ 72, 290–303. https://doi.org/10.1016/S0034-4257(99)00102-9

Quiring, S.M., Papakryiakou, T.N., 2003. An evaluation of agricultural drought indices for the Canadian prairies. Agric For Meteorol 118, 49–62. https://doi.org/10.1016/S0168-1923(03)00072-8

Rahmani, A., Golian, S., Brocca, L., 2016. Multiyear monitoring of soil moisture over Iran through satellite and reanalysis soil moisture products. Int J Appl Earth Obs Geoinf 48, 85–95. https://doi.org/10.1016/j.jag.2015.06.009

Reichle, R.H., De Lannoy, G.J.M., Liu, Q., Ardizzone, J. V., Colliander, A., Conaty, A., Crow, W., Jackson, T.J., Jones, L.A., Kimball, J.S., Koster, R.D., Mahanama, S.P., Smith, E.B., Berg, A., Bircher, S., Bosch, D., Caldwell, T.G., Cosh, M., González-

Zamora, Á., Collins, C.D.H., Jensen, K.H., Livingston, S., Lopez-Baeza, E., Martínez-Fernández, J., McNairn, H., Moghaddam, M., Pacheco, A., Pellarin, T., Prueger, J., Rowlandson, T., Seyfried, M., Starks, P., Su, Z., Thibeault, M., van der Velde, R., Walker, J., Wu, X., Zeng, Y., 2017. Assessment of the SMAP Level-4 Surface and Root-Zone Soil Moisture Product Using In Situ Measurements. J Hydrometeorol 18, 2621–2645. https://doi.org/10.1175/JHM-D-17-0063.1

Reichle, R.H., Koster, R.D., de Lannoy, G.J.M., Forman, B.A., Liu, Q., Mahanama, S.P.P., Toure, A., 2011. Assessment and enhancement of MERRA land surface hydrology estimates. J Clim 24, 6322–6338. https://doi.org/10.1175/JCLI-D-10-05033.1

Reynolds, S.G., 1970. The gravimetric method of soil moisture determination Part I A study of equipment, and methodological problems. J Hydrol (Amst) 11, 258–273. https://doi.org/10.1016/0022-1694(70)90066-1

Rigling, B.D., 2012. Application of Temporal Gap Filling to Natural Power Law Spectrums. IEEE Geosci Remote Sens Lett 9, 624–628. https://doi.org/10.1109/LGRS.2011.2177062

Robinson, D.A., Campbell, C.S., Hopmans, J.W., Hornbuckle, B.K., Jones, S.B., Knight, R., Ogden, F., Selker, J., Wendroth, O., 2008. Soil Moisture Measurement for Ecological and Hydrological Watershed-Scale Observatories: A Review. Vadose Zone Journal 7, 358–389. https://doi.org/10.2136/vzj2007.0143

Robock, A., Vinnikov, K.Y., Srinivasan, G., Entin, J.K., Hollinger, S.E., Speranskaya, N.A., Liu, S., Namkhai, A., 2000. The Global Soil Moisture Data Bank. Bull Am Meteorol Soc 81, 1281–1299. https://doi.org/10.1175/1520-0477(2000)081<1281:TGSMDB>2.3.CO;2

Rodriguez-Iturbe, I., Porporato, A., Ridolfi, L., Isham, V., Coxi, D.R., 1999. Probabilistic modelling of water balance at a point: the role of climate, soil and vegetation, in: Proc Math Phys Eng Sci. https://doi.org/10.1098/rspa.1999.0477

Ropelewski, C.F., Jones, P.D., 1987. An Extension of the Tahiti–Darwin Southern Oscillation Index. Mon Weather Rev 115, 2161–2165. https://doi.org/10.1175/1520-0493(1987)115<2161:aeotts>2.0.co;2

Ross, P.J., 1990. Efficient numerical methods for infiltration using Richards' equation. Water Resour Res 26, 279–290. https://doi.org/10.1029/WR026i002p00279

Rousi, E., Kornhuber, K., Beobide-Arsuaga, G., Luo, F., Coumou, D., 2022. Accelerated western European heatwave trends linked to more-persistent double jets over Eurasia. Nat Commun 13, 1–11. https://doi.org/10.1038/s41467-022-31432-y

Runge, J., 2020. Discovering contemporaneous and lagged causal relations in autocorrelated nonlinear time series datasets. Proceedings of the 36th Conference on Uncertainty in Artificial Intelligence, UAI 2020 124, 1388–1397.

Runge, J., Bathiany, S., Bollt, E., Camps-Valls, G., Coumou, D., Deyle, E., Glymour, C., Kretschmer, M., Mahecha, M.D., Muñoz-Marí, J., van Nes, E.H., Peters, J., Quax, R.,

Reichstein, M., Scheffer, M., Schölkopf, B., Spirtes, P., Sugihara, G., Sun, J., Zhang, K., Zscheischler, J., 2019a. Inferring causation from time series in Earth system sciences. Nat Commun 10, 1–13. https://doi.org/10.1038/s41467-019-10105-3

Runge, J., Nowack, P., Kretschmer, M., Flaxman, S., Sejdinovic, D., 2019b. Detecting and quantifying causal associations in large nonlinear time series datasets. Sci Adv 5. https://doi.org/10.1126/sciadv.aau4996

Sakai, T., Iizumi, T., Okada, M., Nishimori, M., Grünwald, T., Prueger, J., Cescatti, A., Korres, W., Schmidt, M., Carrara, A., Loubet, B., Ceschia, E., 2016. Varying applicability of four different satellite-derived soil moisture products to global gridded crop model evaluation. Int J Appl Earth Obs Geoinf 48, 51–60. https://doi.org/10.1016/j.jag.2015.09.011

Salcedo-Sanz, S., Ghamisi, P., Piles, M., Werner, M., Cuadra, L., Moreno-Martínez, A., Izquierdo-Verdiguier, E., Muñoz-Marí, J., Mosavi, A., Camps-Valls, G., 2020. Machine learning information fusion in Earth observation: A comprehensive review of methods, applications and data sources. Information Fusion 63, 256–272. https://doi.org/10.1016/j.inffus.2020.07.004

Salvia, M., Sánchez, N., Piles, M., Ruscica, R., González-Zamora, Á., Roitberg, E., Martínez-Fernández, J., 2021. The Added-Value of Remotely-Sensed Soil Moisture Data for Agricultural Drought Detection in Argentina. IEEE J Sel Top Appl Earth Obs Remote Sens 14, 6487–6500. https://doi.org/10.1109/JSTARS.2021.3084849

Sánchez, N., Almendra, L., Plaza, J., González-Zamora, Á., Martínez-Fernández, J., 2020. Spatial averages of in situ measurements versus remote sensing observations: a soil moisture analysis. J Spat Sci 00, 1–16. https://doi.org/10.1080/14498596.2020.1833769

Sánchez, N., González-Zamora, Á., Martínez-Fernández, J., Piles, M., Pablos, M., 2018. Integrated remote sensing approach to global agricultural drought monitoring. Agric For Meteorol 259, 141–153. https://doi.org/10.1016/j.agrformet.2018.04.022

Sánchez, N., González-Zamora, Á., Piles, M., Martínez-Fernández, J., 2016. A New Soil Moisture Agricultural Drought Index (SMADI) Integrating MODIS and SMOS Products: A Case of Study over the Iberian Peninsula. Remote Sens 8, 287. https://doi.org/10.3390/rs8040287

Sánchez-Ruiz, S., Piles, M., Sánchez, N., Martínez-Fernández, J., Vall-llossera, M., Camps, A., 2014. Combining SMOS with visible and near/shortwave/thermal infrared satellite data for high resolution soil moisture estimates. J Hydrol (Amst) 516, 273–283. https://doi.org/10.1016/j.jhydrol.2013.12.047

Sandholt, I., Rasmussen, K., Andersen, J., 2002. A simple interpretation of the surface temperature/vegetation index space for assessment of surface moisture status. Remote Sens Environ 79, 213–224. https://doi.org/10.1016/S0034-4257(01)00274-7

Sang, Y.F., Sivakumar, B., Zhu, Y., 2021. Uniform discrete wavelet spectrum for detection of hydrologic variability at multiple timescales. Journal of Hydro-Environment Research 35, 31–37. https://doi.org/10.1016/j.jher.2021.01.005

Sang, Y.F., Sun, F., Singh, V.P., Xie, P., Sun, J., 2018. A discrete wavelet spectrum approach for identifying non-monotonic trends in hydroclimate data. Hydrol Earth Syst Sci 22, 757–766. https://doi.org/10.5194/hess-22-757-2018

Sang, Y.F., Wang, Z., Liu, C., 2014. Comparison of the MK test and EMD method for trend identification in hydrological time series. J Hydrol (Amst) 510, 293–298. https://doi.org/10.1016/j.jhydrol.2013.12.039

Sang, Y.F., Wang, Z., Liu, C., 2013. Discrete wavelet-based trend identification in hydrologic time series. Hydrol Process 27, 2021–2031. https://doi.org/10.1002/hyp.9356

Santanello, J.A., Peters-Lidard, C.D., Kumar, S. v., 2011. Diagnosing the sensitivity of local land-atmosphere coupling via the soil moisture-boundary layer interaction. J Hydrometeorol 12, 766–786. https://doi.org/10.1175/JHM-D-10-05014.1

Scaife, A.A., Folland, C.K., Alexander, L. v., Moberg, A., Knight, J.R., 2008. European climate extremes and the North Atlantic Oscillation. J Clim 21, 72–83. https://doi.org/10.1175/2007JCLI1631.1

Scanlon, T., Pasik, A., Dorigo, W., de Jeu, R.A.M., Hahn, S., van der Schalie, R., Wagner, W., Kidd, R., Gruber, A., Moesinger, L., Preimesberger, W., van der Vliet, M., Stradiotti, P., 2022. Algorithm Theoretical Baseline Document (ATBD) Supporting Product Version 07.1 D2.1 Version 3.

Schmugge, T., Gloersen, P., Wilheit, T., Geiger, F., 1974. Remote sensing of soil moisture with microwave radiometers. J Geophys Res 79, 317–323. https://doi.org/10.1029/JB079i002p00317

Schmugge, T.J., Kustas, W.P., Ritchie, J.C., Jackson, T.J., Rango, A., 2002. Remote sensing in hydrology. Adv Water Resour 25, 1367–1385. https://doi.org/10.1016/S0309-1708(02)00065-9

Scholze, M., Kaminski, T., Knorr, W., Blessing, S., Vossbeck, M., Grant, J.P., Scipal, K., 2016. Simultaneous assimilation of SMOS soil moisture and atmospheric CO2 in-situ observations to constrain the global terrestrial carbon cycle. Remote Sens Environ 180, 334–345. https://doi.org/10.1016/j.rse.2016.02.058

Schubert, S.D., Stewart, R.E., Wang, H., Barlow, M., Berbery, E.H., Cai, W., Hoerling, M.P., Kanikicharla, K.K., Koster, R.D., Lyon, B., Mariotti, A., Mechoso, C.R., Müller, O. v., Rodriguez-Fonseca, B., Seager, R., Senevirante, S.I., Zhang, L., Zhou, T., 2016. Global meteorological drought: A synthesis of current understanding with a focus on sst drivers of precipitation deficits. J Clim 29, 3989–4019. https://doi.org/10.1175/JCLI-D-15-0452.1

Sehgal, V., Gaur, N., Mohanty, B.P., 2021. Global Surface Soil Moisture Drydown Patterns. Water Resour Res 57, 1–26. https://doi.org/10.1029/2020WR027588

Seneviratne, S.I., Corti, T., Davin, E.L., Hirschi, M., Jaeger, E.B., Lehner, I., Orlowsky, B., Teuling, A.J., 2010. Investigating soil moisture-climate interactions in a changing climate: A review. Earth Sci Rev 99, 125–161. https://doi.org/10.1016/j.earscirev.2010.02.004

Sheffield, J., Wood, E.F., 2008. Global trends and variability in soil moisture and drought characteristics, 1950-2000, from observation-driven simulations of the terrestrial hydrologic cycle. J Clim 21, 432–458. https://doi.org/10.1175/2007JCLI1822.1

Sheffield, J., Wood, E.F., 2007. Characteristics of global and regional drought, 1950-2000: Analysis of soil moisture data from off-line simulation of the terrestrial hydrologic cycle. J Geophys Res Atmos 112, 1–21. https://doi.org/10.1029/2006JD008288

Sheffield, J., Wood, E.F., Chaney, N., Guan, K., Sadri, S., Yuan, X., Olang, L., Amani, A., Ali, A., Demuth, S., Ogallo, L., 2014. A drought monitoring and forecasting system for sub-sahara african water resources and food security. Bull Am Meteorol Soc 95, 861–882. https://doi.org/10.1175/BAMS-D-12-00124.1

Sheikh, V., Visser, S., Stroosnijder, L., 2009. A simple model to predict soil moisture: Bridging Event and Continuous Hydrological (BEACH) modelling. Environmental Modelling and Software 24, 542–556. https://doi.org/10.1016/j.envsoft.2008.10.005

Shen, H., Li, H., Qian, Y., Zhang, L., Yuan, Q., 2014. An effective thin cloud removal procedure for visible remote sensing images. ISPRS J Photogramm Remote Sens. https://doi.org/10.1016/j.isprsjprs.2014.06.011

Siebert, S., Döll, P., Hoogeveen, J., Faures, J.M., Frenken, K., Feick, S., 2005. Development and validation of the global map of irrigation areas. Hydrol Earth Syst Sci 9, 535–547. https://doi.org/10.5194/hess-9-535-2005

Silva, F.N., Vega-Oliveros, D.A., Yan, X., Flammini, A., Menczer, F., Radicchi, F., Kravitz, B., Fortunato, S., 2021. Detecting Climate Teleconnections With Granger Causality. Geophys Res Lett 48, 1–10. https://doi.org/10.1029/2021GL094707

Simpkins, G., 2021. Breaking down the NAO–AO connection. Nat Rev Earth Environ 2, 88. https://doi.org/10.1038/s43017-021-00139-x

Smith, P.J., Pappenberger, F., Wetterhall, F., Thielen Del Pozo, J., Krzeminski, B., Salamon, P., Muraro, D., Kalas, M., Baugh, C., 2016. On the Operational Implementation of the European Flood Awareness System (EFAS), Flood Forecasting: A Global Perspective. Elsevier Inc. https://doi.org/10.1016/B978-0-12-801884-2.00011-6

Smola, A.J., Schölkopf, B., 2004. A tutorial on support vector regression. Stat Comput 14, 199–222. https://doi.org/10.1023/B:STCO.0000035301.49549.88

Solomatine, D.P., Wagener, T., 2011. Hydrological Modeling. Treatise on Water Science 2, 435–457. https://doi.org/10.1016/B978-0-444-53199-5.00044-0

Song, X., Song, Y., Chen, Y., 2020. Secular trend of global drought since 1950. Environ Res,Lett 15. https://doi.org/10.1088/1748-9326/aba20d

Spinoni, J., Vogt, J. v., Naumann, G., Barbosa, P., Dosio, A., 2018. Will drought events become more frequent and severe in Europe? Int J Climatol 38, 1718–1736. https://doi.org/10.1002/joc.5291

Spirtes, P., Glymour, C., 1991. An Algorithm for Fast Recovery of Sparse Causal Graphs. Soc Sci Comput Rev 9, 62–72. https://doi.org/10.1177/089443939100900106

Sridhar, V., Hubbard, K.G., You, J., Hunt, E.D., 2008. Development of the Soil Moisture Index to Quantify Agricultural Drought and Its "User Friendliness" in Severity-Area-Duration Assessment. J Hydrometeorol 9, 660–676. https://doi.org/10.1175/2007JHM892.1

Srivastava, P.K., Han, D., Ramirez, M.R., Islam, T., 2013. Machine Learning Techniques for Downscaling SMOS Satellite Soil Moisture Using MODIS Land Surface Temperature for Hydrological Application. Water Resour Manag 27, 3127–3144. https://doi.org/10.1007/s11269-013-0337-9

Su, L., Miao, C., Kong, D., Duan, Q., Lei, X., Hou, Q., Li, H., 2018. Long-term trends in global river flow and the causal relationships between river flow and ocean signals. J Hydrol (Amst) 563, 818–833. https://doi.org/10.1016/j.jhydrol.2018.06.058

Susha Lekshmi, S.U., Singh, D.N., Shojaei Baghini, M., 2014. A critical review of soil moisture measurement. Measurement (Lond) 54, 92–105. https://doi.org/10.1016/j.measurement.2014.04.007

Tabari, H., Willems, P., 2018. Lagged influence of Atlantic and Pacific climate patterns on European extreme precipitation. Sci Rep 8, 1–10. https://doi.org/10.1038/s41598-018-24069-9

Tallec, G., Ansart, P., Guérin, A., Delaigue, O., Blanchouin, A., 2015. Observatoire Oracle. Irstea. https://doi.org/https://dx.doi.org/10.17180/obs.oracle

Thompson, D.W.J., Wallace, J.M., 1998. The Arctic oscillation signature in the wintertime geopotential height and temperature fields. Geophys Res Lett 25, 1297–1300. https://doi.org/10.1029/98GL00950

Thorne, P.W., Diamond, H.J., Goodison, B., Harrigan, S., Hausfather, Z., Ingleby, N.B., Jones, P.D., Lawrimore, J.H., Lister, D.H., Merlone, A., Oakley, T., Palecki, M., Peterson, T.C., de Podesta, M., Tassone, C., Venema, V., Willett, K.M., 2018. Towards a global land surface climate fiducial reference measurements network. Int J Climatol 38, 2760–2774. https://doi.org/10.1002/joc.5458

Thuiller, W., 2007. Climate change and the ecologist. Nature 448, 550–552. https://doi.org/10.1038/448550a

Tibshirani, R., 1996. Regression Shrinkage and Selection Via the Lasso. J R Stat Soc Series B Stat Methodol (Methodological) 58, 267–288. https://doi.org/10.1111/j.2517-6161.1996.tb02080.x

Toreti, A., Desiato, F., Fioravanti, G., Perconti, W., 2010. Seasonal temperatures over Italy and their relationship with low-frequency atmospheric circulation patterns. Clim Change 99, 211–227. https://doi.org/10.1007/s10584-009-9640-0

Toreti, A., Masante, D., Acosta Navarro, J., Bavera, D., Cammalleri, C., De Felice, M., de Jager, A., Di Ciollo, C., Hrast Essenfelder, A., Maetens, W., Magni, D., Mazzeschi, M., Spinoni, J., 2022. Drought in Europe July 2022. Publications Office of the European Union, Luxembourg.

Trenberth, K., 2011. Changes in precipitation with climate change. Clim Res 47, 123–138. https://doi.org/10.3354/cr00953

Trenberth, K.E., 1997. The Definition of El Niño. Bull Am Meteorol Soc 78, 2771–2777. https://doi.org/10.1175/1520-0477(1997)078<2771:TDOENO>2.0.CO;2

Trigo, R.M., Osborn, T.J., Corte-Real, J.M., 2002. The North Atlantic Oscillation influence on Europe: Climate impacts and associated physical mechanisms. Clim Res 20, 9–17. https://doi.org/10.3354/cr020009

Trnka, M., Dubrovský, M., Svoboda, M., Semerádová, D., Hayes, M., Žalud, Z., Wilhite, D., 2009a. Developing a regional drought climatology for the Czech Republic. Int J Climatol 29, 863–883. https://doi.org/10.1002/joc.1745

Trnka, M., Kyselý, J., Možný, M., Dubrovský, M., 2009b. Changes in Central-European soil-moisture availability and circulation patterns in 1881-2005. Int J Climatol 29, 655–672. https://doi.org/10.1002/joc.1703

van der Knijff, J.M., Younis, J., de Roo, A.P.J., 2010. LISFLOOD: A GIS-based distributed model for river basin scale water balance and flood simulation. Int J Geogr Inf Sci 24, 189–212. https://doi.org/10.1080/13658810802549154

van der Schrier, G., Briffa, K.R., Jones, P.D., Osborn, T.J., 2006. Summer moisture variability across Europe. J Clim 19, 2818–2834. https://doi.org/10.1175/JCLI3734.1

Van Loon, A.F., 2015. Hydrological drought explained. WIREs Water 2, 359–392. https://doi.org/10.1002/wat2.1085

van Oldenborgh, G.J., Burgers, G., Tank, A.K., 2000. On the El Niño teleconnection to spring precipitation in Europe. Int J Climatol 20, 565–574. https://doi.org/10.1002/(SICI)1097-0088(200004)20:5<565::AID-JOC488>3.0.CO;2-5

Vapnik, V.N., 1995. The Nature of Statistical Learning Theory. Springer New York, New York, NY. https://doi.org/10.1007/978-1-4757-3264-1

Vautard, R., Yiou, P., D'Andrea, F., de Noblet, N., Viovy, N., Cassou, C., Polcher, J., Ciais, P., Kageyama, M., Fan, Y., 2007. Summertime European heat and drought waves induced by wintertime Mediterranean rainfall deficit. Geophys Res Lett 34, 1–5. https://doi.org/10.1029/2006GL028001

Vaz, C.M.P., Jones, S., Meding, M., Tuller, M., 2013. Evaluation of Standard Calibration Functions for Eight Electromagnetic Soil Moisture Sensors. Vadose Zone Journal 12, vzj2012.0160. https://doi.org/10.2136/vzj2012.0160

Vicente-Serrano, S.M., Domínguez-Castro, F., Murphy, C., Hannaford, J., Reig, F., Peña-Angulo, D., Tramblay, Y., Trigo, R.M., mac Donald, N., Luna, M.Y., Mc Carthy, M., van der Schrier, G., Turco, M., Camuffo, D., Noguera, I., García-Herrera, R., Becherini, F., della Valle, A., Tomas-Burguera, M., el Kenawy, A., 2021. Long-term variability and trends in meteorological droughts in Western Europe (1851–2018). Int J Climatol 41, E690–E717. https://doi.org/10.1002/joc.6719

Vicente-Serrano, S.M., López-Moreno, J.I., Lorenzo-Lacruz, J., Kenawy, A. el, Azorin-Molina, C., Morán-Tejeda, E., Pasho, E., Zabalza, J., Beguería, S., Angulo-Martínez, M., 2011. The NAO Impact on Droughts in the Mediterranean Region, in: Advances in Global Change Research. Springer International Publishing, pp. 23–40. https://doi.org/10.1007/978-94-007-1372-7_3

Visbeck, M.H., Hurrell, J.W., Polvani, L., Cullen, H.M., 2001. The North Atlantic oscillation: Past, present, and future. Proc Natl Acad Sci U S A 98, 12876–12877. https://doi.org/10.1073/pnas.231391598

Wagner, W., Blöschl, G., Pampaloni, P., Calvet, J.-C., Bizzarri, B., Wigneron, J.-P., Kerr, Y., 2007. Operational readiness of microwave remote sensing of soil moisture for hydrologic applications. Hydrology Research 38, 1–20. https://doi.org/10.2166/nh.2007.029

Walker, G.T., Bliss, E.W., 1932. World Weather V. Memoirs of the royal meteorological society IV, 53–84.

Walker, J.P., Houser, P.R., Willgoose, G.R., 2004a. Active microwave remote sensing for soil moisture measurement: a field evaluation using ERS-2. Hydrol Process 18, 1975–1997. https://doi.org/10.1002/hyp.1343

Walker, J.P., Willgoose, G.R., Kalma, J.D., 2004b. In situ measurement of soil moisture: A comparison of techniques. J Hydrol (Amst) 293, 85–99. https://doi.org/10.1016/j.jhydrol.2004.01.008

Wanders, N., Karssenberg, D., de Roo, A., de Jong, S.M., Bierkens, M.F.P., 2014. The suitability of remotely sensed soil moisture for improving operational flood forecasting. Hydrol Earth Syst Sci 18, 2343–2357. https://doi.org/10.5194/hess-18-2343-2014

Wang, C., Liu, H., Lee, S.K., 2010. The record-breaking cold temperatures during the winter of 2009/2010 in the Northern Hemisphere. Atmospheric Science Letters 11, 161–168. https://doi.org/10.1002/asl.278

Wang, G., 2005. Agricultural drought in a future climate: results from 15 global climate models participating in the IPCC 4th assessment. Clim Dyn 25, 739–753. https://doi.org/10.1007/s00382-005-0057-9

Wang, G., Dolman, A.J., Alessandri, A., 2011. A summer climate regime over Europe modulated by the North Atlantic Oscillation. Hydrol Earth Syst Sci 15, 57–64. https://doi.org/10.5194/hess-15-57-2011

Wang, G., Garcia, D., Liu, Y., de Jeu, R., Johannes Dolman, A., 2012. A three-dimensional gap filling method for large geophysical datasets: Application to global satellite soil moisture observations. Environmental Modelling and Software 30, 139–142. https://doi.org/10.1016/j.envsoft.2011.10.015

Wang, G., Kim, Y., Wang, D., 2007. Quantifying the strength of soil moisture-precipitation coupling and its sensitivity to changes in surface water budget. J Hydrometeorol 8, 551–570. https://doi.org/10.1175/JHM573.1

Wang, H., 2018. Soil Moisture Retrieval from Microwave Remote Sensing Observations, in: Civeira, G. (Ed.), Soil Moisture. IntechOpen, London, pp. 29–54. https://doi.org/ht10.5772/intechopen.81476

Wang, L., Qu, J.J., 2009. Satellite remote sensing applications for surface soil moisture monitoring: A review. Frontiers of Earth Science in China 3, 237–247. https://doi.org/10.1007/s11707-009-0023-7

Wang, S., Mo, X., Liu, S., Lin, Z., Hu, S., 2016. Validation and trend analysis of ECV soil moisture data on cropland in North China Plain during 1981–2010. Int J Appl Earth Obs Geoinf 48, 110–121. https://doi.org/10.1016/j.jag.2015.10.010

Wang, T., Franz, T.E., Li, R., You, J., Shulski, M.D., Ray, C., 2017. Evaluating climate and soil effects on regional soil moisture spatial variability using EOFs. Water Resour Res 53, 4022–4035. https://doi.org/10.1002/2017WR020642

Wang, Y.H., Magnusdottir, G., Stern, H., Tian, X., Yu, Y., 2012. Decadal variability of the NAO: Introducing an augmented NAO index. Geophys Res Lett 39, 1–5. https://doi.org/10.1029/2012GL053413

Wanner, H., Brönnimann, S., Casty, C., Gyalistras, D., Luterbacher, J., Schmutz, C., Stephenson, D.B., and Xoplaki, E., 2001. North Atlantic Oscillation – Concepts And Studies. Surv Geophys 22, 321–382. https://doi.org/10.1023/A:1014217317898

Wei, F., Wang, S., Fu, B., Pan, N., Feng, X., Zhao, W., Wang, C., 2018. Vegetation dynamic trends and the main drivers detected using the ensemble empirical mode decomposition method in East Africa. Land Degrad Dev 29, 2542–2553. https://doi.org/10.1002/ldr.3017

Weidong, L., Baret, F., Xingfa, G., Qingxi, T., Lanfen, Z., Bing, Z., 2002. Relating soil surface moisture to reflectance. Remote Sens Environ 81, 238–246. https://doi.org/10.1016/S0034-4257(01)00347-9

Wigneron, J.P., Calvet, J.C., Pellarin, T., van de Griend, A.A., Berger, M., Ferrazzoli, P., 2003. Retrieving near-surface soil moisture from microwave radiometric observations: Current status and future plans. Remote Sens Environ 85, 489–506. https://doi.org/10.1016/S0034-4257(03)00051-8

Wigneron, J.P., Schmugge, T., Chanzy, A., Calvet, J.C., Kerr, Y., 1998. Use of passive microwave remote sensing to monitor soil moisture. Agronomie 18, 27–43. https://doi.org/10.1051/agro:19980102

Wilhite, D.A., 2000. Drought as a Natural Hazard: Concepts and Definitions, in: Drought: A Global Assessment. Routledge, London, pp. 3–18.

Wood, E.F., Roundy, J.K., Troy, T.J., van Beek, L.P.H., Bierkens, M.F.P., Blyth, E., de Roo, A., Döll, P., Ek, M., Famiglietti, J., Gochis, D., van de Giesen, N., Houser, P., Jaffé, P.R., Kollet, S., Lehner, B., Lettenmaier, D.P., Peters-Lidard, C., Sivapalan, M., Sheffield, J., Wade, A., Whitehead, P., 2011. Hyperresolution global land surface modeling: Meeting a grand challenge for monitoring Earth's terrestrial water. Water Resour Res 47, 1–10. https://doi.org/10.1029/2010WR010090

Wu, Z., Huang, N.E., 2009. Ensemble empirical mode decomposition: A noise-assisted data analysis method. Adv Adapt Data Anal 1, 1–41. https://doi.org/10.1142/S1793536909000047

Wu, Z., Huang, N.E., 2005. Statistical significance test of intrinsic mode functions, in: Hilbert-Huang Transform And Its Applications. World Scientific Publishing Co., pp. 107–127. https://doi.org/10.1142/9789812703347_0005

Wu, Z., Huang, N.E., 2004. A study of the characteristics of white noise using the empirical mode decomposition method. Proc Math Phys Eng Sci 460, 1597–1611. https://doi.org/10.1098/rspa.2003.1221

Xiao, Z., Jiang, L., Zhu, Z., Wang, J., Du, J., 2016. Spatially and temporally complete satellite soil moisture data based on a data assimilation method. Remote Sens 8. https://doi.org/10.3390/rs8010049

Xie, X., Li, A., Tan, J., Lei, G., Jin, H., Zhang, Z., 2020. Uncertainty analysis of multiple global GPP datasets in characterizing the lagged effect of drought on photosynthesis. Ecol Indic 113. https://doi.org/10.1016/j.ecolind.2020.106224

Xie, X., Liu, W.T., Tang, B., 2008. Spacebased estimation of moisture transport in marine atmosphere using support vector regression. Remote Sens Environ 112, 1846–1855. https://doi.org/10.1016/j.rse.2007.09.003

Xing, C., Chen, N., Zhang, X., Gong, J., 2017. A machine learning based reconstruction method for satellite remote sensing of soil moisture images with in situ observations. Remote Sens (Basel) 9. https://doi.org/10.3390/rs9050484

Yang, F., White, M.A., Michaelis, A.R., Ichii, K., Hashimoto, H., Votava, P., Zhu, A.X., Nemani, R.R., 2006. Prediction of continental-scale evapotranspiration by combining MODIS and AmeriFlux data through support vector machine. IEEE Trans Geosci Remote Sens 44, 3452–3461. https://doi.org/10.1109/TGRS.2006.876297

Yassin, F., Razavi, S., Wong, J.S., Pietroniro, A., Wheater, H., 2019. Hydrologic-Land Surface Modelling of a Complex System under Precipitation Uncertainty: A Case

Study of the Saskatchewan River Basin, Canada. Hydrology and Earth System Sciences Discussions 1–40. https://doi.org/10.5194/hess-2019-207

Yevjevieh, V., 1987. Stochastic models in hydrology. Stochastic Hydrology and Hydraulics 1, 17–36. https://doi.org/https://doi.org/10.1007/BF01543907

Yoo, C., Kim, S., 2004. EOF analysis of surface soil moisture field variability. Adv Water Resour 27, 831–842. https://doi.org/10.1016/j.advwatres.2004.04.003

Yue, S., Pilon, P., Cavadias, G., 2002. Power of the Mann–Kendall and Spearman's rho tests for detecting monotonic trends in hydrological series. J Hydrol (Amst) 259, 254–271. https://doi.org/10.1016/S0022-1694(01)00594-7

Zacharias, S., Bogena, H., Samaniego, L., Mauder, M., Fuß, R., Pütz, T., Frenzel, M., Schwank, M., Baessler, C., Butterbach-Bahl, K., Bens, O., Borg, E., Brauer, A., Dietrich, P., Hajnsek, I., Helle, G., Kiese, R., Kunstmann, H., Klotz, S., Munch, J.C., Papen, H., Priesack, E., Schmid, H.P., Steinbrecher, R., Rosenbaum, U., Teutsch, G., Vereecken, H., 2011. A Network of Terrestrial Environmental Observatories in Germany. Vadose Zone Journal 10, 955–973. https://doi.org/10.2136/vzj2010.0139

Zawadzki, J., Kędzior, M.A., 2014. Statistical analysis of soil moisture content changes in Central Europe using GLDAS database over three past decades. Cent Eur Geol 6, 344–353. https://doi.org/10.2478/s13533-012-0176-x

Zhang, B., Zhao, X., Jin, J., Wu, P., 2015. Development and evaluation of a physically based multiscalar drought index: The Standardized Moisture Anomaly Index. J Geophys Res Atmos 120, 11,575-11,588. https://doi.org/10.1002/2015JD023772

Zhang, D., Zhou, G., 2016. Estimation of Soil Moisture from Optical and Thermal Remote Sensing: A Review. Sensors 16, 1308. https://doi.org/10.3390/s16081308

Zhang, K., Peters, J., Janzing, D., Schölkopf, B., 2011. Kernel-based conditional independence test and application in causal discovery. Proceedings of the 27th Conference on Uncertainty in Artificial Intelligence, UAI 2011 804–813.

Zhang, R., Li, L., Zhang, Y., Huang, F., Li, J., Liu, W., Mao, T., Xiong, Z., Shangguan, W., 2021. Assessment of agricultural drought using soil water deficit index based on era5-land soil moisture data in four southern provinces of china. Agriculture (Switzerland) 11. https://doi.org/10.3390/agriculture11050411

Zhang, X., Chen, N., 2016. Reconstruction of GF-1 Soil Moisture Observation Based on Satellite and In Situ Sensor Collaboration under Full Cloud Contamination. IEEE Trans Geosci Remote Sens 54, 5185–5202. https://doi.org/10.1109/TGRS.2016.2558109

Zhao, W., Sánchez, N., Lu, H., Li, A., 2018. A spatial downscaling approach for the SMAP passive surface soil moisture product using random forest regression. J Hydrol (Amst) 563, 1009–1024. https://doi.org/10.1016/j.jhydrol.2018.06.081

Zolghadr-Asli, B., Enayati, M., Pourghasemi, H.R., Naghdyzadegan Jahromi, M., Tiefenbacher, J.P., 2021. Application of Granger-causality to study the climate change

impacts on depletion patterns of inland water bodies. Hydrol Sci J 66, 1767–1776. https://doi.org/10.1080/02626667.2021.1944633